ROLLOVER MITIGATION CONTROLLER

DEVELOPMENT FOR A THREE WHEELED PLATFORM

By

RAJA AMER AZIM

A DISSERTATION

Submitted to

National University of Sciences and Technology

in partial fulfillment of the requirements for the degree of

DOCTOR OF PHILOSOPHY

Supervised by

DR WAHEED UL HAQ SYED

DR FAHAD MUMTAZ MALIK

College of Electrical and Mechanical Engineering

National University of Sciences and Technology, Pakistan

2015

In the name of Allah, the most Merciful and the most Beneficent

ABSTRACT

ROLLOVER MITIGATION CONTROLLER DEVELOPMENT FOR A THREE WHEELED PLATFORM

RAJA AMER AZIM

This research work is an investigation of active and passive methods to reduce rollover tendency of a three wheeled platform. This configuration is common in small to medium aircraft landing gears, mobile robots, and fuel efficient futuristic concept vehicles. In developing countries three wheeled vehicles (TWV) have a significant share in point to point public transport. Such vehicles have a higher rollover risk resulting in significant single vehicle fatal crashes, and thus are the main focus of the current research. In Delta configuration the front single wheel offers no roll resistance, hence no lateral load transfer takes place during cornering at the front axle. The effect on directional behaviour is evaluated for this unique lateral load transfer setup. Dynamics of the vehicle are studied in the state space spanned by the yaw rate and side slip angle. These states encompass the directional behaviour of the vehicle fairly well. The effect on roll over and directional behaviour is assessed. For aircraft tricycle landing gears limit handling behaviour in the form of over-steering behaviour appears much before an un-tripped rollover. This is also observed for existing commercial three wheeled vehicles used for public transport when operated on low friction surfaces. This results in immediate loss of control resulting in collision with other vehicles or road sides resulting in tripped rollovers. Factor effecting passive rollover propensity are related to possible changes in directional response of the vehicle. For delta configuration vehicles, braking unloads the rear axle, reducing the lateral load transfer required for rollover. Due relatively low yaw inertia the vehicle response to steering inputs is also better for three wheeled platforms. Based on these observations an

active front steering based sliding mode controller is presented for rollover prevention. A vehicle model for direct control of roll angle using steering as an input is developed. An adapting reference based on roll angle at steady state conditions corresponding to a threshold lateral load transfer ratio, is used for sliding surface design. The robustness of the controller is demonstrated using a nonlinear model of CarSim software. The yaw rate error introduced by increasing the turn radius by the controller is than compensated using a brake based system. Both differential braking based Dynamic Stability Control (DSC) and proportional braking are evaluated for efficacy. Giving a higher priority to rollover mitigation, the active front steering is always activated after a threshold lateral load transfer value. The brake based systems are also evaluated for directional control of the vehicle on low friction surfaces.

A rule based integration scheme based upon performance of the steering and brake based controllers is proposed. Standard critical driving maneuvers are used to gauge efficacy of the integrated controller.

To

My parents, my wife and loving children

ACKNOWLEDGEMENTS

I would like to acknowledge the guidance and cooperation of all my teachers whose earnest efforts have made possible the successful completion of this work. The knowledge I gained from them proved helpful throughout the course of my studies. The persons to whom I would like to address very special thanks are my supervisor Dr Waheed ul Haq Syed and co-supervisor Dr Fahad Mumtaz Malik, both for accepting me as a PhD student and for providing valuable guidance, advice and support over the years resulting in the completion of this thesis. I would always cherish the long hours of technical discussions.

I would like to express my sincere gratitude to Dr Ejaz Muhammad (HITEC University), Dr Muhammad Afzaal Malik (Air University), Dr Shahab Khushnood (UET Taxila), Dr Bilal Malik and Dr Aamer Ahmed Baqai for their valuable guidance in my research.

I am grateful to my colleagues Dr Khalid Munawwar, Dr Imran Akhtar, Dr Ali Usman for their cooperation and beneficial academic discussions I have had with them.

I am grateful to all my family members for their support. My parents have been source of inspiration for me and their prayers have accompanied me throughout my life. I am also indebted to my wife and children who have been very supportive and have shown extraordinary patience all the way along.

I would also like to acknowledge National University of Sciences & Technology (NUST) for the multi-faceted support they provided for my studies and research.

TABLE OF CONTENTS

LIST OF FIGURES

LIST OF TABLES

LIST OF ABBREVIATIONS USED

ABS	Anti lock Braking System
AGV	Automated Guided Vehicle
ARB	Anti-Roll Bar alternately known as stabilizer bar, sway bar, anti sway bar
DOF	Degrees of freedom
DSC	Dynamic Stability Control (brake based) Alternately known as Electronic Stability Program (ESP) and Direct Yaw moment Control (DYC)
ESC	Electronic Stability Control
FAR	Federal Aviation Register
ISO	International Standards Organisation
NHTSA	National Highway Traffic Safety Administration (US Dept of Transportation)
SAE	Society of Automotive Engineers
TWV	Three Wheeled Vehicle

CHAPTER 1

INTRODUCTION

Three wheeled configurations provide compact, cost-effective and sometimes due to packaging constraints like in aircrafts, the only feasible solutions for mobility requirements. They have an essential role in ground mobility of aircrafts, low cost point to point road transport and wheeled robots. Component and passenger placement constrains the single wheel to be placed either at the front or rear. Such vehicles have significantly high rollover propensity. While regulations limit lateral accelerations for aircraft ground operations, cost has inhibited the use of active systems for rollover control in commercial three wheeled vehicles. Recent studies focus on handling characteristics of this configuration as well as control. New concept vehicle designs with active leaning of chassis have been explored and some companies have started limited production of such vehicles. The major bulk of the three wheeled vehicles (TWV) still remain vulnerable as no active rollover prevention systems has been implemented for these vehicles. This chapter provides an overview of the problem, and existing solutions.

1.1 Motivation

Road traffic accidents are currently the 9th leading cause of death worldwide[1]. It is projected that it would become the fifth leading cause of death by year 2030 [2]. Of all the reported deaths about 60% deaths occur in lower and lower middle income countries. Almost 36 per cent (about 596 million) of which live in Asia [3]. The vehicle ownership per 1000 individuals is less than 10 in these countries. In such countries, intermediate transport mediums play a pivotal role to complement the public transport systems. Three

wheeled vehicles provide a significant share of this mode [4]. The role of these vehicles have been re-emphasized in a report of World Resource Institute[5]. In capital of Bangladesh, Dhaka 48% of the total km travelled per day are by three wheeled vehicles[6]. In an iconic Asian city Mumbai, three wheeler auto rickshaws grew by 420 per cent during 1991–2005 which is one of the highest in India[3]. In china almost 16 million three wheeled vehicles are owned in the rural area[7]. The production of such vehicles increased by an annual rate of 38% during 1985 to 2000. The annual vehicle miles travelled by these three wheeled vehicles was estimated to surpass that of cars in year 2030 and the trend will continue till 2050 as projected in the report by Argonne National Laboratory of US state department [8].

These three wheeled vehicles while providing a cost effective, agile transport means, are prone to rollover. Rollover of three wheeled vehicles have resulted in serious injuries to the passengers and even fatalities. On the average, of the total traffic related fatalities reported in India in 2009~2011[9]–[11], three wheeled vehicle were involved in 5%. The share in serious injuries was 8%. The estimated share in total transport was 3.5%. This indicates a serious threat to human life due to rollover and crash worthiness properties of the vehicle. A major share of fatalities 29% involves tempos, truck, mechanized agricultural vehicles (MAV) and tractors. Tempos and most of the MAVs are three wheeled vehicle variations with rigid chassis. In Pakistan where only 8 out of 1000 owns a car[12], public and commercial transport plays a very vital role. Two and three wheeled vehicles are 51% of the total registered vehicles. It was also highlighted that the reported accidents are less than 2.5% of real data. Accident data reported does not have a breakdown of three wheeled and two wheeled vehicles but both account for more than 60% of fatalities.

According to Jooma et al [13] in Karachi, the fatalities due to accidents in which three wheeled vehicles are involved, rose by 33% in 2011.

Three wheeled all-terrain vehicles (ATVs) have been banned in several countries due to poor safety record[14], The accidents reported have been attributed to its poor rollover crash record. According to accident data provided by Bangladesh Road Transport Authority, 75% single vehicle crashes of three wheeled vehicles involved rollover. In India large number of people prefer this mode of transport and are vulnerable to such accidents. In a study by Schmucker et al [15] single-vehicle collisions (54%) were more frequent than multivehicle collisions (46%) amongst motorized rickshaw occupants. The occurrence of overturning of motorized rickshaw was observed in 73% of the single-vehicle collisions. Mortality (12%), the mean Injury Severity Score (5.8) and rate of multiple injured (60%) indicated a substantial trauma load.

The major cause, in 77.5% of reported accidents, was identified as driver's mistake[9]. This includes over reacting to emergency situations, improper speed etc. This indicates the potential of active chassis control systems that can assist in mitigating crashes. The need to reduce the risk for human lives as well as eliminate the effects of human error in operating vehicles has motivated research in understanding dynamics of wheeled platforms and allied control systems at different levels along with extensive testing. Cost effectiveness has been the key to adaption of such technologies.

Rollover propensity of narrow commercial vehicles with high center of gravity has been a major area of research[16]–[19]. Generally passive measures alone are not sufficient to provide the required safety against rollover crashes. National Highway Testing and Safety Association (NHTSA), report DOT HS 809 790[20] reports that, (Electronic

Stability Control) ESC systems reduce fatalities by 34% in multiple vehicle crashes for passenger cars and sports utility vehicles (SUVs). Single vehicle crashes resulted in up to 74% less fatalities in SUVs using ESC systems. Single vehicle crashes in SUVs are dominantly rollover events. The three wheelers and SUVs share similar stability parameters values defined as Static Stability Factor (SSF) and Static Stability Factor Margin (SSFM) [21], [22].

1.2 The Three Wheeled Platform

Simplicity of construction has led to an early adaption of a three-wheeled platform for wheeled vehicles, as the first purpose built vehicle of Nicolas-Joseph Cugnot[23] in 1769. Low polar moment of inertia, layout favoring less drag[24] and less complicated steering design are main advantages of a three wheeled platform. The average maneuverability of three wheeled vehicles was shown to be superior to an equivalent four wheeled vehicle [25]. There are two main variants of three wheeled platform which were evaluated for rollover propensity reported first by Huston et al [22] as shown in Figure 1-1

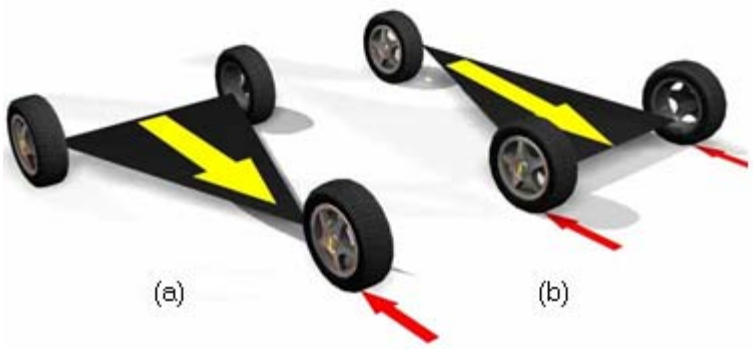

Figure 1-1 Three wheeled Vehicle configurations: a) Delta and b) Tadpole wheel layouts[26]

The delta configuration has one wheel in front and two wheels in the rear (1F2R) as in Figure 1-2(a). A two wheel in front with one rear wheel (2F1R) as in Figure 1-2 (b) is

referred to as a tadpole configuration. In the study by Valkenburgh [21] keeping all other factors same, tadpole configuration is less prone to rollover as compared to delta configurations in situations where braking is applied while the vehicle is turning. Both configurations have been extensively used in aircrafts varying slightly to accommodate design and packaging requirements. Recently most of the aircraft have a delta layout for the compliant wheel assemblies to support and steer the aircraft on ground. It has found application in unmanned ground vehicles and robots. Even without the use of suspension all three wheels can maintain contact with ground and have a deterministic ground contact force leading to adaption in robots for challenging terrains [27] and easy evaluation of stability[28] for control. The most significant three wheeled platform was conceived by Enrico Piaggio in 1948 after the second world war[29]. This got the name Ape [bee] in Italian. This contributed significantly in the rebuilding of Italian economy after war. The success led to adoption of this platform to developing and under developed countries in the form of tuk-tuks, rickshaws, Qing qi in Asia, Bajaj, keke-marwa in Africa, Ape, Bajaj in South America and Europe, all have rigid chassis and are in delta configuration. Futuristic personal mobility solutions like Carver[30] and Clever[31], which use active stability control systems to lean the front part of a split chassis. These have a delta layout for wheels. Stability in turns while braking led to adoption of tadpole configuration which is still less favorable for commercial vehicle passenger and goods layout. Automotive giants realizing the potentials of this platform for personal and limited passenger mobility have led to the development of Mercedes-Benz F 300 Life-Jet in 2005, Volkswagen GX3 in 2006, and Peugeot HYmotion3 in 2008. Except Clever all have a tadpole wheel layout. Independent companies started work on this platform and produced many variants. These were claimed

as the missing (required) link between a four wheeled vehicle and a two wheeled motorcycle. The main catalysts for adapting a three wheeled platform are rising fuel prices, road congestion caused by larger vehicles with less passengers and safety considerations that cannot be guaranteed by motorcycles. The modern non-tilting concept vehicles are focusing on individual, personal mobility. These vehicles are and cannot be adapted for public transport as is the case of Ape'.

A representative list of variants used for public transport and moving goods with three wheels can be found at[32]–[36]. The variants use different propulsion systems, from simple gasoline and diesel engines to hydrogen internal combustion engines, designed by ICHET in collaboration with Mahindra & Mahindra of India[37]plying the roads of Delhi in 2010. In 2007 EPA funded project at University of Michigan, USA resulted in the first publically known electric-hydraulic hybrid vehicle, was built upon a three-wheeled platform Xebra by ZAP[38]. ZAP founded in USA in 1994 focuses on plug in electric technology. Its three-wheeled product Zap Alias has a top speed 140 km/h, capable of doing 0 - 100 km/h in about 8 seconds. The cruising range claimed is 160 km on a single charge[36]. The Peugeot HYmotion3, another futuristic three wheeled vehicle is powered by a gasoline electric hybrid power plant.

The bulk of three wheeled vehicles used in developing countries with delta configuration, serve as a sustainable low cost commercial transport. An estimated 65% of the world's three and two wheeled vehicles are in Asia. India alone has an estimated production capacity of more than 1,100,000 units [39]. In Pakistan the installed capacity is not well documented with varying numbers being quoted. A conservative number is 200,000 based upon company websites and Engineering Development Board Pakistan. The main three

wheeled vehicle with a two-stroke engine, now is being phased out by 4-stroke gasoline (with CNG/LPG kits) or diesel engines. The designs mainly focus on low cost, with no active controls for handling or rollover prevention. UNDP and other government agencies have sponsored different Studies[40]. Most focus on the economic and environmental impact of this platform. A common conclusion as in reports by Mani et al [41] and Breithaupt et al [6], is that these three wheeled commercial vehicles serve as one of the major mode of transport in congested-urban and now rural areas of Asia, South America and Africa. Almost all of these public transport versions are with delta configuration. Primary focus on cost has led to low directional and rollover stability. Single vehicle accidents typically involve rollover.

1.3 Previous Research on TWV Rollover and Directional Stability

The factors affecting the rollover tendency of three wheeled vehicles were experimentally evaluated by Valkenburgh *et al*.[21]. They used a simple steady state model to predict rollover and related the results with experiments. Limit handling behavior was experimentally also evaluated. They concluded that a three wheeled setup in delta configuration always over-steers while a tadpole configuration predominantly under steers. Huston et al. [22] used analytical modeling without including suspension and other secondary nonlinear effects, evaluated steady state steering response in terms of understeer and over steer behavior. Rollover was evaluated for both tadpole and delta configurations in accelerating while turning and breaking while turning. The tadpole configuration was more prone to rollovers in breaking while turning maneuvers. As in an emergency obstacle avoidance maneuver or while correcting vehicle heading in a turn, breaking along with steering is typically used. This further highlights the vulnerability of the delta design and

points towards the limitations of any possible control schemes utilizing braking for stability in high speed turns. Another important finding was the absence of front to rear roll stiffness distribution tuning ability in three wheelers. Analytical prediction of rollover stability in terms of limiting value of lateral acceleration was given as in equation (1-1) with reference to Figure 1-2 . The ratio $\frac{a_{threshold}}{g}$ is known as the static stability factor and is used by NHTSA for rating vehicles for rollover tendency [42].

$$\begin{aligned} \frac{a_{threshold}}{g} &< \frac{b}{2h} \quad \text{for four wheeled vehicles} \\ \frac{a_{threshold}}{g} &< \frac{b}{2h}\frac{l_1}{L} \quad \text{for delta three wheeled vehicle} \end{aligned} \tag{1-1}$$

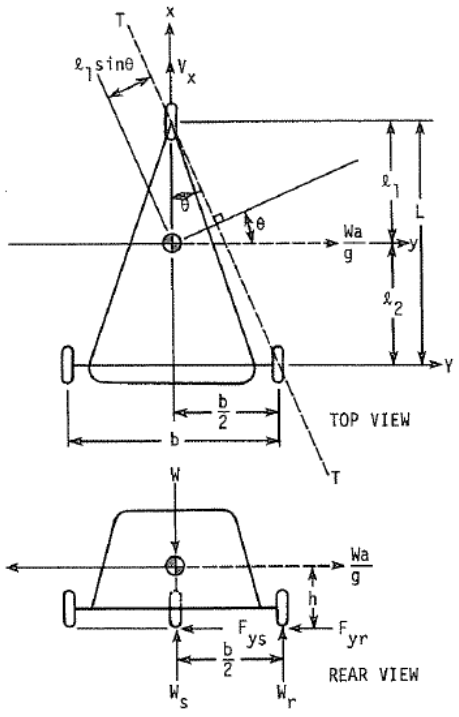

Figure 1-2 Three wheeled vehicle (Delta) showing rollover axis T-T[22]

The tadpole design had a reduced rollover threshold as compared to an unchanged stability factor for a four wheeled vehicle. The ratio $\frac{l_1}{L}$ between the longitudinal distances of *cg* from the front axle to the total wheel base scaled the rollover resistance as compared to a four wheeled vehicle. The static stability factor used neglected the compliance of suspension elements and linear tire behavior was used for vehicle limit handling boundaries. Three wheeled motorized vehicle commonly used in Asia was analyzed by Raman et al [43]. The vehicle was represented as a rigid triangular body with wheels at corners connected through vertical spring damper combination representing suspensions. Camber changes during vehicle roll were neglected. Transmission and suspension inertia was taken negligible as compared to the sprung mass inertia. Parameters of a popular commercial three wheeled vehicle were used. Constant power turn, accelerated turn and avoidance with braking were simulated. The vehicle was shown most vulnerable to rollover in avoidance while braking maneuver. The increase in track width was shown to have an increasing effect on stability which can be explained by the quadratic term in roll stiffness related to track width [44]. While height of vehicle center of gravity effects linearly and stability decreases with increase in height. The effect of suspension was shown to have a nonlinear effect. This can be explained by the equivalent roll stiffness which doubles with a unit increase in stiffness of both rear suspension springs. A decrease in roll angle also contributes to decrease in the over-turning moment of the displaced center of gravity. A decrease in ride performance is expected with increase in suspension stiffness. Stability was shown to improve with damping. Again this has a negative effect on ride quality. Rao *et al*. [45] used the model of Raman and extended the study using Simulink software. The

handling behavior of the three wheeled vehicles were discussed in some limited detail in the experimental evaluation by Valkenburgh but were generally not related to the parameters effecting rollover. In all of these studies effect of using an anti-roll bar was not reported. The effect on rollover and directional behavior of a three wheeled vehicle with tilting wheel assemblies (variable camber) in two front one rear wheel configuration (2F1R) was investigated recently by Azadeh [46]. A three degree of freedom analytical model was used in the study. A camber angle on all the three wheels was considered in different combinations. The requirement for left and right hand turns require opposite camber angle corrections leading to an increase in rollover threshold by almost 20%. The authors did not report the mechanism required to achieve this camber. It is assumed that this additional mechanism with sufficient structural strength would add significant weight and cost to the vehicle.

Typical robotic applications use three wheeled platforms without any suspension. Saha and Angeles in a representative work [47] presented a 2-DOF kinematic and dynamic model of a three wheeled AGV. The rear wheels were actuated with independent motors. A castor wheel in the front provided with the desired motion stability, preventing the tires to skid, however only planer motion was considered. A light weight mobility concept was presented by Honorati et al [48] based on hub motors. The emphasis was on the electrical power management. Optimal velocity as determined for a specified path. To offset environmental concerns, electric power as an alternate to internal combustion engines have been reported by Caricchi et al [49] for a rigid chassis delta design while Cossalter et al [50] used electric power for a tilting three wheeled vehicle. A more comprehensive electric

drive model was presented by Mulhall et al [51] with possibility of solar energy utilization. The rollover prevention and handling concerns were not addressed.

Rollover propensity is compensated in two wheeled motorcycle by leaning inwards in a turn, researchers started to work on tilting three wheelers with narrow wheel base as in [52], [53]. Kim et al [28] used model predictive control of an autonomous three wheeled vehicles in a delta configuration without suspension. Only the front single wheel was powered as well as steered. Measurements and a linear model were used to predict tire adhesion status and control action was generated. The efficacy was ascertained for trajectory following on flat and inclined surfaces. The departures from the planned trajectory were significant but the tire slippage and tip over have been mitigated. Finite element models in PAM-CRASH software were developed to study the crash worthiness of three wheeled vehicles by Chawla et al [54]. A maneuver entrance speed of 35 km/hr was used which corresponds to an average velocity of a TWV involved in crashes. The various simulations carried out declared the present design as ‘dangerous’. This indicates a serious threat to human life due to rollover and crash worthiness properties of the vehicle. Yu et al [55] using analytical models with arbitrary parameter values applied full control concept on a three wheeled platform. Delta and tadpole configurations were modeled using Newton-Euler approach. The study uses linear tire and suspension models. Zero body sideslip and zero body motions were targeted for desired motion trajectory. Six control parameters were needed from the eight available i.e. three tractive forces at wheels, three active suspension forces and steering angle at front and rear axle. Control modes (input combinations) were evaluated for force demand. In constant radius turn steering inputs at both axles and active suspension provide a favorable combination. An active suspension

would add considerable cost and weight. A stiff suspension may provide some stability in the absence of active suspension. For better handling, the results favored active steering control over braking. Yavin and Frangos [56] modeled a tadpole configuration using Lagrange approach. Without any suspension front wheels rotate freely and can be steered whereas the rear wheel were powered. A planer TWV model for ride characterization was presented by Gawade et al [57]. Wheel lift-off over a bump along with associated vibrations over different bump profiles were investigated for comfort. A cycloidal profile having maximum acceleration for the same bump height initiates liftoff and vibrations. The induced vibrations were reported to be within ISO 2631 tolerance limits. The same group of researchers presented rollover propensity of three-wheel scooter taxis [58]. Six degrees of freedom model was simulated for slowly increasing steer, NHTSA J turn, and Road Edge Recovery maneuvers. Experimental results for vertical accelerations while traveling over a bump were used for model validation. Using Magic tire model a comparison was made with NHTSA one star rated 2001 Chevrolet Blazer. The maneuver entrance speed is 2.17 and 1.79 times more for Chevrolet Blazer as compared to the three wheeled taxi. The difference was attributed to the different rollover lines (axis) for the two vehicles as indicated earlier by Huston et al [22]. The authors suggested moving the center of gravity rearwards for improved stability. A lateral acceleration of $3 m/s^2$ was reported as the limiting value for wheel lift off. It is important to note that static stability factor of the vehicle was 0.8 g. A refined form of model development and validation was later published [59]. The combined results of [54], [58] were presented in [60]. The results were expanded by the same research group using MADYMO^{TM} [61].

Directional stability and handling performance are strongly influenced by the distribution of roll stiffness among the axles of a vehicle because of the nonlinear relationship between normal tire load and cornering stiffness, particularly for truck tires. In the absence of torsional frame flexibility, axles with greater roll stiffness will carry a greater proportion of the total lateral load transfer generated during cornering[44]. This leads to an effective reduction of cornering stiffness at those axles, affecting the handling balance. Anti-roll bars are used to fine tune the lateral load transfer ratio for achieving desirable understeer behavior. In three wheeled vehicles, roll stiffness is available only on the axle with two wheels. This peculiar setup introduce inherent roll over steer. Hac [62] demonstrated that addition of anti-roll bar (ARB) resulted in an increase in the rollover threshold of a four wheeled sports utility vehicle. The suggested method is adding or increasing the auxiliary roll resistance (stiffness) uniformly on both front and rear axles. Research on effect of adding an ARB on rollover and lateral stability of a three wheeled vehicle is very limited.

A typical aircraft has a three wheeled configuration as shown in Figure 1-3. The front wheel is steered similar to a ground vehicle for turning [63]. A large number of commercial and military aircraft utilize three wheeled landing gear for ground mobility (taxiing). Significant research on ground maneuvers[63]–[69] has been carried out but has focused only on directional behavior of the aircraft. Safety has more significance than performance and hence ground maneuvers are regulated to a higher degree in aircraft as compared with other ground mobility platforms. The current Federal Aviation Register[70] regulation FAR25.495, for an aircraft during a high-speed turn on ground, limits the lateral load to half the vertical load at each landing gear. This according to Tipps et al[71] was considered to be too conservative. Landing gear tires selection result in spin/skid at low

speeds and not rollover as discussed in [64], [72]. The primary interest of previous studies was hence in directional stability. A detailed analysis for directional behavior was given in [67]. A more comprehensive study is presented in [73]. In these studies, bifurcation and continuation methods were applied to study the behavior of an aircraft on ground. A nonlinear look ahead control and command filter was proposed by Chen et al[63] for runway keeping. The roll dynamics were neglected. As in this study and other representative work[68], [69], [74]–[76], nose wheel steer angle is regulated by the controller to achieve desired performance. A steering based rollover control would augment the existing controller and extend the ground operational envelope of an aircraft.

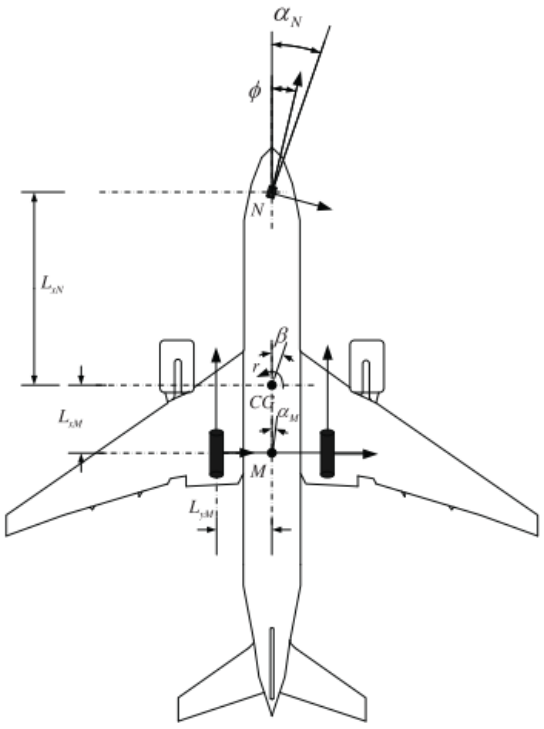

Figure 1-3 Aircraft Ground Maneuver Model [63]

1.4 Existing Active rollover mitigation Techniques

The research in active rollover control systems for four wheeled and multi axle road vehicles is quite an active area of research. A study [77] suggested that some form of electronic stability control (ESC) on a vehicle reduces single vehicle crashes up to 49%. In [20] collected single vehicle accident data shows up to 65% fatal crash reduction for SUVs using some form of electronic stability control system.

The following Five actuation schemes are currently utilized for rollover prevention of four-wheeled vehicle.

- Differential braking [78]–[81]
- Active steering control [82]–[85]
- Active suspension control [81], [86], [87]
- Active anti-roll bar [84], [88]
- Combination of above [89]–[91]

Recently research activity has started in the area of three wheeled vehicle control. An electric vehicle having two wheels in front and one in rear is being developed at University of Zagreb, Croatia [92]. Only analytical modeling was presented with in-wheel motors and nonlinear tire model. The significant part was the additional variables added in

the model to cater for additional inertia due to payload changes. Plans have been revealed for the development of electronic differentials, traction and stability control systems. Bartolozzi et al [93] and Sponziello et al [94] presented work on a tilting three wheeled vehicle Piaggio MP3. They have used analytical model for directional stability studies with linear tire models. MSC Adams was used to investigate dynamic handling characteristics of the vehicle and were validated using experimental results. The roll was introduced by a roll follower controller. Results suggest that the vehicle was driven as an ordinary two wheeler with better handling and stability characteristics. The other major development in three wheeled vehicle has been tilting three wheeled vehicle with split chassis in delta configuration. EU funded CLEVER project at University of Bath, United Kingdom is an iconic work in the area of tilting three wheeled vehicle research. Barker [95] and Berote [96] gave a detailed account of the tilting mechanics and controls. The vehicle uses Direct Tilt Control DTC. Speed and steer angle was measured and tilt angle based on a static map was achieved using two hydraulic actuators. MATLAB SimMechanics software was used for model development and validated by experimental data. The vehicle's response was found to be satisfactory in steady state operation. Gohl et al [97] presented the development of a tilting three wheeled vehicle at university of Minnesota. A controller utilized the steady state tilt angle as desired value for tilt and a proportional derivative arrangement was used to achieve the desired tilt angle. Kidane et al [98] presented combination of Steering Tilt Control (STC) and Direct Tilt Control (DTC) discussed earlier.

A hierarchical tracking controller for a three wheeled platform was presented in [99]. The roll and pitching motion were not considered making it a planer mobility problem. [100] uses adaptive neuro-fuzzy based controller to enhance rollover stability of a three wheeled

mobile manipulator. A 4-DOF spatial manipulator was mounted at center of gravity of a triangular three wheeled platform without suspensions. The platform was made to move in a sinusoidal path. The manipulator was controlled so that the forces on the rear left and right wheels remain equal. In [101] a three wheeled platform taken as a unmanned ground vehicle was made to follow a sinusoidal trajectory. Adaptive control was implemented. A planer model with two powered rear wheels was used. The front wheel was a free castor wheel. The controller was compared with a proportional-integral-derivative (PID) controller. In [102] a sliding mode controller was proposed for tilting the vehicle. The tilt angle deviation from the desired and forward velocity deviation from the desired speed for the desired turn was used to define the sliding functions. The study suggests that a simple multivariable controller using sliding mode control can effective stabilize the vehicle in turns.

1.5 Need for Research

Commercial three wheeled vehicles, aircrafts and most of three wheeled robots use a delta configuration. For Safety enhancement and handling improvement further research is required. Characteristics and shortcomings of existing available research can be summarized as follows.

- A large number of existing commercial public transport vehicles prone to rollover have no existing sensor/actuator installed and limited space is available for such additions
- Studies are limited primarily to directional behaviour of three wheeled configurations

- Rollover tendency is addressed by regulations, passive systems and vehicle layout for fixed single-unit-chassis urban vehicles, aircrafts and mobile robots
- Active measures primarily rely on tilting the whole vehicle or part of it as in split chassis during turns
- Limited evidence on effect of factors effecting rollover on directional handling of three wheeled vehicles

1.6 Approach Used

Based on the established need, six degrees of motion of a delta configuration three wheeled vehicle is modeled using nonlinear tire model and suspension behavior. This model is then used to assess the effect of various vehicle parameters effecting rollover on the directional behavior of the vehicle. Based upon the outcomes, control objectives are ascertained. Actuators and controller design are chosen based upon robustness, cost and adaptability to existing three wheeled platforms. Keeping rollover prevention as the primary objective, individual control schemes based upon steering and braking are proposed. A rule based integration of the controllers is considered for operational safety of the vehicle over a range of road conditions.

1.7 Thesis Overview

The thesis is organized as follows: In CHAPTER 2, models used for rollover propensity and directional behavior are developed. A nonlinear model for controlling roll angle through steering input is developed. Tire modeling based upon available data on three wheeled vehicles is presented. In CHAPTER 3, analysis of a three wheeled vehicle is

presented. Effect of adding an anti-rollover bar on rollover propensity and its possible effect on directional behavior is established. A detailed analysis to relate parameters effecting rollover with the directional behavior of the TWV is presented. In CHAPTER 4, development of a rollover mitigation controller based on active front steering is presented. Its efficacy on low and high friction road conditions is discussed. Subsequently in CHAPTER 5, brake based controller design for directional stability and vehicle response fidelity is presented. Steering and brake based controllers are integrated through a rule based logic. The thesis will be concluded in CHAPTER 6 with future work suggestions given in CHAPTER 7.

CHAPTER 2

VEHICLE MODELING

In this chapter, various vehicle models for the proposed study and controller design are presented. A 6dof vehicle model for assessing the open loop dynamics of three wheeled vehicle and low order models for direct control of roll and yaw plane dynamics controller design are presented.

Adequate vehicle dynamics models are essential to simulate handling, design control systems and evaluate control performance when the vehicle is subjected to specific maneuvers. A simplified model is always preferred due to less computational expense and number of model parameters to be identified and correlated with the physical system. The simplification is limited by the significant dynamic modes required for adequate representation of the phenomenon.

A vehicle undergoes motion with six degrees of motion: three translational components and three rotational components. The translational degrees of freedom are defined along the vehicles longitudinal, lateral and vertical direction. Rotation about the lateral longitudinal and vertical axis are defined as the pitch, roll and yaw respectively. The number of sprung and un-sprung mass components and their significant motions considered yield models with corresponding number of states. For this research three different models have been used.

2.1 Full Vehicle Simulation Model

A vehicle model full vehicle model based on the earlier work of Gawade *et al* [59], [103] is used. They have developed a six degree of freedom model to investigate the rollover

propensity of a three wheeled vehicle. Model complexity has been set to include commonly measurable parameters of the vehicle. The same model has been extended to include effects of track width change during roll motion and an anti-rollover bar has been added at the rear axle. SAE standard coordinate system as shown in the figure is used for the vehicle. In total three coordinate frames are used for writing the equations of motion.

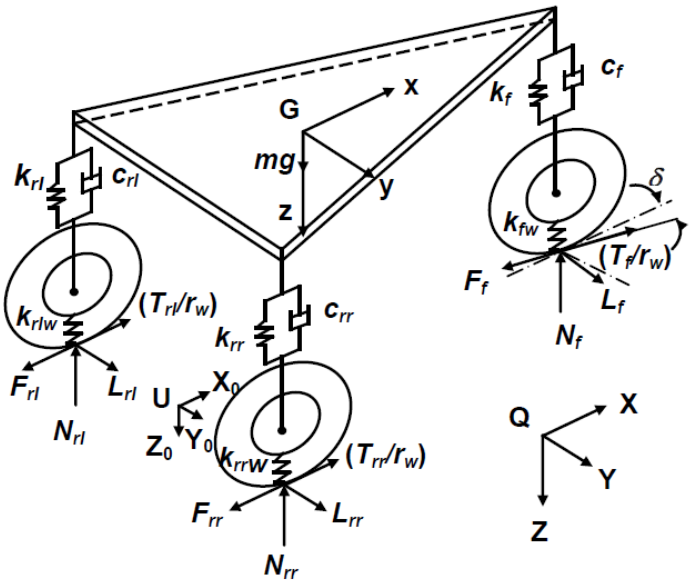

Figure 2-1 6-dof three wheeled vehicle model[59]

An inertial frame of reference Q is used to describe external forces including acceleration due to gravity. A body fixed frame G positioned at center of mass is used to derive the equations of motion. A local frame G' is used to describe an intermediate frame to represent local vehicle states to evaluate tire forces w.r.t. the road. Considering a globally flat road, this frame has its z-axis aligned with the Q frame and x-axis aligned with the vehicle heading direction. This frame is referred to as the local flat earth frame (LFEF). The vehicle is shown with N_{ij} as the normal reaction at the tire contact patches, L_{ij} as the

lateral forces and F_{ij} as the longitudinal tire forces. Subscripts i, j represent wheel location. Equations of motion are derived using Newton-Euler method while expressing quantities in the body fixed frame G. Euler angles are used to describe the orientation of each frame with respect to the inertial frame Q. The transformation matrix $[T]$ to transform quantities from any frame to the inertial frame is generated using composition of three intrinsic rotations in the following sequence: φ radians about x-axis of the frame, θ radians about current y-axis and finally ψ radians about current z-axis. The intrinsic rotation matrices are as given in equations(2-1), (2-2)and (2-3)

$$R_x(\phi) = \begin{bmatrix} 1 & 0 & 0 \\ 0 & \cos\phi & -\sin\phi \\ 0 & \sin\phi & \cos\phi \end{bmatrix} \tag{2-1}$$

$$R_y(\theta) = \begin{bmatrix} \cos\theta & 0 & \sin\theta \\ 0 & 1 & 0 \\ -\sin\theta & 0 & \cos\theta \end{bmatrix} \tag{2-2}$$

and

$$R_z(\psi) = \begin{bmatrix} \cos\psi & -\sin\psi & 0 \\ \sin\psi & \cos\psi & 0 \\ 0 & 0 & 1 \end{bmatrix} \tag{2-3}$$

which give the overall rotation matrix from any arbitrary frame to the inertial frame and is calculated as in equation (2-4). As the pitch angle remains small the singularity corresponding to $\theta = \pm\frac{\pi}{2}$ is easily avoided.

$$[T] = R_z(\psi).R_y(\theta).R_x(\phi) \tag{2-4}$$

An arbitrary quantity X in a reference frame $Oxyz$ is expressed in inertial frame $OXYZ$ as in equation (2-5)

$$\{\mathrm{X}_{OXYZ}\} = [T]\{\mathrm{X}_{Oxyz}\} \tag{2-5}$$

The instantaneous values of Euler angles are generated through integration of equation (2-6), which relates the angular velocities of the vehicle expressed in body fixed frame to Euler angle rates.

$$\begin{bmatrix} \dot{\phi} \\ \dot{\theta} \\ \dot{\psi} \end{bmatrix} = \begin{bmatrix} 1 & \sin\phi\tan\theta & \cos\phi\tan\theta \\ 0 & \cos\phi & -\sin\phi \\ 0 & \sin\phi\sec\theta & \cos\phi\sec\theta \end{bmatrix} \begin{bmatrix} \omega_x \\ \omega_y \\ \omega_z \end{bmatrix} \tag{2-6}$$

The equations of motion expressed in body attached frame are as given in equations (2-7) and (2-8).

$$\begin{aligned} \ddot{x} &= \frac{F_x}{m} + \omega_y \dot{z} + \omega_z \dot{y} \\ \ddot{y} &= \frac{F_y}{m} - \omega_z \dot{x} + \omega_x \dot{z} \\ \ddot{z} &= \frac{F_z}{m} - \omega_x \dot{y} + \omega_y \dot{x} \end{aligned} \tag{2-7}$$

$$\begin{aligned} \dot{\omega}_x &= (M_x - (I_{zz} - I_{yy})\omega_y\omega_z + I_{xz}(\dot{\omega}_z + \omega_y\omega_x)) / I_{xx} \\ \dot{\omega}_y &= (M_y - (I_{xx} - I_{zz})\omega_x\omega_z + I_{zx}(\omega_z^2 - \omega_x^2)) / I_{yy} \\ \dot{\omega}_z &= (M_z - (I_{yy} - I_{xx})\omega_x\omega_y + I_{zx}(\omega_y\omega_z - \dot{\omega}_x)) / I_{zz} \end{aligned} \tag{2-8}$$

The forces F_x and F_y are primarily the sum of longitudinal and lateral tire forces expressed in body fixed frame and discussed in detail in the tire forces section. Summation of forces in the z direction, F_z includes gravitational forces and suspension forces expressed in body fixed frame. The cross product terms I_{xy} and I_{yz} are assumed negligible because of dominant symmetry about vehicle Gxz plane due to component layout and driver seating.

The moments M_x, M_y, M_z are generated because of the forces mentioned earlier and are first calculated in local flat earth coordinates as in equation (2-9) and then expressed in the local body fixed frame of the vehicle.

$$\begin{aligned} M_x &= -(F_{yf} + F_{yrr} + F_{yrl})h_{cg} + (F_{ZRR} - F_{ZRL})c\cos(\phi) + mgh_{rc}\sin(\phi) \\ M_y &= -F_{zf}a\cos(\theta) + (F_{zrr} + F_{zrl})b\cos(\theta) + (F_{xf} + F_{xrr} + F_{xrl})h_{cg} \\ Mz &= -(F_{yrr} + F_{yrl})b\cos(\theta) + F_{yf}a\cos(\theta) + (F_{xrl} - F_{xrr})c\cos(\theta) \end{aligned} \tag{2-9}$$

2.1.1 Suspension Modelling

The vertical force at each suspension mounting point are given by the equations(2-10) ,(2-11) and(2-12). Where $k_{ij}, c_{ij}, \dot{z}_{ij}$ and z_{ij} are suspension stiffness, damping , travel rate and suspension travel at respective locations indicated by subscripts i, j .

$$N_f = \begin{cases} -(k_f z_f + c_f \dot{z}_f) & \text{if } z_f > z_{fbs} \\ 0 & \text{otherwise} \end{cases} \tag{2-10}$$

$$N_{rr} = \begin{cases} -(k_{rr} z_{rr} + c_{rr} \dot{z}_{rr} + k_{arb}\phi / c) & \text{if } z_{rr} > z_{rrbs} \\ 0 & \text{otherwise} \end{cases} \tag{2-11}$$

$$N_{rl} = \begin{cases} -(k_{rl} z_{rl} + c_{rl} \dot{z}_{rl} - k_{arb}\phi / c) & \text{if } z_{rl} > z_{rlbs} \\ 0 & \text{otherwise} \end{cases} \tag{2-12}$$

To account for lift off when the wheel travel exceeds z_{ijbs} (the bump stop limited travel of the suspension) no force is transmitted to the body at that suspension point. Also as the suspension cannot pull the body the force is zero if the net value becomes positive. It is important to note that this can occur if there are significant suspension travel velocities over a bump. For a $+ve$ roll angle ϕ about the longitudinal axis, the anti-roll bar resists the roll motion in proportion to its torsional stiffness. Consequently the outer wheel (rear

right) gets an additional vertical force reaction $k_{arb}\phi/c$ and the same is reduced from the inner (rear left) wheel. The action is such that the roll angle is reduced but the corresponding load transfer due to suspension movement mostly remains the same. The anti-roll bar arrangement in typical commercial vehicles usually adds stiffness whereas only a small amount of damping is added which is ignored in this modeling approach. Another departure from the typical auxiliary roll stiffness modelling is that in full vehicle models, the auxiliary stiffness is added along with the un-sprung masses. Shim and Ghike [104] in a comparison of different models for rollover dynamics studied four wheeled vehicles, observed that ignoring the sprung masses would slightly increase the net roll moment acting on the sprung mass. They also observed an increase in roll angle peaks and lateral load transfer. These assumptions made the model to slightly over predict the lateral load transfer. While computationally less intensive, this model provides significantly accurate results when compared to highly non-linear models of MSC.Adams software of the same vehicle setup. As the primary reason for developing this analytical model was assessing the relative effect of vehicle parameters especially addition of anti-roll bar on rollover limits as well as directional stability of the vehicle hence this model was assumed

sufficient for the study. For simulation, the sequence of calculations as in Figure 2-2 is followed.

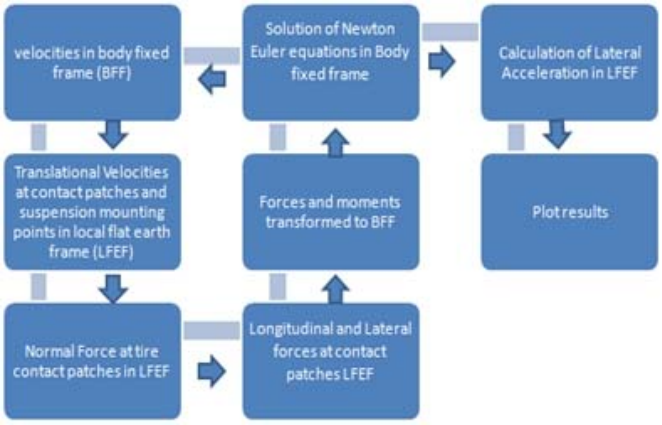

Figure 2-2 Flow chart for calculations

2.1.2 Tire Modelling

The most significant force/moment inputs a vehicle is subjected to while moving on road come from the tire-road contact patches. It is considered the most complex subsystem of the vehicle. There is a large variety of tires used for three wheeled vehicle configurations. For typical tricycle landing gear of aircraft, tubeless radial tires are preferred over bias-ply tires due to better failure properties [105]. A large number of commercial three wheeled taxis use bias ply tires due to the motorcycle platform of which they are derived. Off road ATVs use large tread patterns and are mostly of radial construction. Due to hysteresis in the rubber compound of the tire, resistance to rolling is offered. The ratio between rolling resistance F_r and the vertical load F_z on the tire is known as the *coefficient of rolling resistance* μ_R with a typical value of 0.02 for flat roads[44].

Lateral motion of tire results in direction of travel of the wheel making an angle with the wheel heading. This angle α is known as the slip angle. This results in lateral forces generated at tire contact patch as shown in the Figure 2-3.

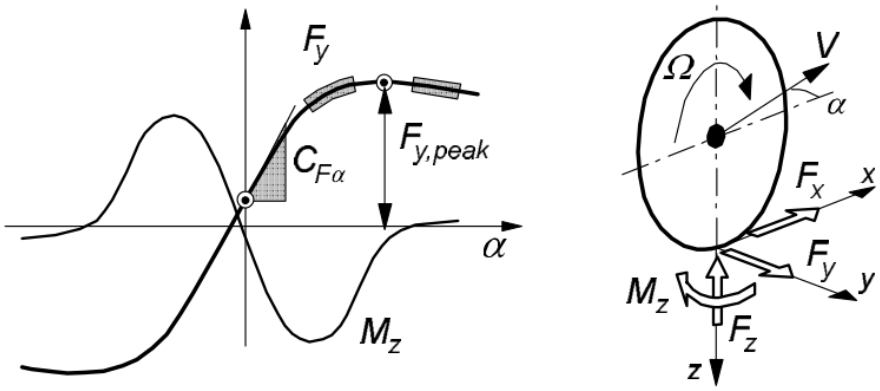

Figure 2-3 Tire Force F_y variation with change in slip angle α

The slip angles at the three contact patches are obtained by first calculating the tire contact patch velocities in the local flat earth frame and then using the relations in equations (2-13)

.

$$\begin{aligned}\alpha_f &= \frac{\dot{y}+a\omega_z}{\dot{x}} - \delta_f \\ \alpha_{rr} &= \frac{\dot{y}-b\omega_z}{\dot{x}-c\omega_z} \\ \alpha_{rl} &= \frac{\dot{y}-b\omega_z}{\dot{x}+c\omega_z}\end{aligned} \tag{2-13}$$

Two main types of tire models are used for vehicle dynamics study: physical models, which use physical parameters to define the relationship between tire forces and kinematics; and empirical models, which use curve fitting of arbitrary models to experimental data. Commonly used physical models include Fiala and Dugoff[106]. These models are based

on the brush model for tire force generation. The most commonly used empirical model was developed by Hans Pacejka [107] and referred to as the Magic Tire Formula.

In this work the lateral forces are calculated using two variants of magic formula and its parameters. The first one is based on the data made available in the work of Gawade et el[59] for three wheeled vehicle used for passenger transport in Asian countries. It would be referred to as Tire-A in the next sections. The relation is as provided in equation(2-14) and the graphical explanation of various parameters is given in Figure 2-3 and Figure 2-4

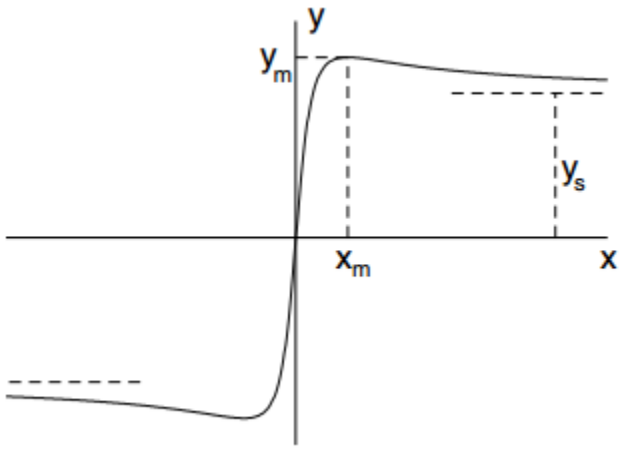

Figure 2-4 Magic formula parameters

$$Y = D\sin(C)\arctan(Bx - E(Bx - \arctan(Bx))) \tag{2-14}$$

The parameter B the stiffness factor, C the shape factor, D the peak factor and the curvature factor E are calculated using eq (2-15) to (2-18). The value of x is the tire slip angle α, and Y is the tire lateral force F_y.

$$B = (CD)^{-1}\left(dY/dx\right)_{x=0} \tag{2-15}$$

$$C = 2 - (2/\pi)\arcsin(y_s / y_m) \tag{2-16}$$

$$D = y_m \tag{2-17}$$

$$E = \frac{Bx_m - \tan(\pi / 2C)}{Bx_m - \arctan(Bx_m)} \tag{2-18}$$

The parameters used are given in Table 1.

Table 1 Tire-A parameters used in Magic formula for Lateral forces[59]

Parameter	$(dy/dx)_{x=0} = C_\alpha$	y_s	y_m	x_m
Value	$C_f = 3885$ N/rad $C_r = 4050$ N/rad	$0.75F_z$	$0.8F_z$	0.175^*

The value of slip angle corresponding to maximum lateral force α_m was not explicitly available. A value of 0.175 radians was used which is typical for such small tire constructions [108] . The resulting behaviour for different values of vertical load is shown in Figure 2-5

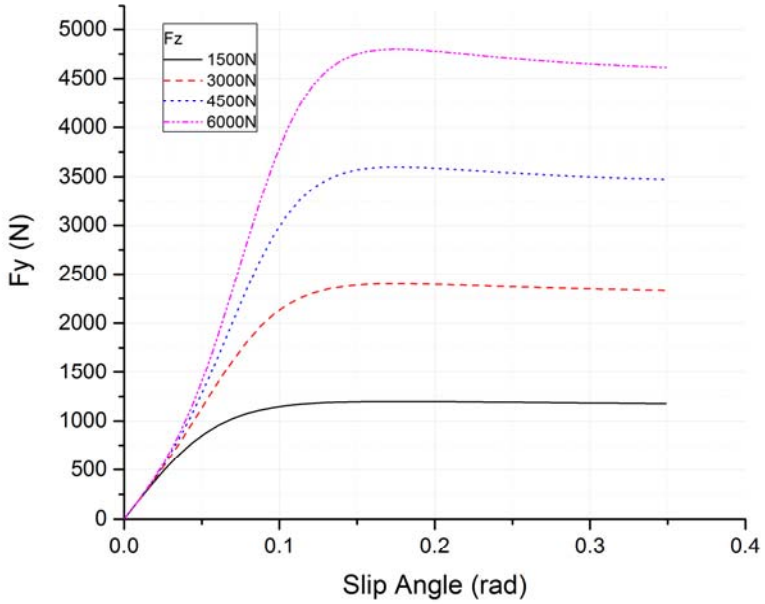

Figure 2-5 Lateral Force plot showing no change in cornering stiffness at low slip angles for tire model A

While encapsulating the major nonlinear behaviour of the tire, this model uses measurable values of physically relatable parameters mentioned in Table 1. The most significant issue with tire represented by this model is that the initial slope corresponding to the linear operating range of a tire is same for different vertical loads. In practice, increase in vertical tire load results in increase of contact area and hence cornering stiffness. The effect of lateral load transfer would not appear before the tire starts to saturate. For a well design three wheeled platform the lateral acceleration that may cause lateral sliding (tire lateral force saturation) is less than the lateral acceleration required for rollover initiation. e.g. tricycle landing gear tires for aircrafts and it is evident from the work of Coetzee [109]. While in common three wheeled vehicles used as taxis, the rollover threshold appears much

earlier than the tire saturation limit on normal dry road conditions. The limit over steer behaviour is also significantly dependent on the tire vertical load sensitivity at low slip angles.

For this work, an eight coefficient generalisation of the Pacejka tire model is used to capture these variations in cornering stiffness at low slip angles and this would be taken as the Tire-B. The formula for this tire model is given in equation (2-19) and the values of coefficients used are given in table Table 2

$$
\begin{aligned}
D_y &= ay_1 F_z^{\,2} + ay_2 F_z \\
BCD_y &= ay_3 \sin(ay_4 \arctan(\mathrm{ay}_5 F_z) \\
B_y &= BCD_y / (C_y D_y) \\
E_y &= ay_6 F_z^{\,2} + ay_7 F_z + ay_8 \\
YY &= (1 - E_y)(\alpha + E_y \arctan(B_y \alpha) / B_y) \\
F_y &= D_y \sin(C_y \arctan(B_y YY))
\end{aligned}
\tag{2-19}
$$

Table 2 Pacejka Coefficients used for Tire model Tire-B

C_y	ay_1	ay_2	ay_3	ay_4	ay_5	ay_6	ay_7	ay_8
1.3	-22.1	1011	1078	1.82	0.208	0.0	-0.354	0.707

The resulting curves for various vertical loads is given in Figure 2-6. As apparent from the figure the dependence of cornering stiffness is more at lower vertical load values this model uses most of its coefficients for typical motorcycle tires.

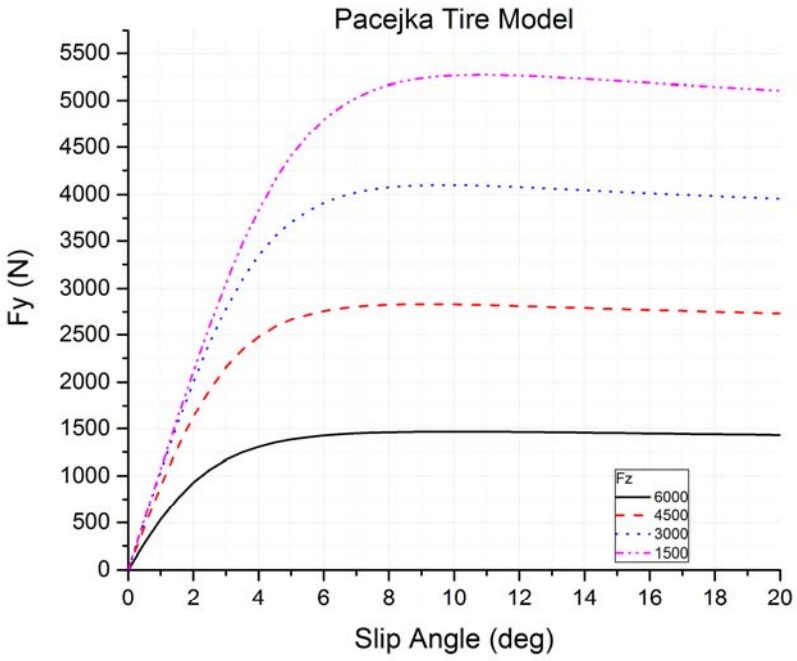

Figure 2-6 Lateral Force plots tire model for Tire-B

The other significant variation required was the variation of lateral force behaviour with changing road friction. A different set of coefficients would be required for different road friction. As the characteristics of the lateral force curve remain the same and only the lateral force curve mainly gets scaled for different values of friction. A known (nominal) behaviour is scaled using similarity method, to account for the effect of various road conditions. There are two variations available for such scaling based upon similarity method. Pacejka [107] used equation (2-20), while Pacejka and Sharp [110] used relation as given in equation(2-21) for scaling lateral force based on friction coefficient value. The subscript '0' is used for reference value for which the parameters are available.

$$F_{y\mu} = \frac{\mu}{\mu_0} F_{y0} \tag{2-20}$$

$$F_{y\mu} = \frac{\mu}{\mu_0} F_y \left(F_z, \frac{\mu}{\mu_0} \alpha \right) \tag{2-21}$$

Another variation at parameter level is as in equations(2-22). For the sake of computational convenience and consistency in results with the nonlinear full vehicle model of CarSim software equation (2-21) would be used as the same equation is used in the software[111].

$$\begin{aligned}
&C_{y\mu} = C_{y0}(5-\mu)/4 \\
&D_{y\mu} = (ay_1 F_z^{\,2} + ay_2 F_z)\mu \\
&BCD_{y\mu} = ay_3 \sin(ay_4 \arctan(\mathrm{ay}_5 F_z) \\
&B_{y\mu} = (2-\mu)BCD_{y\mu} / (C_{y\mu} D_{y\mu}) \\
&E_{y\mu} = ay_6 F_z^{\,2} + ay_7 F_z + ay_8 \\
&YY = (1-E_{y\mu})(\alpha + E_{y\mu} \arctan(B_{y\mu}\alpha)/B_{y\mu}) \\
&F_{y\mu} = D_{y\mu} \sin(C_{y\mu} \arctan(B_{y\mu} YY))
\end{aligned} \tag{2-22}$$

Linear tire model is used for controller development as shown in equation (2-23). The effective cornering stiffness c_α is sensitive to loading and road conditions and needs to be estimated for any particular scenario. In case of significant lateral accelerations an average value is used.

$$F_y = c_\alpha \alpha \tag{2-23}$$

2.2 Test Maneuvers for Rollover Propensity Evaluation

Roll over studies are based upon wheel lift off during a maneuver which is related to zero vertical reaction force for that wheel. Several maneuvers are used to establish dynamic roll over propensity. A detailed comparison of different maneuvers was compiled by Forkenbrock et al [112]. In this study J-Turn and Fishhook maneuvers as proposed by

National Highway Traffic Safety Administration (NHTSA) would be used and are presented in the following sections.

2.2.1 Slowly Increasing Steer (SIS)

In order to characterize lateral dynamics of a ground vehicle, SIS maneuver is based on constant speed with variable steer. Maneuver entrance speed is fixed typically at 50 mph, the hand wheel angle is slowly increased from zero to 270 degrees at a rate of 13.5 degrees per second. The steering wheel is held constant at 270 degrees for two seconds after which the maneuver concludes. It is used for establishing several important handling characteristics including the initial linear and limit handling behavior. The steering profile as given in Figure 2-7 is used.

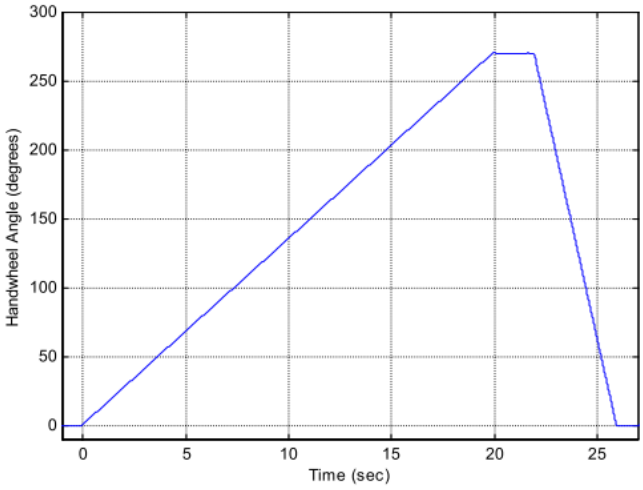

Figure 2-7 Steering Profile for NHTSA Slowly Increasing Steer Maneuver[112]

2.2.2 NHTSA J-Turn Maneuver

A steer angle corresponding to an average linear lateral response is established by using the SIS maneuver. The value of steer angle at which the lateral acceleration is 0.3g is established. A maneuver entrance speed is achieved while driving with zero steer angle on a flat road. The throttle is released and the steering profile in Figure 2-8 is applied. The test is repeated for different maneuver entrance speeds to establish lift-off threshold to establish relative rollover tendency of a tested vehicle.

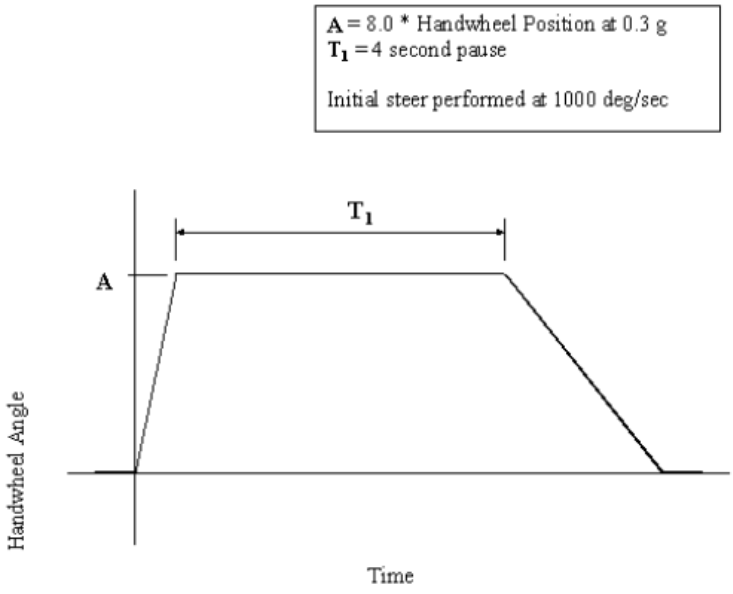

Figure 2-8 Steering Profile for NHTSA J-Turn Maneuver[112]

2.2.3 NHTSA Fishhook Maneuver

As in the J-Turn maneuver the steering angle corresponding to lateral acceleration of 0.3g is established using SIS maneuver. The steering profile as shown in Figure 2-9 is used at different maneuver entrance speed to find out the relative rollover tendency of a test

vehicle. The significant difference is the steering reversal after a dwell time of 250ms once the first ramp steer input is complete.

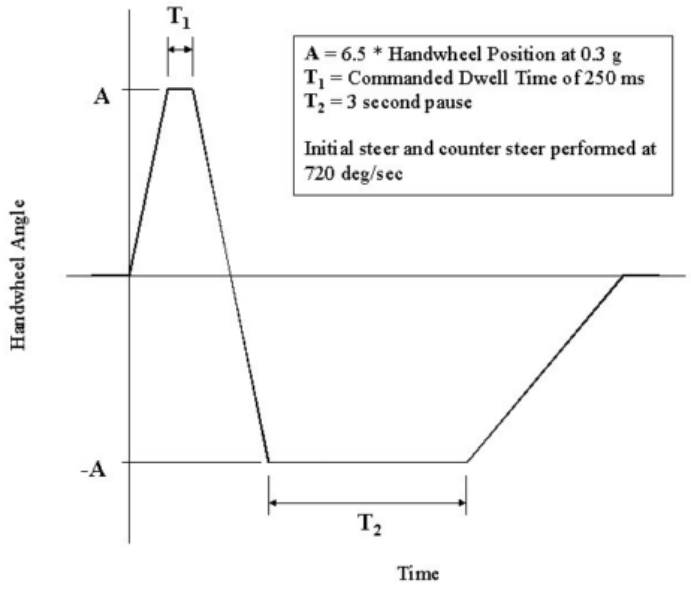

Figure 2-9 Steering Profile for NHTSA Fishhook Maneuver[112]

2.3 Model Validation

A full nonlinear simulation model of a typical TWV was prepared in CarSim software. This includes nonlinear suspension behavior including roll center movements, transient tire force generation etc. The steering input profile for the maneuver is given in Figure 2-10. The steering wheel ratio for such vehicles is 1:1 between steering wheel input and road wheel angle.

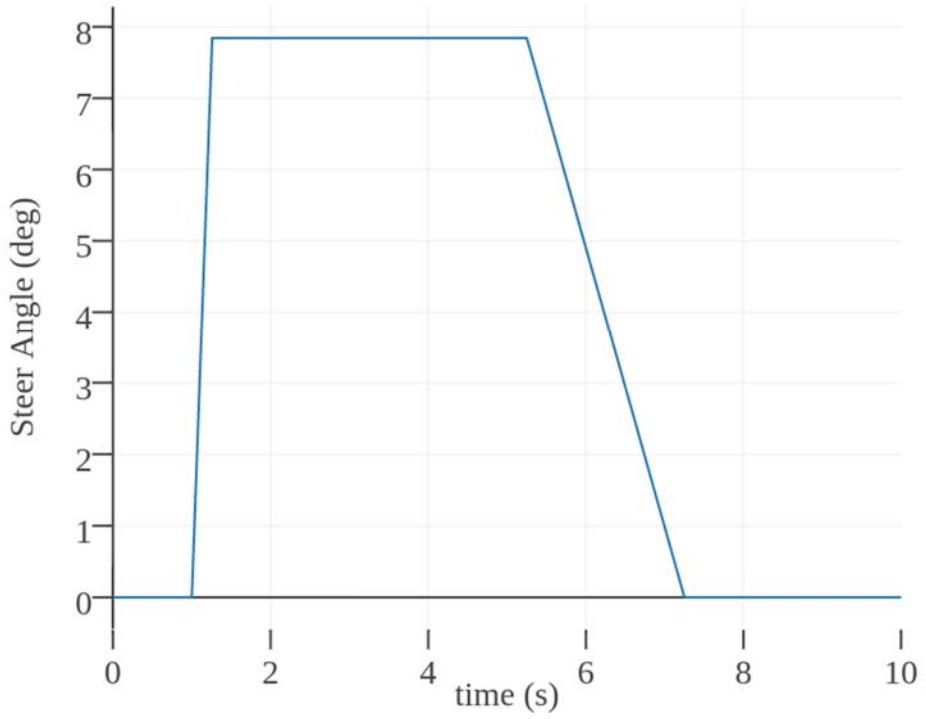

Figure 2-10 Steer profile NHTSA J-turn maneuver

The roll angle of the vehicle during this maneuver is shown in Figure 2-11. The slight difference is due to the nonlinear suspension behaviour which is approximated as linear in the 6dof model. The effect of roll center movement and un-sprung mass also have a significant effect. The results for vertical load of rear right tire during a right hand turn is shown in Figure 2-12. The variations are indicative of lateral movement of sprung mass during the maneuver.

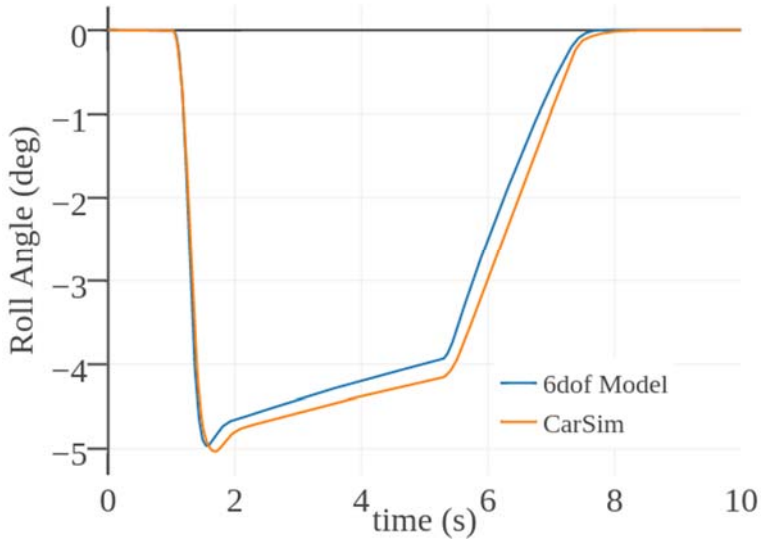

Figure 2-11 Roll angle during NHTSA J-Turn Maneuver

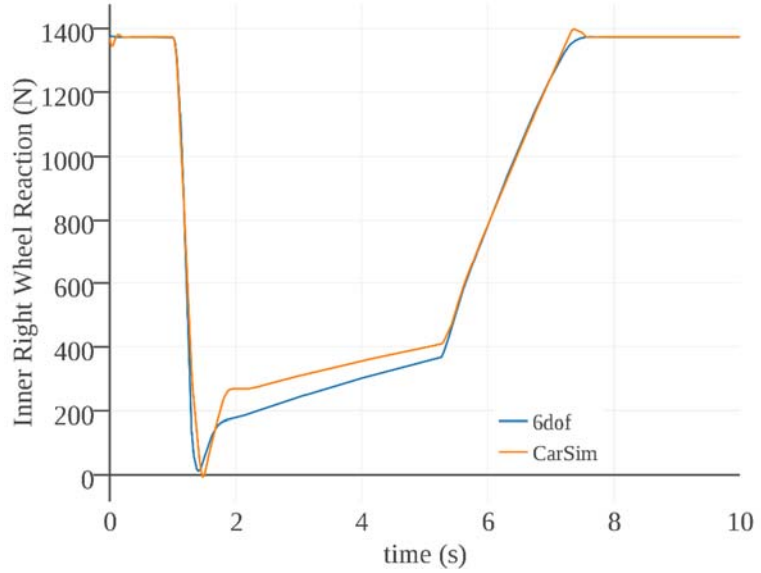

Figure 2-12 Vertical Reaction at the inner right wheel during NHTSA J-turn Maneuver

2.4 2 DOF directional Stability model with lateral load transfer

Lateral stability concerns dominate on low friction surfaces. The roll dynamics approximated by simple load transfer models have been shown to be effective for four wheeled vehicle analysis [113]. This reduces model complexity and computational expense for phase plane study as compared to a complex 6dof model. A planer 2-dof model is developed in this section. Yaw rate $\dot{\psi}$ and vehicle side slip angle β are chosen as states for this planer model as shown in Figure 2-13

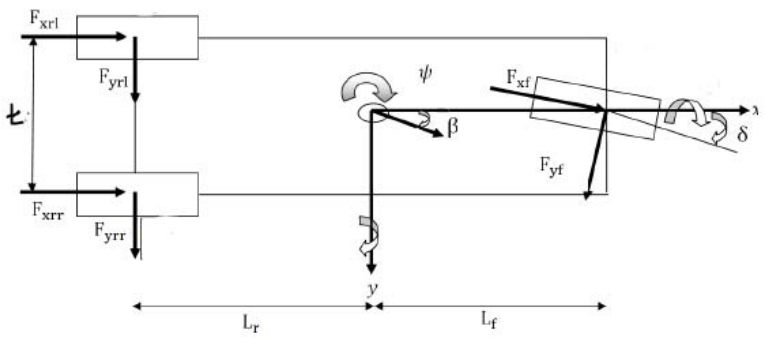

Figure 2-13 2-dof Model for study of vehicles directional behaviour

The Pacejka tire model is used. As both height of cg and track width t effect lateral load transfer therefore tire behavior which is sensitive to vertical load would affect the vehicle response. Wheel loads without considering suspension were considered. The equations governing the motion of the vehicle are shown in equations (2-24)

$$\begin{aligned} \dot{\beta} &= (F_{yf}\cos\delta + F_{yrr} + F_{yrl})/m - \dot{\psi} \\ \ddot{\psi} &= ((F_{yf}\cos\delta)l_f - (F_{yrr} + F_{yrl})l_r)/I_{zz} \end{aligned} \tag{2-24}$$

The relations for tire vertical loads for lateral force calculations are as given in equation (2-25)

$$\begin{aligned} F_{zf} &= mgl_r / l \\ F_{zrr} &= m(gl_f / 2l - 2a_y h / \mathrm{t}) \\ F_{zrl} &= m(gl_f / 2l + 2a_y h / \mathrm{t}) \end{aligned} \tag{2-25}$$

The inclusion of a_y makes the system of equations implicit. Tire lateral forces are calculated using (2-19) with similarity principle to simulate the behavior at low friction surfaces.

2.5 6 DOF TWV Simplified model for Steering based Rollover Mitigation Controller (RMC) Development

With the objective of directly controlling vehicle roll motion based on roll angle, a less complex roll dynamics model with steering input appearing explicitly, is required. To achieve this, a relatively simpler, full vehicle model adapted from [43] is used. Small angle approximations were used neglecting un-sprung mass and roll axis effects. In a typical rollover controller design, roll-yaw motion coupling is exploited to control roll dynamics. As in the work of Chen et al[114] the lateral acceleration, yaw rate and side slip angle is limited to achieve rollover mitigation. Imine et al [115] translate the lateral acceleration corresponding to limiting value of LLTR into a sliding surface. Whereas the model employed in this research enables direct control of roll motion using steering input. The modeling scheme used also facilitates finding equivalent control. A rigid chassis model with six degrees of freedom is used. Un-sprung mass is lumped with the sprung mass.

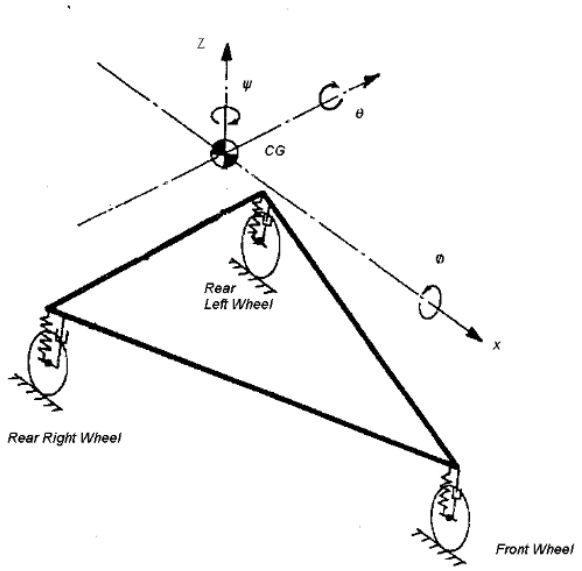

Figure 2-14. Vehicle layout used for 6dof Model for RMC control development.

Using a vehicle fixed coordinate system at the center of gravity as shown in Figure 2-14, equations of motions are derived as given below.

$$\ddot{x} = \dot{y}\dot{\psi} + \frac{P(t)}{m\dot{x}} - \frac{\mu_r}{m}(Fz_{rl} + Fz_{rr} + \mathrm{Fz}_f) - \frac{(Bx_{rl} + Bx_{rr} + Bx_f)}{m} \tag{2-26}$$

$$\ddot{y} = \dot{x}\dot{\psi} + \frac{(Fy_f + Fy_{rl} + Fy_{rr})}{m} \tag{2-27}$$

$$\ddot{z} = -g + \frac{(Fz_f + Fz_{rl} + Fz_{rr})}{m} - \frac{\dot{\phi}\dot{y}}{m} \tag{2-28}$$

$$\ddot{\phi} = \frac{1}{I_{xx}}[b(Fz_{rl} - Fz_{rr}) - (h_0 + z)(\mathrm{Fy}_f + Fy_{rl} + Fy_{rr}) - \dot{\theta}\dot{\psi}(\mathrm{I}_{zz} - I_{yy})] \tag{2-29}$$

$$\begin{aligned}\ddot{\psi} = \frac{1}{I_{zz}}&[b\mu_r(\mathrm{Fz}_{rr} - Fz_{rl}) + b(Bx_{rr} - Bx_{rl}) \\ &+ Fy_f l_f - l_r(Fy_{rl} + Fy_{rr}) - \dot{\phi}\dot{\theta}(I_{yy} - I_{zz})]\end{aligned} \tag{2-30}$$

$$\ddot{\theta} = \frac{1}{I_{yy}}[l_f Fz_f - l_r(Fz_{rl} + Fz_{rr}) + (h_0 + z)(\frac{P(t)}{\dot{x}} - \mu_r \sum Fz - \sum Bx)] \quad \textbf{(2-31)}$$

Linear tire model is used for calculating lateral forces as follows

$$Fy_f = C_{\alpha f}\alpha_f \quad \textbf{(2-32)}$$

$$Fy_{rl} = C_{\alpha r}\alpha_{rl} \quad \textbf{(2-33)}$$

$$Fy_{rr} = C_{\alpha r}\alpha_{rr} \quad \textbf{(2-34)}$$

where $C_{\alpha r}$ and $C_{\alpha f}$ are rear and front cornering stiffness; and the slip angles $\alpha_f, \alpha_{rl}, \alpha_{rr}$ are expressed in terms of vehicle states as follows

$$\alpha_f = \delta_f - \frac{(\dot{y} + l_l\dot{\psi})}{\dot{x}} \quad \textbf{(2-35)}$$

$$\alpha_{rl} = -\frac{\dot{y} - l_r\dot{\psi}}{\dot{x} - b\dot{\psi}} \quad \textbf{(2-36)}$$

$$\alpha_{rr} = -\frac{\dot{y} - l_r\dot{\psi}}{\dot{x} + b\dot{\psi}} \quad \textbf{(2-37)}$$

where δ_f is the front steering angle. The vertical forces on each wheel are calculated as follows

$$Fz_f = Fz_{fi} + K_f(-z + l_f\theta) + c_f(-\dot{z} + l_f\dot{\theta}) \quad \textbf{(2-38)}$$

$$Fz_{rl} = Fz_{rli} + K_r(-z - l_r\theta - b\phi) + c_r(-\dot{z} - l_r\dot{\theta} - b\dot{\phi}) \quad \textbf{(2-39)}$$

$$Fz_{rr} = Fz_{rri} + K_r(-z - l_r\theta + b\phi) + c_r(-\dot{z} - l_r\dot{\theta} + b\dot{\phi}) \quad \textbf{(2-40)}$$

Where subscript i denotes initial static forces; K is the effective suspension stiffness and c is the effective suspension damping as tire characteristics are lumped with the suspension compliance characteristics. It may be noted here that the $-l_r\theta$ and $-l_r\dot{\theta},$ terms unload the rear wheels in breaking and hence reduce the total lateral load transfer required to unload the rear wheels.

The roll dynamics equation in terms of state variables can be written as follows

$$\ddot{\phi} = \frac{1}{I_{xx}}\{(h+z)[-\frac{2\dot{x}(\dot{y}-l_r\dot{\psi})C_{\alpha r}}{(\dot{x}^2 - b^2\dot{\psi}^2)}] - 2b^2(K_r\phi + c_r\dot{\phi})$$

$$-(h+z)[\frac{(\dot{y}+l_f\dot{\psi})C_{\alpha f}}{\dot{x}}] - \dot{\theta}\dot{\phi}(I_{zz} - I_{yy})\} + \frac{(h+z)}{I_{xx}}\delta_f \quad \textbf{(2-41)}$$

Nominal values for parameters l_r, l_f, b, m, l are directly used from previous studies on three wheeled vehicle [43], [57]–[59]. While the parameters $C_{\alpha f}, C_{\alpha r}, h$ are adapted by minimizing a cost function J as given in equation (2-42) , which is the summation of normalized errors of roll angle and roll rate between values obtained from equation (2-41) and CarSim. This ensures that the model used for controller design, represents vehicle behavior with reasonable accuracy.

$$J = \sum \left(\frac{\left| \phi_{CarSim} - \phi_{Model} \right|}{\max \left| \phi_{CarSim} \right|} + \frac{\left| \dot{\phi}_{CarSim} - \dot{\phi}_{Model} \right|}{\max \left| \dot{\phi}_{CarSim} \right|} \right) \quad \textbf{(2-42)}$$

The response in terms of roll angle and roll rate to a step input of 3 degrees at 40 km/hr speed is shown in Figure 2-15.

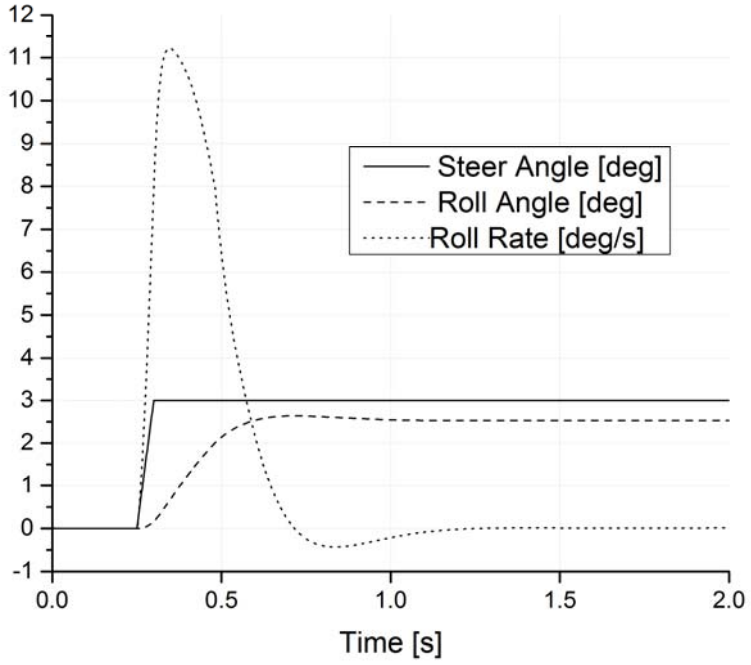

Figure 2-15. Roll angle and roll rate of vehicle resulting from a step steer input of 3 degrees.

The response clearly indicates a delay of almost 0.55 seconds for the roll angle to evolve. Although close to a nominal step input of this type is uncommon in typical road vehicles due to the rate at which an average person can turn the wheel coupled with the reduction in steer angle input from hand-wheel to the road wheel. The steer input rate used in NHTSA

J-turn test is 720 deg/sec, which effectively translates into 36 degrees per second for a typical 20:1 reduction. In the absence of any reduction in the steering system of a common three-wheeled vehicle using motorcycle steering assemblies. A driver when suddenly confronted with an obstacle, impulsively gives a large steering input in a relatively short time, resulting in almost a step steering profile.

2.6 Summary

Analytical model to evaluate the effect of adding anti roll bar on rollover mitigation and handling characteristics of a three wheeled vehicle is developed. Two different tire models, representative of available literature are presented. The most significant difference in the two tire models is their sensitivity to vertical loads at lower slip angles.

To establish handling characteristics a planer model with weight transfer effects has been described. This would help in creating phase portrait of handling dynamics, cost effectively.

A nonlinear model for roll dynamics was also presented which incorporates steering input in the equations for roll dynamics of the vehicle. This enables development of a unique, steering based controller for the roll states of the vehicle.

The roll dynamics lags the steering input. This should be considered while developing control.

CHAPTER 3

ROLLOVER AND DIRECTIONAL CHARACTERISTICS OF DELTA CONFIGURATION THREE WHEELED VEHICLES

In order to establish design guidelines for safer and more agile wheeled vehicles and to assist in controller objective formulation and design, a parametric study of factors effecting rollover tendency and their relation to lateral stability/handling characteristics are required. As described by Metz[116] handling constitutes three important aspects namely resistance to rollover, steady-state behavior, and transient behavior in response to driver inputs and environmental disturbances. Vehicle rollover can be broadly classified into two categories: un-tripped and tripped rollover[117]. Tripped rollovers are caused by vehicle laterally striking an object or due to vertical disturbance on the road or mostly when the vehicle leaves the road. Un-tripped rollover occurs when the moment due to maneuver induced lateral forces overturning the vehicle exceed the restoring moment due to tire forces. Vehicle responsiveness, in a drivers perceptive, is subjective in nature and many metrics have been proposed [118], [119]. Objective measures and combination of objective and subjective methods like in the work of Crolla et al [120] have been used to assess vehicle response to steering inputs. As the primary objective of the study is safety, hence the focus would be rollover and transient behavior leading to rollover and/or instability characterized by skidding of front or rear wheels referred to as limit over steer and understeer behavior in the work of Valkenburgh et al [21] which may lead to tripped rollover or impact due to loss of control. The tadpole configurations tested have demonstrated a limit over steer response while all the delta configurations skid out of a turn signifying limit understeer

even if the initial steady state response of the vehicles was understeering. The directional response and its control as discussed in [22], [63], [121]–[123] have more subjective handling goals, maintaining vehicle steering response close to perceived linear response at relatively low speeds. This adds to actuator energy demands and cost of operation of a vehicle. Significant departure from this linear behavior is observed at limit handling scenarios. Hence parameters that improve rollover resistance are studied for their possible effect on limit handling behavior. Rollover event is described by wheel liftoff on one side of the vehicle. In case of delta three wheeled vehicle, it would be a single rear wheel lifting off the ground. This is in turn is detected by the vertical reaction turning to zero of the corresponding wheel..

The rollover will occur only if the forces generated due to road friction are greater than the inertial forces required to tip over the vehicle. The vehicle would skid or spin at higher speeds while turning before rolling over. This can be considered as a safety margin to rollover as mentioned in [21] to un-tripped rollover only. This may lead to excursions from the road and hence tripped rollover may result. To assess this, a phase plane analysis for lateral stability is used. A phase portrait of physically relatable quantities yaw rate and side slip angle $(\dot{\psi} - \beta)$ is used to assess the lateral stability of TWV of delta configuration with reference to changes in factors effecting rollover at high friction road conditions.

The most significant parameters effecting rollover behavior of the three wheeled vehicle are discussed in the following subsections.

3.1 Effect of Adding Antiroll Bar (ARB) on Rollover Propensity

The model is simulated for changes in stiffness of antiroll bar and evaluated for using NHTSA J-turn maneuver. The baseline used is the one without any auxiliary roll stiffness. The roll angle evolution during this maneuver is shown in Figure 3-1. The reduction in roll angle with increasing ARB torsional stiffness is observed. A slight delay in evolution of roll angle is observed. The reduction in roll angle would be also of a perceptible level for the driver.

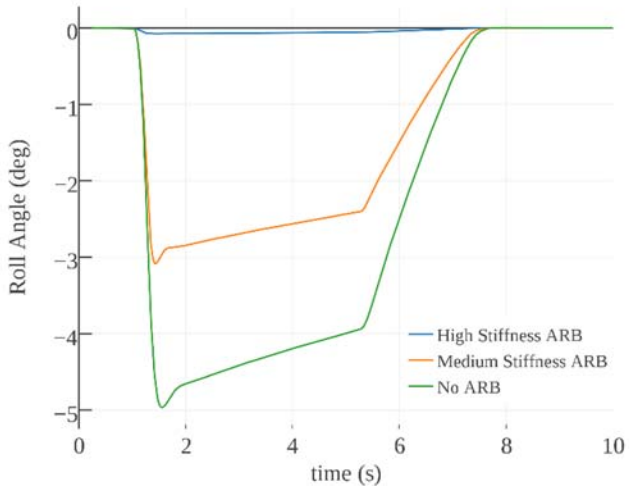

Figure 3-1 Roll Angle during NHTSA J-turn Maneuver using different ARB Stiffness

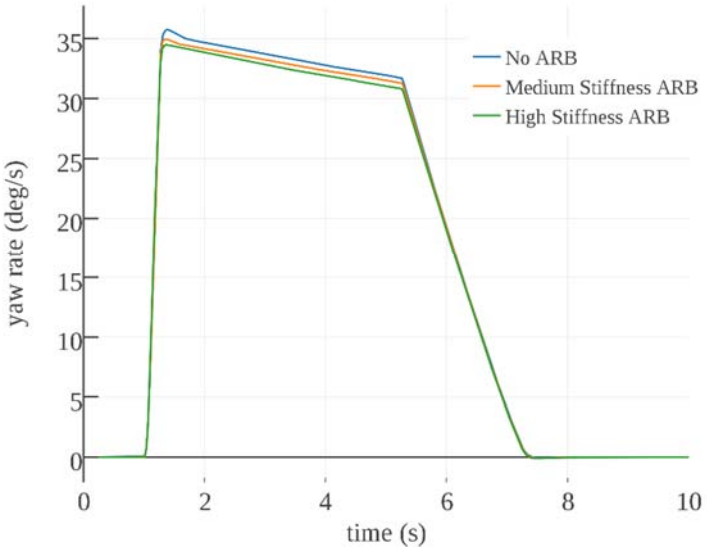

Figure 3-2Yaw rate during NHTSA J-Turn Maneuver with different ARB Stiffness

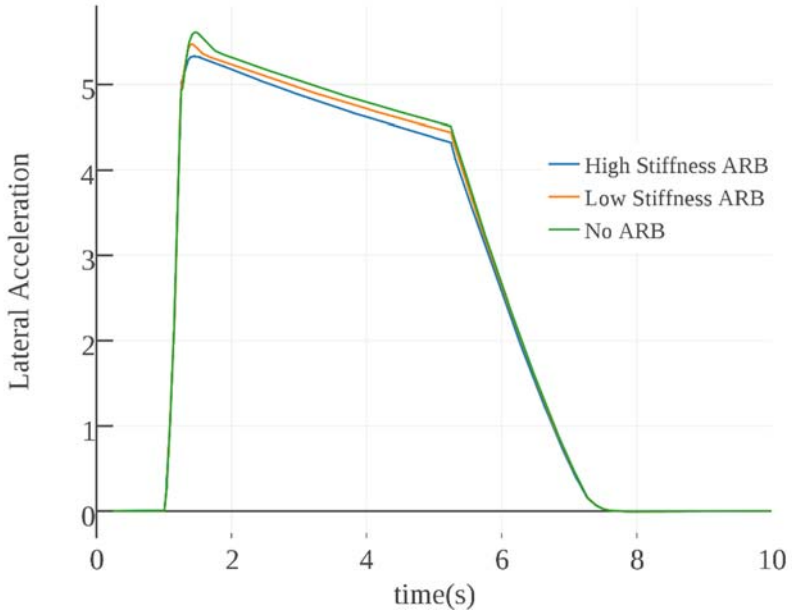

Figure 3-3 Lateral Acceleration during NHTSA J-Turn Maneuver with different ARB Stiffness

The evolution of yaw rate and lateral acceleration is shown in Figure 3-2 and Figure 3-3 respectively. A slight decrease in lateral acceleration and increase in yaw rate is observed

with increase in roll stillness. This can be attributed to reduced lateral motion of the center of mass due to reduced roll motion. This can be interpreted as a slightly tighter turn with reduced lateral acceleration or in other words a quicker directional response of the vehicle with increase ARB stiffness. The lift off of inner wheel changed significantly as shown in Figure 3-4. This would reduce the lateral load transfer, hence rollover propensity for the vehicle by almost 15% in this setup, and that too without effecting the lateral behaviour represented by the comparatively small changes in lateral acceleration and yaw rates. This is possible in four wheeled setups if ARB on front and rear axles are increased in the same ratio as the basic setup else lateral load transfer ratio between front and rear would change resulting in over steer if load transfer is greater at the rear or under steer if load transfer is more at the front. The only drawback is the increased oscillation in the roll motion with increase in torsional stiffness of ARB. This would be felt as a degradation in ride quality of the vehicle. Another documented effect of increased torsional stiffness would appear as less independence of rear wheels i.e. any vertical displacement of one side of the vehicle would be transferred to the other wheel transferring partially to the vehicle. Torsional stiffness maybe set to be one third of the primary roll stiffness as practiced by suspension tuning experts which keeps the independence of wheel in single wheel bumps, reduces body roll while keeping roll oscillations to their minimum. Additional roll damping may be provided to reduce oscillations associated with increased stiffness. Too much roll stiffness will not further reduce lateral load transfer as load transfer associated with vehicle inclination is primarily reduced.

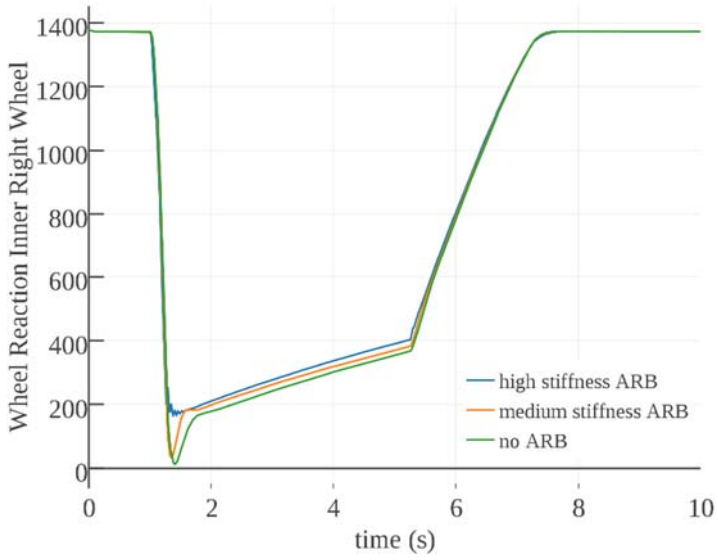

Figure 3-4 Inner Right Wheel vertical reaction during the J-Turn Maneuver with different ARB stiffness

The maneuver entrance speed of 9m/s is used. Road friction is set at 0.2 corresponding to slippery road conditions. Tire model A with significantly low vertical load sensitivity is used. The results shown in Figure 3-5, indicate yaw rate remaining at low values despite large steering input. Vehicle demonstrates a limit understeer behavior. Oscillations in wheel vertical loads with higher ARB stiffness is evident. As the front wheels have saturated before the rear wheels, the vehicle in this condition would 'slide' out of turn with less response to steer inputs, but would not be unstable. This can be seen from the bounded value of all states and returning of the vehicle states to zero with zero steer input later. This is referred to as drift by drivers.

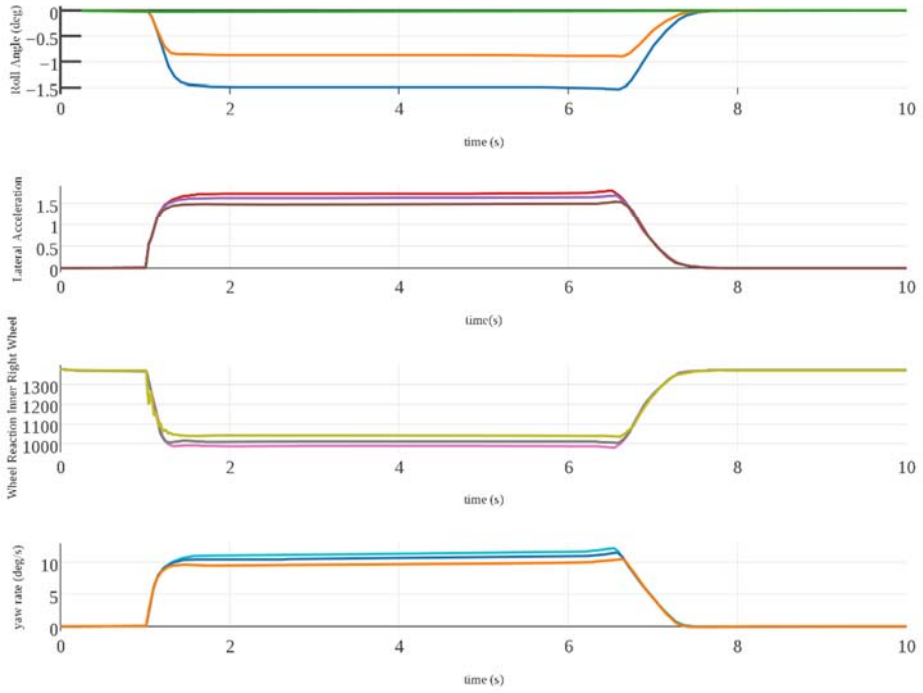

Figure 3-5Vehicle states on low friction surface using tire-A

A more elaborate picture would appear on a phase plane with yaw rate and lateral velocity plotted for a fixed values for longitudinal velocity as shown in Figure 3-7. Phase portraits are representative set of solutions, plotted as parametric curves on a Cartesian plane. Pair of states used for characterization of directional behavior are yaw rate and vehicle side slip [124]–[126] and side slip angle and side slip angle rate [127]. As yaw rate and side slip angle are physically relatable states, hence used in this research work. Three stable equilibria appear. The main stable node corresponding to (0,0) dominates. Stable spirals with very small basins of attraction appear near the corresponding tire saturation behavior. These basins of attraction are more prominent in Figure 3-7 when the state trajectory is

projected on the $\dot{\psi} - v_y$ plane. The max steady state yaw rate depending on front tire coefficient of friction μ_f and is given by equation (3-1) . The limiting value of max steady state yaw rate if applied leaves the probability of only one stable node at $(0,0)$ in less aggressive maneuvers. The vehicle has a predominant understeering behavior even beyond tire saturation.

$$\dot{\phi}_{\max,ss,understeer} = \frac{\mu_f g}{v_x} \tag{3-1}$$

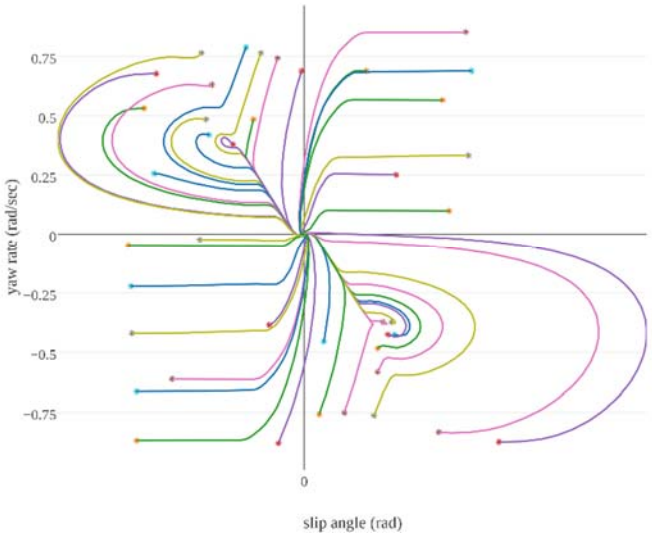

Figure 3-6 State trajectory projection on $\dot{\psi} - \beta$ plane on low friction road with Tire-A using zero Steer input and no ARB

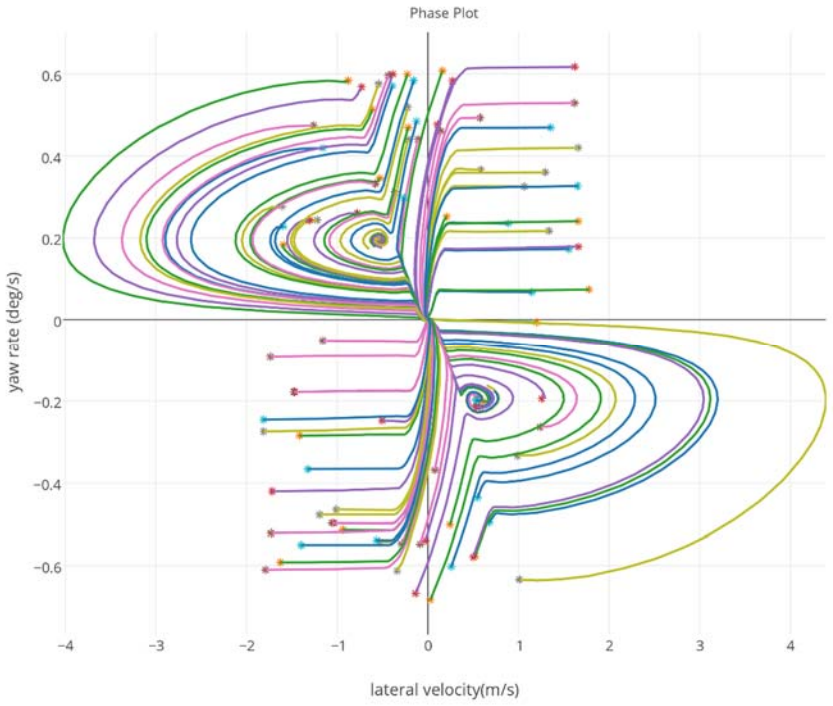

Figure 3-7 State trajectory projection on $\dot{\psi} - v_y$ plane on low friction road with Tire-A using zero Steer input and no ARB

With increase in steer angle the stable middle stable node move to the corresponding limit in yaw rate and removes the small basin of attraction for limit over steer. The other unstable equilibrium corresponds to a counter steer input with yaw rate is in the negative direction with positive side slip as shown in Figure 3-8.

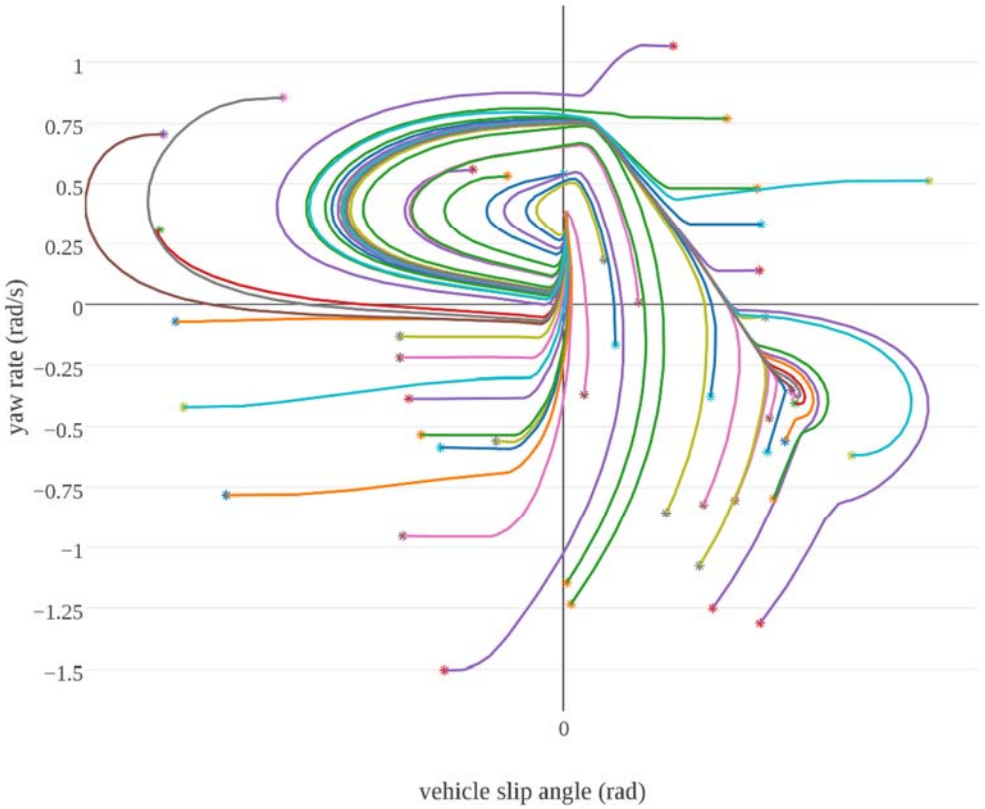

Figure 3-8 Phase portrait at 10deg steer angle at low friction road surface with no ARB

With increased ARB stiffness the phase portrait for zero steer is as shown in Figure 3-9. The unstable nodes are more prominent in the projection of state trajectories on the $\dot{\psi} - v_y$ plane as shown in Figure 3-10. The only significant change is that along with the dominant attracting stable node, two unstable spiral equilibrium points near the tire saturation limit given by equation(3-1). This signifies a small domain of limit over steer. The limit over steer behavior is not maintained for long and the vehicle easily recovers and under-steer behavior dominates the state space. When using such tires possibility of an oscillating behavior of vehicle entering into an over-steer instability and recovering may appear. The

vehicle states with 10^{o} steer angle is shown in Figure 3-11and Figure 3-10. A stable under steer behavior dominates the plausible state space. This is due to the yaw rate limited by the front tire saturation. The vehicle would not be following the driver's intent still is considered as a stable state. A rear wheel braking intervention can help recover from this situation easily.

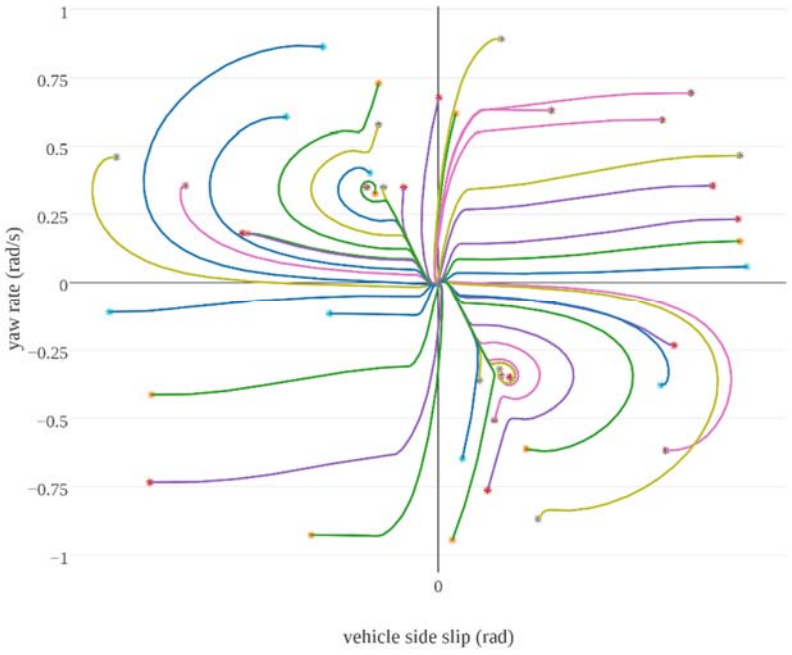

Figure 3-9 State trajectory projection on $\dot{\psi} - \beta$ plane on low friction road with Tire-A using zero Steer input and High stiffness ARB

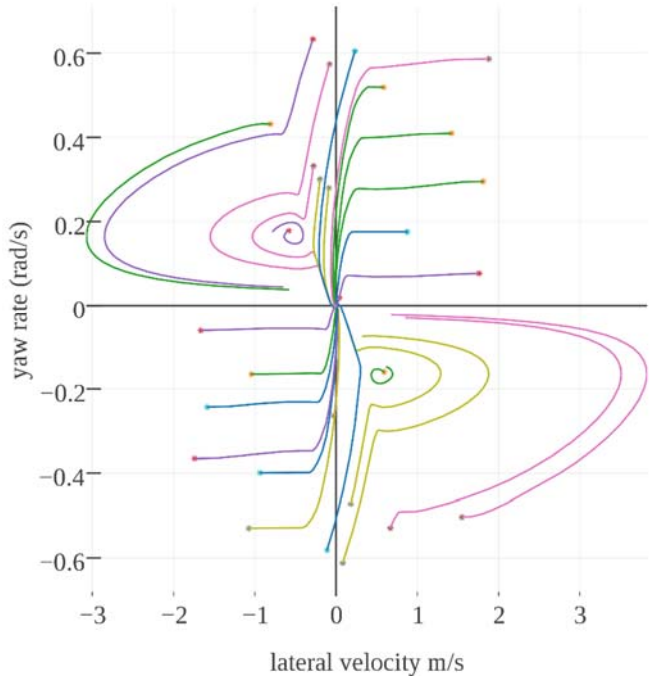

Figure 3-10 State trajectory projection on $\dot{\psi} - v_y$ plane on low friction road with Tire-A using zero Steer input and High stiffness ARB

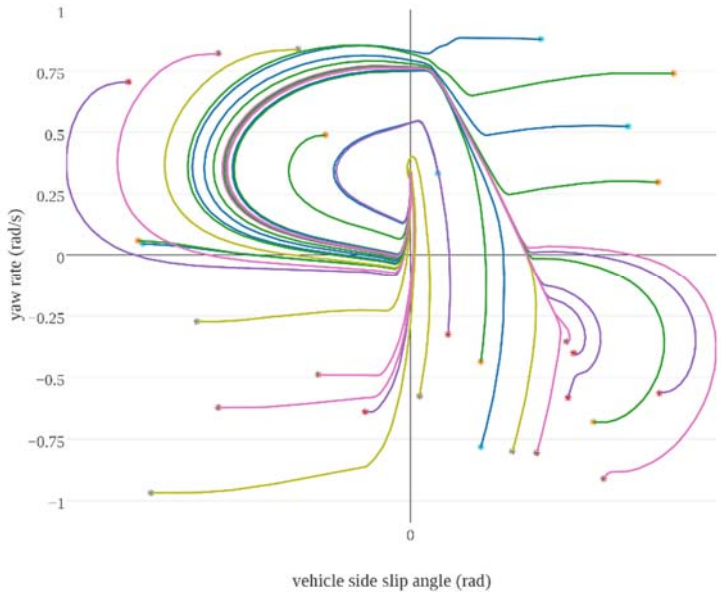

Figure 3-11 State trajectory projection on $\dot{\psi} - \beta$ plane on low friction road with Tire-A using 10 degree Steer input and High stiffness ARB

When the same vehicle is simulated using tire model B (which has more lateral stiffness sensitivity at lower slip angles to vertical load) limit over-steer is evident from Figure 3-12, which shows evolution of yaw rate in a slowly increasing steer maneuver keeping vehicle speed constant. The vehicle does not show a distinct over steer limit but it starts to spin out at 12secs, but recovers then finally it spins out again for a significant instability. The reason for this is primarily the torque variation at the rear wheel to compensate for loss of longitudinal speed during spin out. The phase portraits with yaw rate and side slip angle as the states would be projections of the state trajectory on this plane.

The phase portrait for TWV with tire-B without ARB, keeping front wheel straight (zero steer) is shown in Figure 3-13. The appearance of a stable node at $(0,0)$ and two unstable saddle nodes are typical of limit over steer behavior. The intersection of projected state trajectory indicates energy transfer between modes of motion represented by states other than represented by yaw rate and side slip. Typically the roll of sprung mass is not in phase with the yaw motion in transients and planer and roll motions exchange energy.

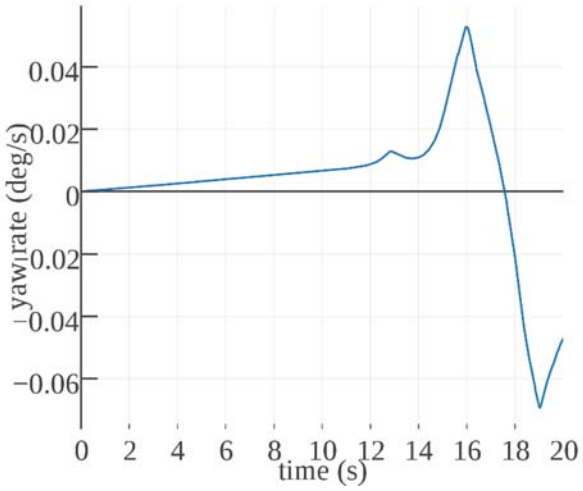

Figure 3-12Yaw rate for TWV with tire-B on low friction road surface when subjected to slowly increasing steer at constant vehicle speed

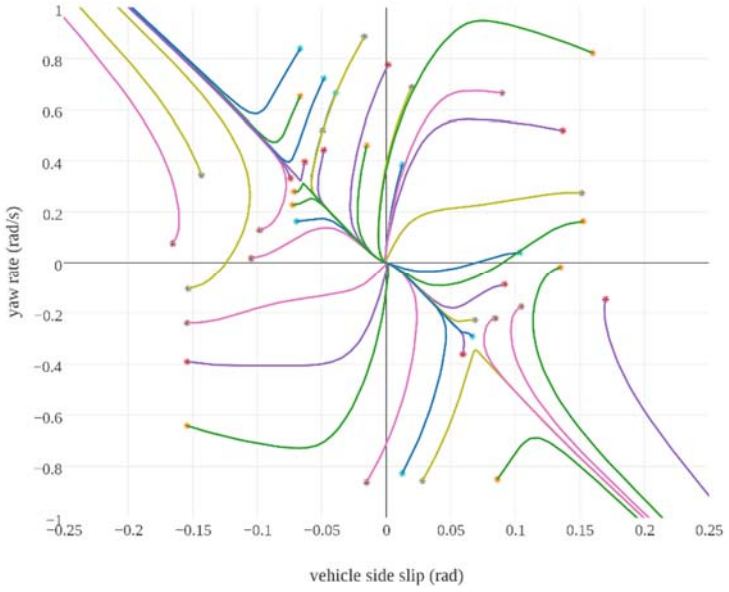

Figure 3-13 State trajectory projection on $\dot{\psi} - \beta$ plane on low friction road with Tire-B using zero Steer input and no ARB

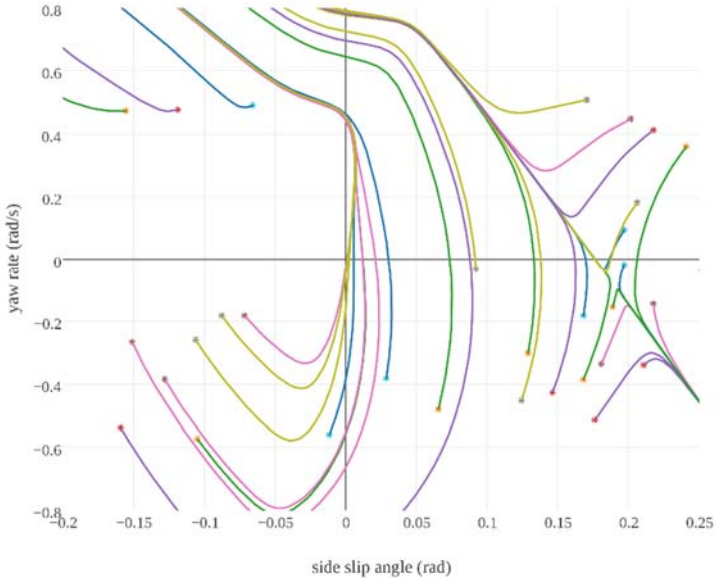

Figure 3-14 State trajectory projection on $\dot{\psi} - \beta$ plane on low friction road with Tire-B using 10 deg Steer input and no ARB

With increasing steer angle the stable middle node approaches the corresponding unstable node and then they both collide and disappear. The projection of state trajectories on $\dot{\psi} - \beta$ plane is shown inFigure 3-14. The plot shows a single unstable saddle equilibrium point in the plausible range of state variables and a general instability is corresponding to over steer behavior. For higher lateral velocities opposite in sign to yaw rate of smaller magnitude, the vehicle initially drifts laterally before spinning out.

With this tire behavior if ARB of higher stiffness is incorporated, the projection of state trajectories for a zero steer angle is given in Figure 3-15. The nature of equilibrium points do not change, however the side slip angle limit for instability increases slightly. Yaw rate is still limited by the tire adhesion limit. Reduced rollover motion results in relatively fewer intersecting projections.

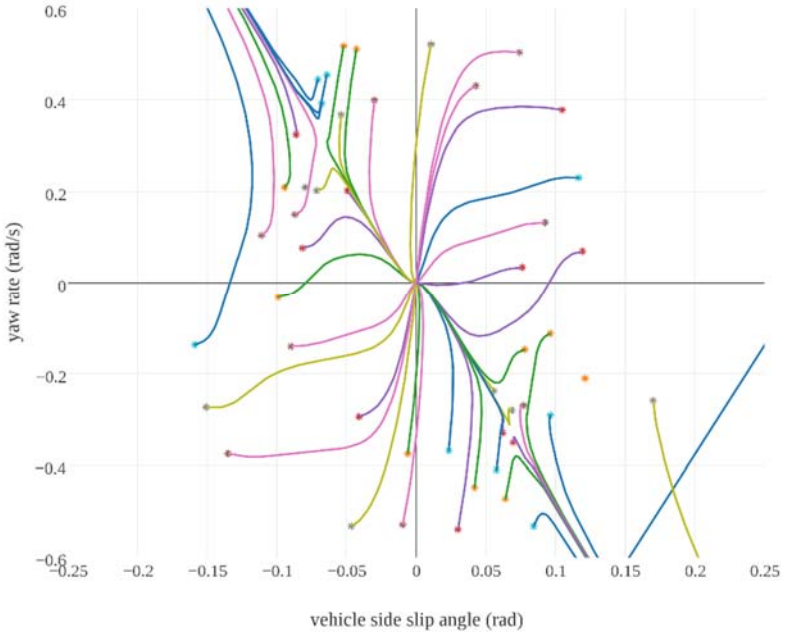

Figure 3-15 State trajectory projection on $\dot{\psi} - \beta$ plane on low friction road with Tire-B using 10 deg Steer input and High Stiffness ARB

It can be concluded that with the two distinct tire behaviors based on vertical load sensitivity at low slip angles, result in different directional behavior in transient maneuvers. The addition of an ARB would slightly increase the side slip angle limit on low friction roads, hence a small improvement in handling behavior. The real advantage of adding an ARB would be increased rollover threshold on high friction roads. Based upon majority of single chassis, non-tilting delta three wheeled vehicles tested and reported [21], [64], [66], [67] limit over-steer dominates and chances of spinning out of control on relatively low adhesion roads increase which, may result in a tripped rollover apart from high possibility of collision with other vehicles causing serious damage. A directional stability control augmentation would be essential in preventing such rollovers.

3.2 Effect of Factors Effecting Rollover Propensity on Directional Stability

Passive parameters effecting rollover tendency of a three wheeled vehicle has been studied by several researchers [21], [43], [128]. The effects can be summarized as given in Table 3. The effect of such changes on directional behavior is not established for a three wheeled setup. The planer 2-dof model developed earlier for establishing this relationship is used. Yaw rate $\dot{\psi}$ and vehicle side slip angle β are chosen as states for this planer model as shown in Figure 3-16

Table 3 Factors effecting roll over resistance

	Parameter	Effect on Rollover
1	Track width	Rollover resistance increases with increase in track width
2	cg height	Rollover resistance increases with decrease in cg height
3	Longitudinal location of cg w.r.t. rear axle	Rollover resistance increases with cg located closer to the rear axle
4	Increasing suspension stiffness (with or without ARB)	Roll over resistance increases. The beneficial effect diminishes with increasing stiffness.

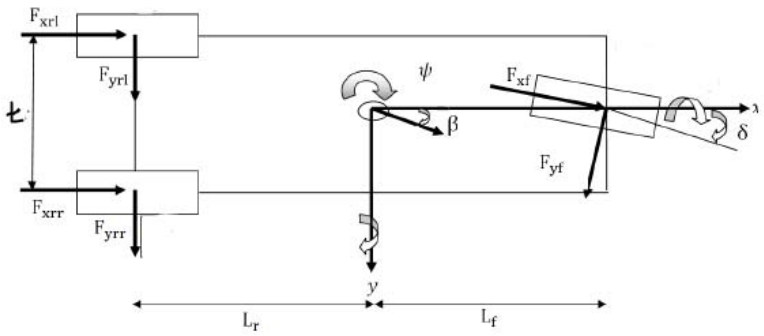

Figure 3-16 2dof Model for study of vehicle directional behaviour [122]

The tire model B resulting in spin out in earlier full vehicle model analysis was used. As both, height of cg and track width t effect lateral load transfer therefore tire behavior which is sensitive to vertical load would affect the vehicle response. Wheel loads were considered without suspension effects. Tire lateral forces are calculated using (2-19) with similarity principle to simulate the behavior at low friction surfaces. The base line phase portrait is shown in Figure 3-17 at zero steer angle. The value of friction was kept sufficiently high to make the vehicle slide before rollover while making maximum lateral load transfer to enhance the effects of factors effecting this load transfer. The presence of stable node at (0,0) and two saddle nodes are noticeable. This behavior is typical of an over-steering vehicle. This resulted in a saddle node bifurcation at higher speed and steer angles as discussed in [113] and might result in unstable limit cycles as in [129]. These bifurcations and post bifurcation behavior is not considered in detail as the primary focus is to understand and extend the handling limits of the three wheeled vehicle when operated over low friction roads and to define thresholds for controller actuation. The same concept has been utilized by researchers like Bobier [126] to define vehicle operational envelope.

The effect of different parameter variations which have a positive effect on rollover resistance are presented in the following sections using phase portraits.

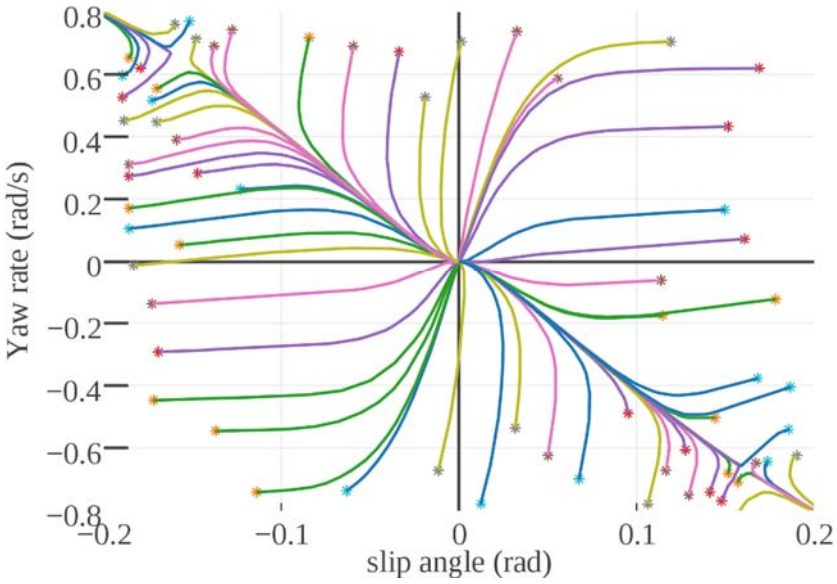

Figure 3-17 Phase portrait of baseline vehicle

3.2.1 Increase in track width

An increase in track width increases rollover resistance. To study its effect on directional behaviour, the track width was increased by 25% of its base value, and the corresponding phase plane trajectories are presented in Figure 3-18. The presence of equilibrium points and their stability does not change in the plausible limits of phase plane. However there is an increase in the domain of attraction as the unstable saddle nodes move away from the middle stable node. Hence increase in track width would result in improved directional stability of the vehicle. The increase in restoring moment due to ground reaction resisting roll motion increases linearly with increase in track width.

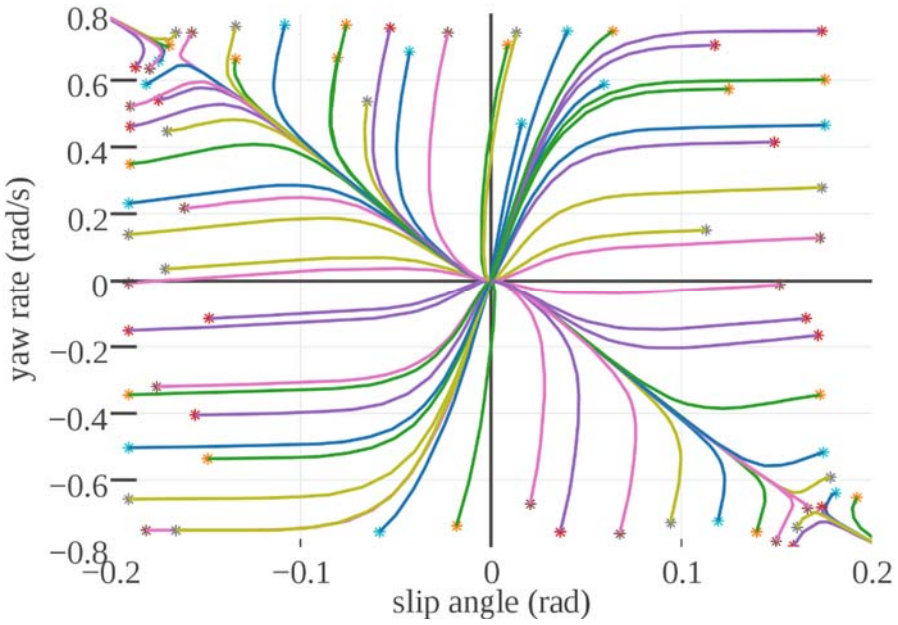

Figure 3-18Phase plot of vehicle at low friction road with zero angle and track width increased by 25% of the base vehicle parameter

3.2.2 Effect of decrease in height of center of gravity

Decrease in center of gravity height was done by 25% and the resulting behaviour is represented in Figure 3-19. Again there is no qualitative change in the behaviour of the vehicle. The location of saddle points moved away, increasing the domain of attraction for the stable node in the middle. This increase is almost of the same order as that resulting from increase in the track width.

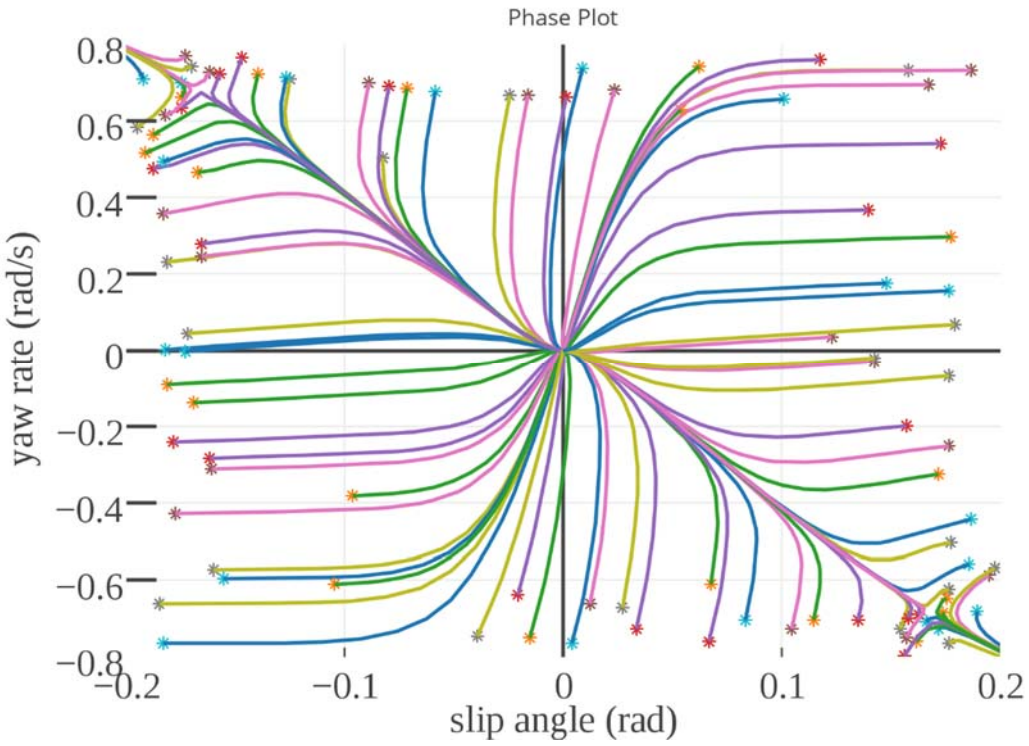

Figure 3-19 Vehicle states for height of cg reduced by 25 % of the base vehicle parameter

3.2.3 Effect of moving the cg rearward

The most significant rollover behaviour departure of a three wheeled vehicle from a four wheeled vehicle results from moving the center of gravity to the axle with two wheels. For a four wheeled vehicle this has no direct effect on the rollover propensity but over steer effect starts to dominate. The trajectories projected on the yaw rate – slip angle plan is shown in the Figure 3-20. The rear to forward axle distance from cg has a 80:20 bias and is changed to 95:5 setup. This has a very significant effect on the directional behaviour of the vehicle as compared to change in track width and cg height. The domain of attraction of the stable node is comprised more of one dominating Eigen direction aligned with the

unstable saddle points. The unstable nodes although have drifted away more in side slip direction, indicating that the vehicle is able to return to the stable equilibrium point from larger slip angles. This is can be attributed to the tire vertical load sensitivity characteristics. To further investigate this effect, the location of cg was moved forward. The results are shown in Figure 3-21

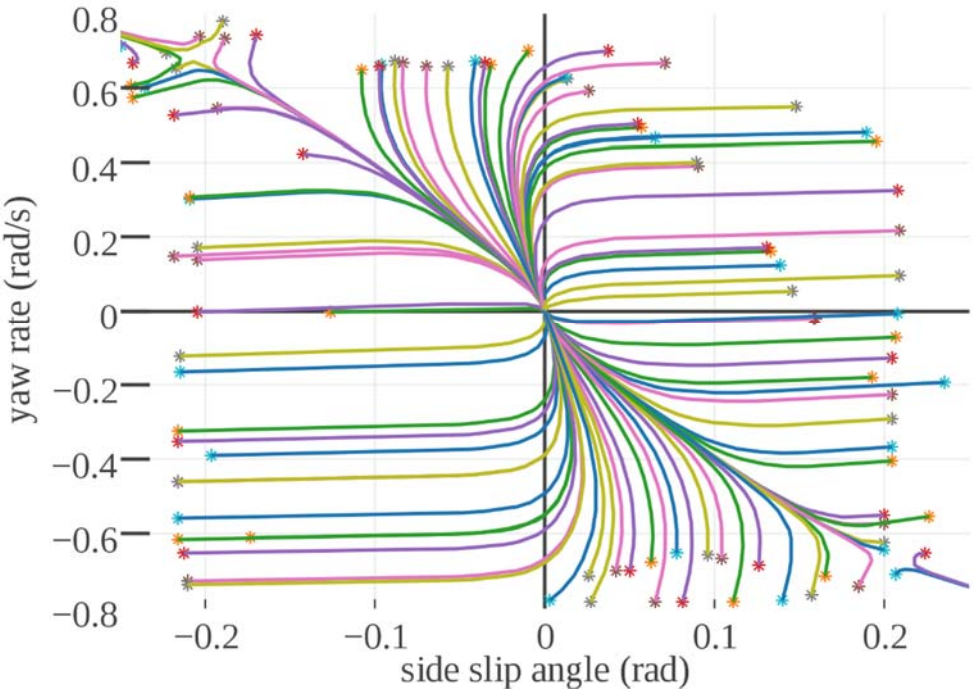

Figure 3-20 State trajectories for 95:5 l_f, l_r ratio with zero steer angle

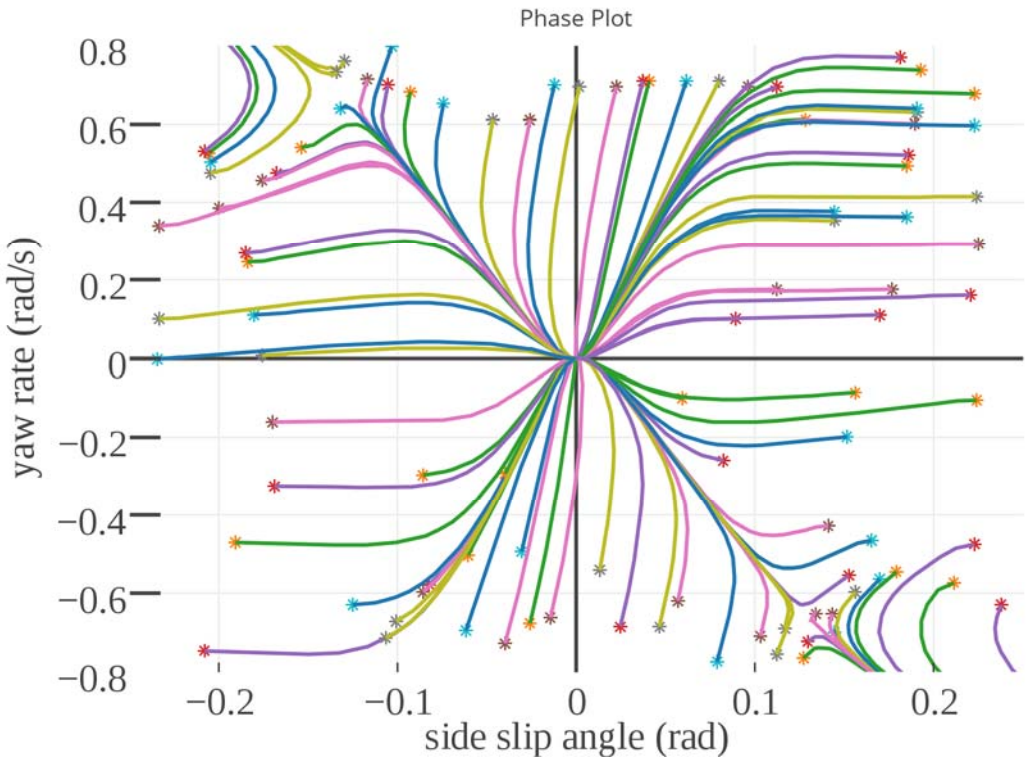

Figure 3-21 State trajectories for 50:50 l_f, l_r ratio with zero steer angle

A clear limit over steering exists with both eigen directions for the stable node are equally attracting. This would result in recovery of both yaw rate and side slip angle with the same speed in the domain of attraction of the stable node. The domain of attraction is reduced with the unstable saddle nodes moving closer to the yaw rate axis.

Further moving the cg towards the front would compromise the rollover resistance. A 40:60 rear front weight split would have state trajectories possible only for small value of road friction so that the vehicle could slide for limiting handling behaviour without over turning first. The results are shown in Figure 3-22. The two saddle nodes have disappeared and the middle stable node turned into a stable node. This implies limit understeering behaviour of the vehicle. Such behaviour would be at the cost of rollover stability which

would imply that this limit understeer behaviour would be achievable only at very low road friction conditions else the vehicle would rollover at very low lateral accelerations.

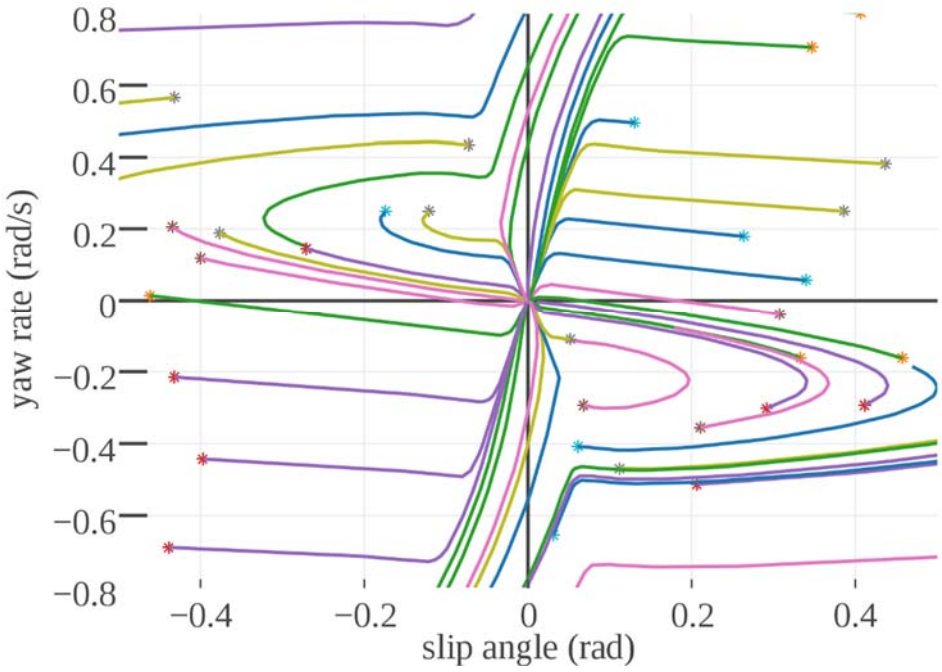

Figure 3-22 state trajectories for 40:60 rear/front weight distribution with zero steer angle

3.3 Conclusions

The effect of various parameters on the rollover propensity and directional behaviour of the three wheeled vehicle can be summarized as follows

- Addition of an ARB increases rollover resistance with very minor effect on directional behaviour. This is attributed to the absence of roll stiffness distribution between front and rear effecting lateral load transfer distribution.

- Increase in track width and reduction in height of cg from ground increases rollover resistance. There is less corresponding improvement in handling.
- The changes in directional behaviour become significant only on low friction road, otherwise the behaviour is dominantly under steering.
- Tire vertical load sensitivity has a significant effect on directional behaviour. A moderately sensitive tire would always lead to a limit over steer condition. Relatively large tires with low to negligible vertical load sensitivity always under steer at handling limits.
- Moving the center of gravity rearward has the most significant effect on side-slip stability. The range and rate of recovery to equilibrium becomes higher for slip angle perturbations as compared to yaw rate perturbations.
- Moving the cg forward would ensure limit understeer behaviour but only on very low friction roads. The rollover resistance would be reduced significantly. The vehicle would rollover much before any limiting directional response starts.

As an under steering behavior is not considered as an instability and an average skilled driver can adjust vehicle response by applying corrective steer input and/or braking. This behavior is related to the steer-ability of the vehicle. A desired under steer response can be achieved using a controller reducing the burden on the driver for corrective actions, hence would be more of a subjective intervention. Limit over steering vehicle will spin out too quickly and it would be too difficult for even a skilled driver to recover on his own. The vehicle can only be recovered from this instability with the help of active control elements.

Un-tripped roll over which is primarily maneuver induced and as discussed earlier, results from driver judgment errors or negligence. A roll over mitigation system becomes necessary to prevent such accidents.

3.4 Identification of control objectives

Based on the rollover tendency and directional behaviour of the vehicle, the primary and secondary control objectives are defined as in Table 4 with priority level indicated. The primary objective is to mitigate rollover. The fidelity of vehicle response to driver steering command is more subjective therefore steer ability interventions is given a low priority.

Table 4 Identification of control objectives

Control Objective		Priority
Primary	a. To prevent maneuver induced un-tripped rollover at higher lateral accelerations	Very High
	b. To prevent vehicle from entering into limit understeer and over steer behaviour on low friction roads	High
Secondary	a. Minimum effect of longitudinal dynamics of the vehicle	Low

The most vulnerable vehicle configuration depending upon number of vehicles involved and fatalities is the three wheeled taxi used in the developing countries. These vehicles still do not have any electronic stability equipment. Majority of the vehicles have a limit over steer behaviour on low friction roads. The limit under steer behaviour is managed using

brake based direct yaw control. Controller design, actuation thresholds of individual controllers is discussed in the following chapters.

CHAPTER 4

ROLLOVER MITIGATION CONTROLLER BASED ON ACTIVE FRONT STEERING

Development of a steering based rollover mitigation controller is presented in this chapter. The three wheeled vehicle in delta configuration at higher lateral acceleration typically has one or both the rear wheels near saturation. A Steering controls have been used to prevent rollover. These actuators generally have less latency and are available for larger bandwidths than the brake actuator [130]. Decrease in rollover resistance of three wheeled vehicles when brakes are applied also favors active front steering for rollover prevention. Considering robustness and simplicity, sliding mode control technique has been used.

4.1 Sliding Mode Control

Vehicle behaviour is nonlinear and subject to heavy uncertainties. The most frequently varying and uncertain phenomenon is the tire road interaction. Sliding mode control (SMC) utilises discontinuous control action to reach and remain on a surface defined in the state space. This surface represents a constraint on a subset of system states, possibly with some desired dynamics. State trajectories when confined to this surface, appear to be 'sliding' on the prescribed 'sliding surface', as shown in Figure 4-1 which gives the name to this technique. This motion has two major advantages: firstly the system has a reduced order dynamics as compared to the original system: and secondly the dynamics on this surface is insensitive to matched uncertainties and perturbations. These uncertainties and perturbations could be due to un-modeled dynamics, parameter variations, state estimation errors and external bounded disturbances. Sliding mode control technique has also gained

prominence amongst several robust control techniques (Adaptive, LMI, H_∞ etc.) as it yields low complexity laws which are more suitable for implementation in electronic stability control units of a vehicle[131]. Simpler, lower order models can be used to design controllers that perform well despite parameter variations, un-modeled dynamics and other uncertainties. Based on these properties SMC technique would be used in this thesis to investigate rollover mitigation using active steering and brake based systems.

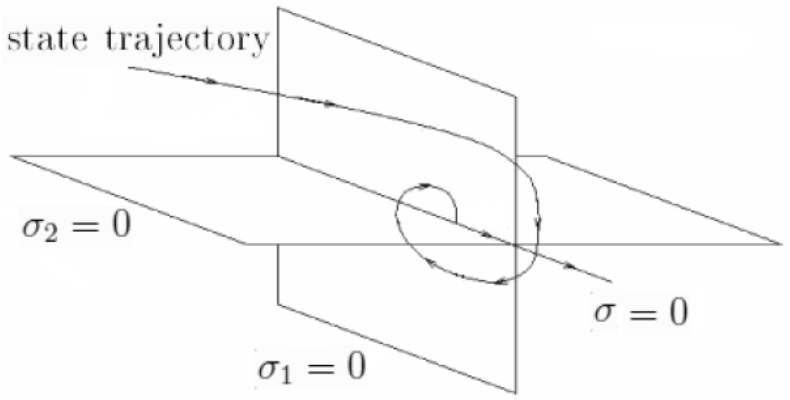

Figure 4-1State trajectories reaching and then staying on the manifold described by $\sigma_i = 0$ constraints

The design process can also be divided into two significant phases.

I. Design or selection of constraints or sliding surface such that the controlled plant has a desired dynamics when confined to the sliding manifold

II. Design of a discontinuous law that forces the state trajectories towards this manifold and keeps it there.

A general nonlinear system with affine control input is represented in equation(4-1), where $x(t) \in \mathbb{R}^n, u(t) \in \mathbb{R}^m$, $f(t,x) \in \mathbb{R}^{n\times n}$, and $g(t,x) \in \mathbb{R}^{n\times m}$. The discontinuous feedback $u(t)$ is used.as in equation (4-2),

$$\dot{x} = f(t,x) + g(t,x)u(t) \tag{4-1}$$

$$u_i = \begin{matrix} u_i^+(t,x), & \text{if } \sigma_i(x) > 0 \\ u_i^-(t,x), & \text{if } \sigma_i(x) > 0 \end{matrix} \quad i = 1,2,....,m \tag{4-2}$$

where $\sigma_i(x) = 0$ is the i-th sliding surface and the sliding manifold which is $(n-m)$ dimensional and is defined as

$$\sigma(x) = \left[\sigma_1(x), \sigma_2(x), ..., \sigma_m(x)\right]^T = 0 \tag{4-3}$$

With a proper definition of sliding manifold the existence of sliding motion requires that the trajectories in some vicinity of the manifold are attracted towards the manifold. This can be ensured using the concepts of generalised stability as outline in the Lyapunov's second method[132]. A domain D in the manifold $\sigma = 0$ is a sliding mode domain if for each $\varepsilon > 0$, there is $\delta > 0$, such that any motion starting within a n-dimensional vicinity of D may leave the n-dimensional vicinity of D only through the n-dimensional δ-vicinity of the boundary of D as shown in Figure 4-2 . The existence is then established using theorem 2.1.[133]

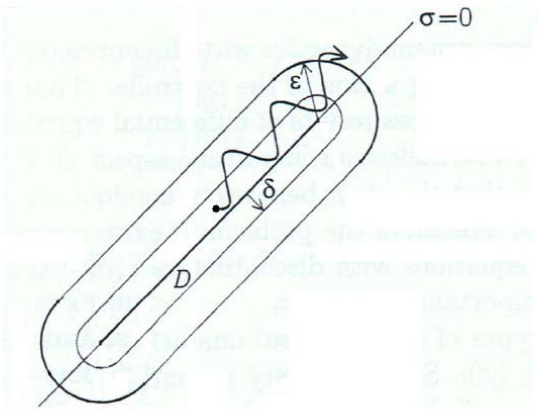

Figure 4-2 Sliding mode domain

Theorem 2.1 *For the (n-m)-dimensional domain D to be the domain of a sliding mode, it is sufficient that in some n-dimensional domain* $\Omega \supset D$*, there exists a function* $V(t,x,\sigma)$ *continuously differentiable with respect to all of its arguments, satisfying the following conditions:*

i. $V(t,x,\sigma)$ *is positive definite with respect to* σ *, i.e.,* $V(t,x,\sigma)>0$*,with* $\sigma \neq 0$ *and arbitrary t,x and* $V(t,x,\sigma)=0$*; and on the sphere* $\|\sigma\| = \rho$*, for all* $x \in \Omega$ *and any t, the following relations hold*

i. $\inf_{\|\sigma\|=\rho} V(t,x,\sigma) = h_\rho, \quad h_\rho > 0$

ii. $\sup_{\|\sigma\|=\rho} V(t,x,\sigma) = H_\rho, \quad H_\rho > 0$

where h_ρ *and* H_ρ*, depend on* ρ $\quad (h_\rho \neq 0 \text{ if } \rho \neq 0)$

ii. The total time derivative of $V(t,x,\sigma)$ *for the system (2.1) has a negative supremum for all* $x \in \Omega$ *except for x on the switching surface where the*

control inputs are undefined, and hence the derivative of $V(t,x,\sigma)$ *does not exist.*

A suitable Lyapunov function $V(t,x)$ used for single input systems is as in equation(4-4) which is clearly positive definite.

$$V(t,x)=\frac{1}{2}\sigma^2 \tag{4-4}$$

The stability of state trajectories can be assured by equation(4-5) and often referred to as the *reachability condition*. The design of sliding surface would have control input appearing in equation(4-5). The reachability condition would dictate selection of a suitable control action.

$$\dot{V}(t,x,\sigma)=\sigma\frac{\partial\sigma}{\partial t}<0 \tag{4-5}$$

The reachability condition is often modified as in equation (4-6) which is referred to as the η - reachability condition. The integration of this equation is given in equation

$$\sigma\frac{\partial\sigma}{\partial t}\le-\eta|\sigma|<0 \tag{4-6}$$

$$|\sigma[x(t)]|-|\sigma[x(0)]|\le-\eta t \tag{4-7}$$

This ensures a finite time convergence to the sliding manifold $\sigma(x)=0$. The time to reach the surface is then limited to a finite value depending upon the initial conditions as shown in equation (4-8)

$$t_r\le\frac{|\sigma[x(0)]|}{\eta} \tag{4-8}$$

A control u satisfying the reachability condition would drive the state trajectories to the sliding surface in finite time and will keep it there. In this research conventional sliding mode controls have been applied based upon simplicity and robustness. In this work the selection of sliding manifold and reachability conditions have been elaborated with the corresponding control allocation used.

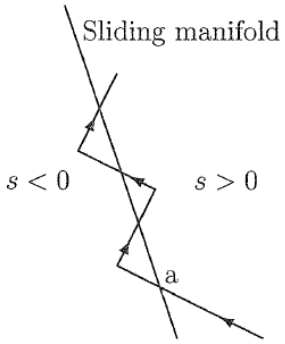

Figure 4-3 Chattering due to Actuator Delay[134]

In theory, the control would be switching at infinite frequency which in realization would require high control effort and fast response of the actuators. Coupled with inherent actuator, and system delays and actuator limits, it appears as finite frequency, finite amplitude oscillations, referred to as chattering[135] and is shown in Figure 4-3. The approach used in this work is based on relaxing the requirement of enforcing the trajectory to slide on the manifold and allow it to remain in a small vicinity of the manifold.

4.2 Rollover Detection

During cornering, the inner wheel(s) in a turn are unloaded and the load is transferred to the outer wheel(s). NHTSA defines lift-off when both wheels of the vehicle side lift of the ground. This loss of contact means lesser influence of driver input and loss of roll damping provided by the suspension. It is for this reason that wheel lift off condition is taken as the

threshold or limiting value for all control scheme developments. Several factors such as track width, height of center of gravity and suspension characteristics effect the rate at which this load transfer occurs hence specific rollover propensity for a particular vehicle setup exists as elaborated in [62], [136], [137]. The lateral load transfer ratio (LLTR) is given by equation (4-9) as in [138]

$$LLTR = \frac{Fz_r - Fz_l}{\left|Fz_r + Fz_l\right|} \tag{4-9}$$

where Fz_r and Fz_l are the total vertical forces on the right and left side wheels. The value varies from -1 to 1. A value of zero is for no lateral load transfer. A maximum value of ± 1 signifying total load on wheels on one side of the vehicle hence represents wheel(s) lift off. In a four-wheeled vehicle, a single wheel maintaining contact on either side would keep significant roll motion damping in effect. In a three-wheeled vehicle, only the axle having two wheels provides the roll motion damping hence a single wheel lift off is critical enough. In a delta configuration, braking unloads the rear wheels as shown in equations (2-39) and (2-40) reducing the threshold for lateral load transfer. Hence, for three wheeled vehicles, the following lateral load transfer ratio is suggested and is used in this research, depending only on wheel loads at the rear axle.

$$LLTR = \frac{Fz_r - Fz_l}{\left|Fz_{rr} + Fz_{rl}\right|} \tag{4-10}$$

where Fz_{rr} and Fz_{rl} denote rear right and rear left vertical tire forces.

4.3 Steering Based Rollover Mitigation Controller

A rollover mitigation controller based on steering alone is proposed. Sliding mode control is one of the many promising control techniques being used for vehicle control. Rollover mitigation controller as proposed by Imine et al [115] used a reference lateral position and its derivative as the tracking error which were found by integrating lateral acceleration corresponding to threshold LLTR. Bo-Chiuan Chen et al [114] proposed a sliding manifold using yaw rate following error, sideslip angle and lateral acceleration. The controller exploits the yaw-roll coupling and the roll motion is indirectly influenced by differential braking.

In this study a roll angle ϕ corresponding to the target LLTR at steady state is set as limiting value. A superposition steering system as suggested by F. Joachim [139] can be utilized for realization of this system and the layout is proposed as shown in the Figure 4-4. This reduces the input required for the controller and only compensation steer input is required from the controller.

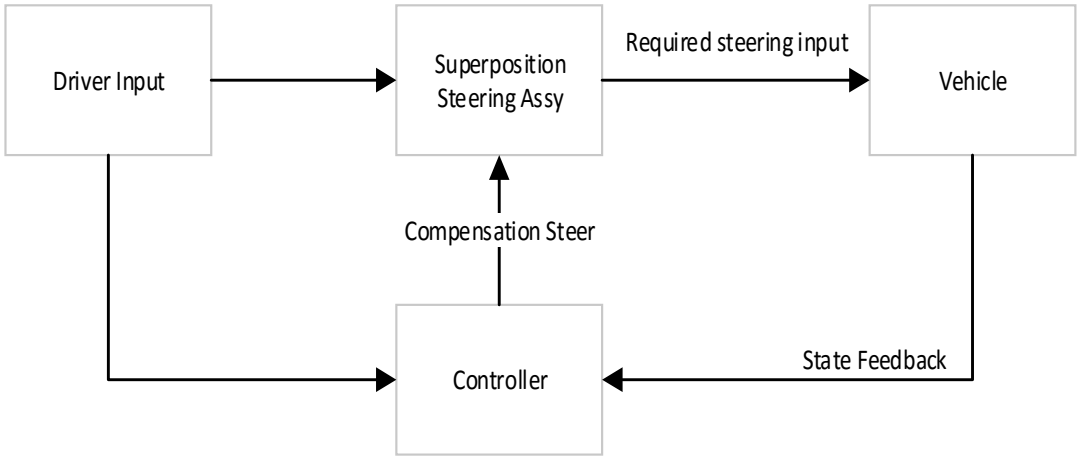

Figure 4-4. Layout suggested for Superposition steering system for controller realization.

A direct mechanical linkage between steering wheel and road wheel along with feedback to the driver to an extent, is maintained, conforming to existing road vehicle standards for steering systems. To limit the LLTR in finite time the sliding variable σ is defined as follows

$$\sigma = \dot{e} + \alpha e \tag{4-11}$$

Where $\alpha > 0$ and $e = \phi_{th} - \phi$. The state feedback sliding mode control design is based upon roll dynamics equation (2-41) , which in standard form including disturbances is written as Follows

$$\ddot{\phi} = f(\phi, \dot{\phi}) + g(\mathrm{z}, \phi, \dot{\phi})u + d(\mathrm{z}, \phi, \dot{\phi}) \tag{4-12}$$

where

$$\begin{aligned} f(\phi, \dot{\phi}) = \frac{1}{I_{xx}} \{ (\mathrm{h}+\mathrm{z})[-\frac{2\,\dot{\mathrm{x}}(\dot{\mathrm{y}} - l_r\dot{\psi})C_{\alpha r}}{(\dot{x}^2 - b^2\dot{\psi}^2)}] - 2b^2(K_r\phi + c_r\dot{\phi}) \\ -(h+z)[\frac{(\dot{\mathrm{y}} + l_f\dot{\psi})C_{\alpha f}}{\dot{x}}] - \dot{\theta}\dot{\phi}(I_{zz} - I_{yy}) \} \end{aligned} \tag{4-13}$$

$$g = \frac{(h+z)}{I_{xx}} \tag{4-14}$$

This disturbance term $d(z, \phi, \dot{\phi})$ represents modeling uncertainties. The control law has two components as follows

$$u = u_{eq} + u_s \tag{4-15}$$

where u_{eq} is the equivalent control and u_s is the conventional switching control. The equivalent control is based upon the nominal model and is given by

$$u_{eq} = \left(-f(\phi,\dot{\phi}) - \alpha\dot{\phi}\right) \Big/ g(z,\phi,\dot{\phi}) \tag{4-16}$$

The switching component u_s is given by

$$u_s = \rho sign(\sigma) \tag{4-17}$$

where

$$\rho = M + \kappa \tag{4-18}$$

and M is the bound on the disturbance term $d(z,\phi,\dot{\phi})$ that satisfies

$$\left|d(z,\phi,\dot{\phi})\right| \le M \tag{4-19}$$

for all $z,\phi,\dot{\phi}$ in the domain of interest. The finite time convergence to the sliding surface is guaranteed by the positive constant κ and the rate of convergence depends on its magnitude as discussed by Y. Shtessel et al [135] .

An important consideration in the controller implementation is that the controller attempts to regulate the roll angle at the limiting value as soon it is activated. A threshold LLTR activates the controller. The evolution of LLTR in response to a step steer is shown in Figure 4-5 .

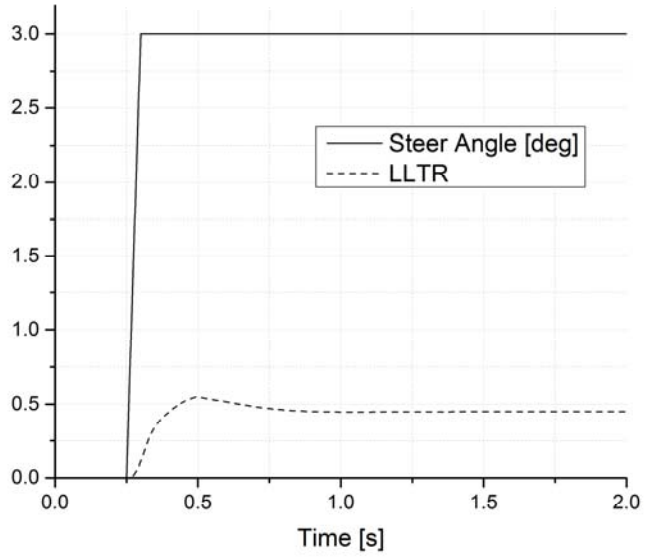

Figure 4-5 Evolution of LLTR in response to a step steering input of 3 degrees

When compared with the evolution of roll angle as shown in Figure 2-15, the roll angle value lags behind the LLTR by approximately 0.1 seconds with increasing LLTR reaching a level of critical value, the value of roll angle was still less than the critical value corresponding to steady state LLTR. If the controller is activated based on LLTR, it will try to immediately push the roll angle to the set value, increasing the LLTR overshoot significantly. To account for this, the reference roll angle threshold in this condition is set as the current roll angle if it is less than the threshold steady state roll angle corresponding to desired LLTR. The evolution of roll angle is thus restricted significantly. Furthermore, the driver steering input is compared with the value of required steering input for maintaining the vehicle roll angle at threshold value. To provide for the switching control to work with less oscillations due to one sided fencing of the roll angle, the controller output value is used with correction even if it is up to 5% less than steering input of the driver. In

this work the controller was activated prior to reaching the critical LLTR value. The switching relay part of the controller can have a larger gain for robustness requiring a larger operating range of controller output with respect to the driver input. It would result in delayed switch-off of the controller input even if the driver has turned the steering wheel back. To cater for this, the dynamic regularization of the relay part of the controller, several continuous approximations are used [140]. For this work sigmoid approximation of $sign(.)$ is used as shown in the equation (4-20) below

$$sign(s) = \tanh(\frac{s}{\varepsilon}) \tag{4-20}$$

4.4 Controller Evaluation

In order to evaluate the efficacy of the proposed controller, a high fidelity model of a three-wheeled vehicle is setup in CarSim software. This model includes nonlinear effects of roll center movement, tire force nonlinearities including tire relaxation length causing a further lag in response of the vehicle as discussed in the previous section 2.5. The suspensions are also modeled using nonlinear dampers and stiffness which are typical of light vehicle suspension systems. The controller is coded as a level-1 S-function in Matlab/Simulink. NHTSA J-Turn test is used for evaluating the efficacy of the controller. A co-simulation is setup in Matlab/Simulink using simulation model of CarSim.

While assessing the available data on three wheeled vehicles, it was observed that most of the un-tripped rollover accidents were caused by sudden large steer to avoid an obstacle on the road. The second major cause was over speeding while cornering [9], [11]. Considering the steer input severity pattern and available standards, NHTSA Fishhook maneuver was selected for evaluation of the proposed controller. A slowly increasing steer input at

constant speed was given. A steer input corresponding to a lateral acceleration of 0.3g is measured. This steer angle was scaled by a factor of 8 to account for maneuver severity and used as the amplitude of ramp steer on each direction. The angle was changed with a rate of 720 degrees per second during the first two ramps and a dwell period of three seconds after the steering reversal is maintained. The corresponding road wheel steer angle profile for a typical Asian three-wheeled vehicle is as shown in Figure 4-6.

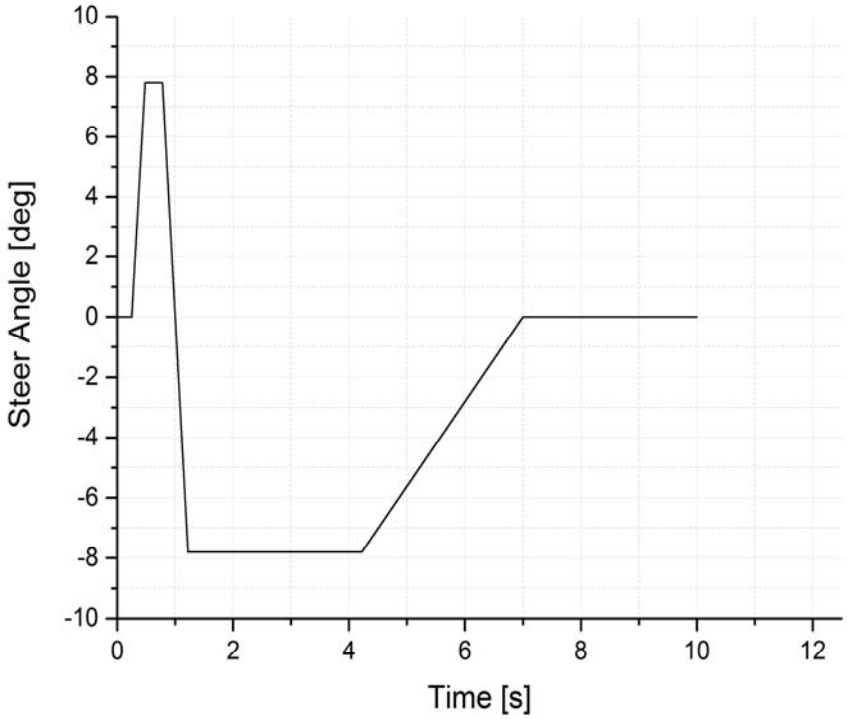

Figure 4-6. NHTSA Fishhook Steer profile used for evaluating rollover propensity.

A maneuver entrance speed of 35 km/hr is used. A threshold roll angle is set at a steady state LLTR of 0.8 arbitrarily considering a margin of safety. The LLTR with and without controller is shown in Figure 4-7. A value of 1 and -1 for LTTR indicates wheel lift off,

while the controller is able to maintain these values near 0.8. The transients are managed in finite time as apparent in the dwell period from 1.7 to 4.2 seconds.

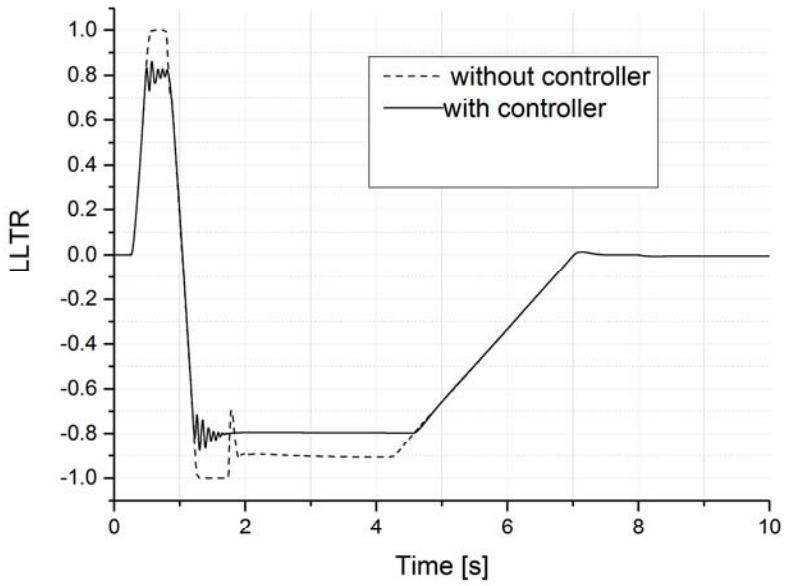

Figure 4-7. Evolution of LLTR during NHTSA Fishhook maneuver with and without controller. The maneuver entrance speed is set to correspond to wheel lift off during this maneuver without controller.

The overshoots of roll angle when reduced, results in controller action which is restricted by the switching threshold on the lower side with a value of 0.75. The adapted roll angle threshold is shown in Figure 4-8.

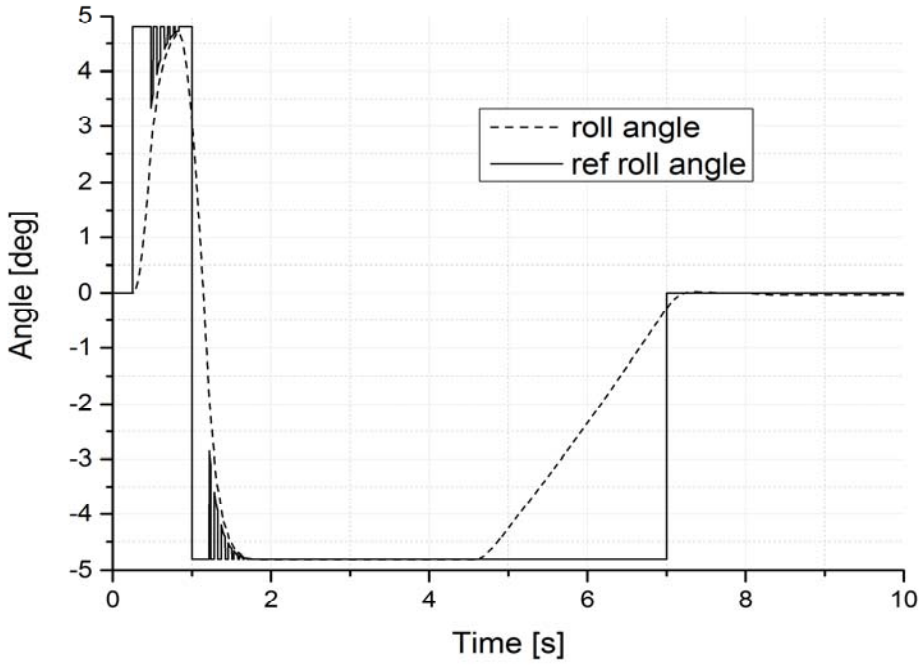

Figure 4-8. Proposed adapting reference roll angle and the actual roll angle during NHTSA Fishhook Maneuver. The adaption is based on the value of LLTR.

The adaption algorithm was used to compensate for the delay between the steer angle and the evolving roll angle. The value of roll angle reference for the controller is as follows

$$\phi_{ref} = \phi_{set\_point} + (\phi_{setpoint} - \phi_{actual}) \tag{4-21}$$

The value is updated only if the LLTR is greater than the threshold value which is 0.8 in this study and the actual roll angle is less than the set point steady state roll angle corresponding to the threshold LLTR. The evolution of roll angle with and without controller is shown in the Figure 4-9 below. A threshold value for roll angle has been set at 4.8 degrees.

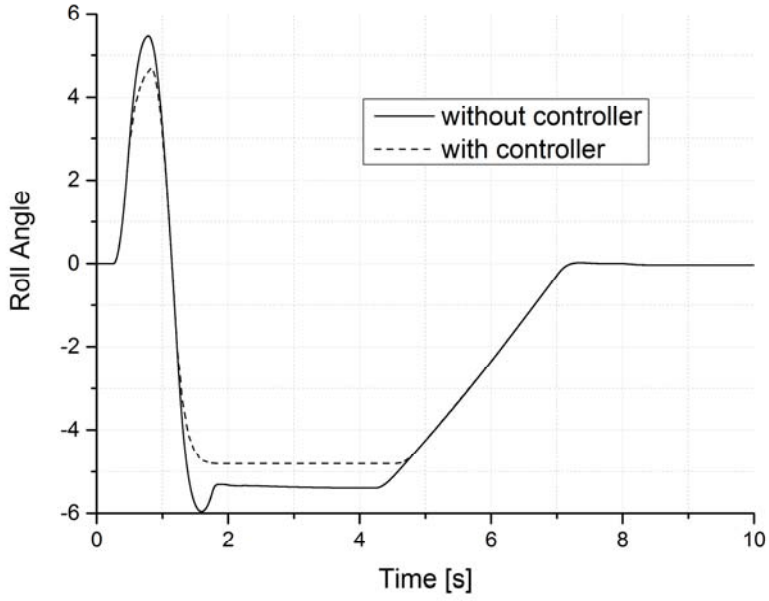

Figure 4-9. The evolution of roll angle of vehicle during NHTSA Fishhook maneuver with and without control.

As the roll angle is the focus of the controller, it is effectively regulated at the set point value despite approximate model and model parameters. The steer angle output is given in .Road uncertainties, slight increase in vehicle speed and lack of driving skills may result in rollover as indicated in the Figure 4-11 below indicating a roll angle profile with the same steering profile for a maneuver entrance speed of 38 km/hr.

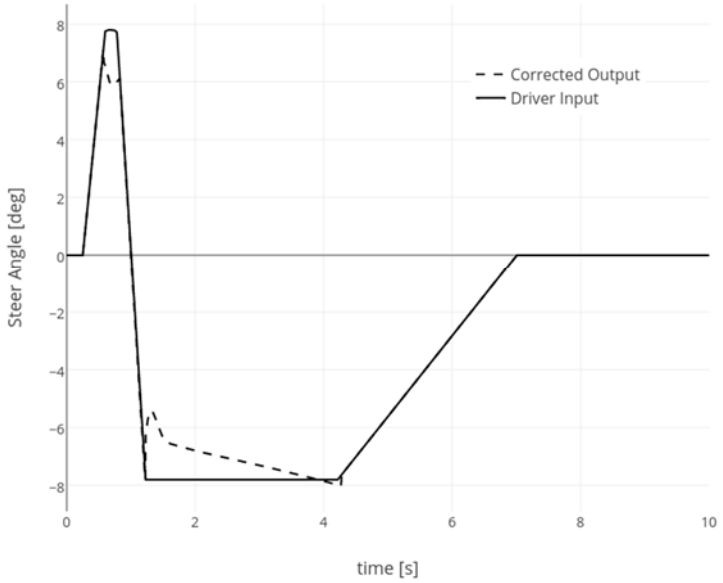

Figure 4-10 Steering input of the driver compared with the corrected output of the controller

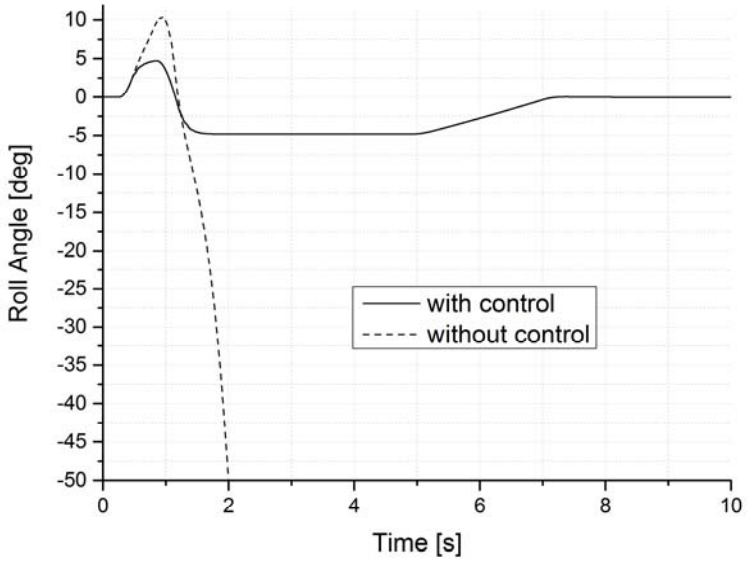

Figure 4-11. Roll angle evolution during fishhook maneuver with an elevated speed of 38 km/hr. The controller was successful in limiting roll angle and mitigating rollover.

As evident from Figure 4-11, the vehicle did not recover without controller after steering reversal with this slight increase in vehicle speed. However the controller was still able to limit the roll angle and LLTR despite this change in longitudinal speed signifying robustness. Next the controller was evaluated with $\pm 10\%$ variations in height of cg from the ground and mass. The results are presented in Figure 4-12 and Figure 4-13 respectively.

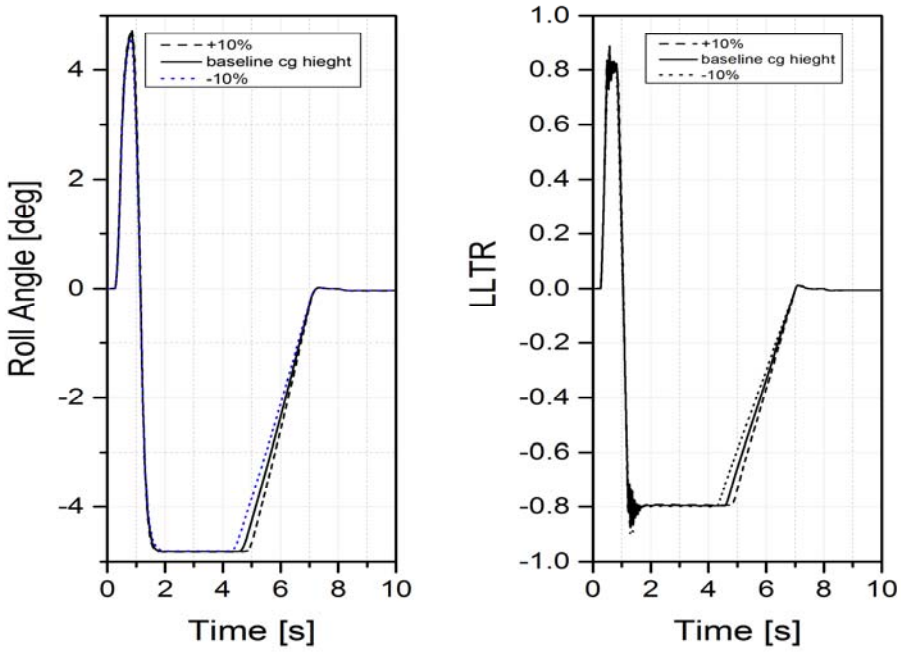

Figure 4-12. Evolution of roll angle and LLTR with 10% variation in cg height. Controller was able to able to limit both with reasonable efficacy.

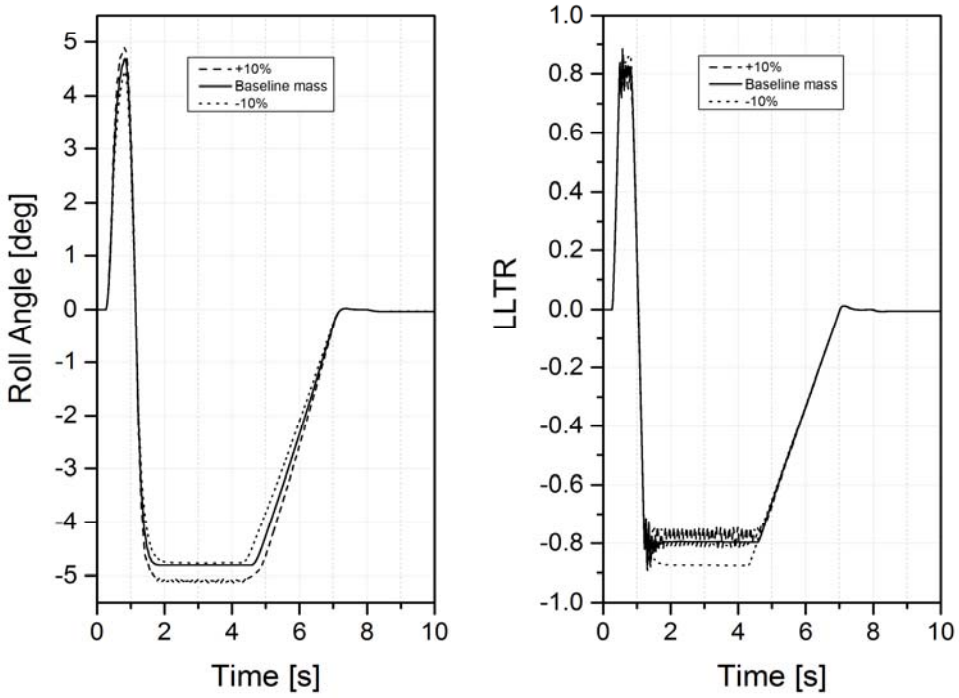

Figure 4-13. Evolution of roll angle and LLTR with 10% variation in vehicle mass. Controller was able to able to limit both with reasonable efficacy. With less mass, increase in roll angle results in more lateral load transfer.

These results show that the controller adapted better to cg-height changes as compared to mass increase but still was able to maintain LLTR below one i.e. maintaining contact with ground. With additional mass the static deflection of suspension increases, reducing the suspension travel and at higher roll angles the bump stops starts interacting, resulting in sudden change in stiffness. This results in oscillations about the steady state roll angle. The mass increase results in increased lateral force on the sprung mass for the same lateral acceleration. This results in an increase in roll angle. When the controller tries to regulate the roll angle, lateral load transfer is reduced, hence a better rollover mitigation. With reduced mass, the roll angle corresponding to the same maneuver reduces. When the controller tries to regulate it to a higher level, relatively more lateral load transfer results.

This is evident from Figure 4-13. To overcome this, it is suggested that the controller should be tuned for lowest operational vehicle total mass. This would ensure robustness with load variations. Based on the performance of controller with reduced vehicle mass, it is recommended that the baseline mass properties used for controller design should correspond to the minimum anticipated operational loading instead of the nominal fully laden vehicle state. This would lead to maximum efficacy and robustness of the proposed controller. The rollover is mitigated at the expense of path following fidelity as the steering would increase the radius of turn to reduce lateral load transfer. In other words, it would limit the steering angle to be equal or smaller than the steer angle for threshold roll angle for any given speed. For smaller steering excess by the driver, this effect would be hardly noticeable but for larger input from the driver, it may lead to significant departure from intended path.

4.5 Rollover Mitigation controller performance on low friction Road

The controller is then evaluated on a low friction road (μ =0.2). The maneuver entrance speed is 35 km/hr. The LLTR evolution during NHTSA fishhook maneuver is shown in Figure 4-14. The controller which performed well in mitigating vehicle rollover on normal road conditions, failed to limit the LLTR below the threshold set and wheel lift-off is evident. This can be explained by the evolution of yaw rate during the maneuver, shown in Figure 4-15. The sudden increase in yaw rate after 0.25 seconds indicate a limit over steer situation, hence instability. This leads to wheel lift off signified by LLTR value reaching 1 after one second. The vehicle does not completely turn over but recovers with steering reversal. The lateral acceleration gets limited by the skidding of tires at the rear, hence

despite the high spin out, the vehicle recovers from lift off condition and does not roll over completely. After the vehicle achieved a large yaw rate, the steering inputs had negligible effect on the vehicle behavior indicating instability. Such situations generally lead to collision with other vehicles or excursions from the road resulting in tipped rollovers.

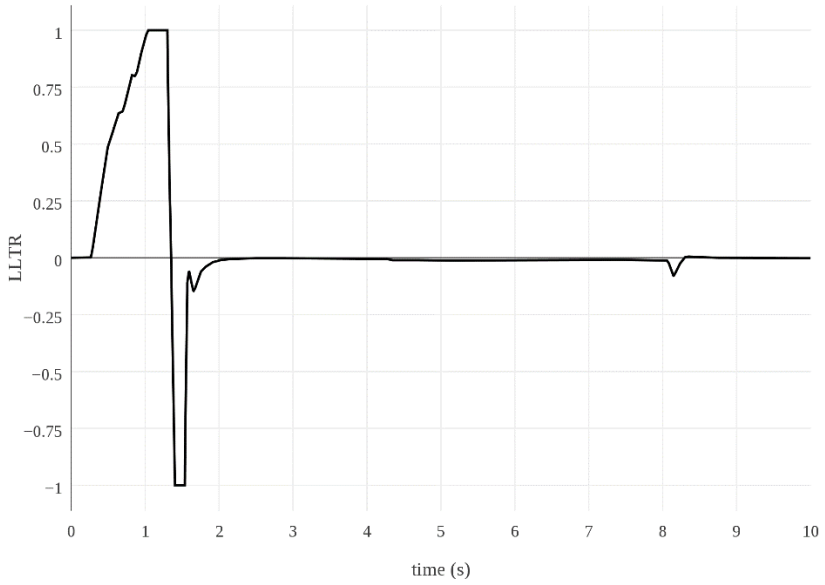

Figure 4-14 LLTR during NHTSA Fishhook maneuver with controller on a low friction road

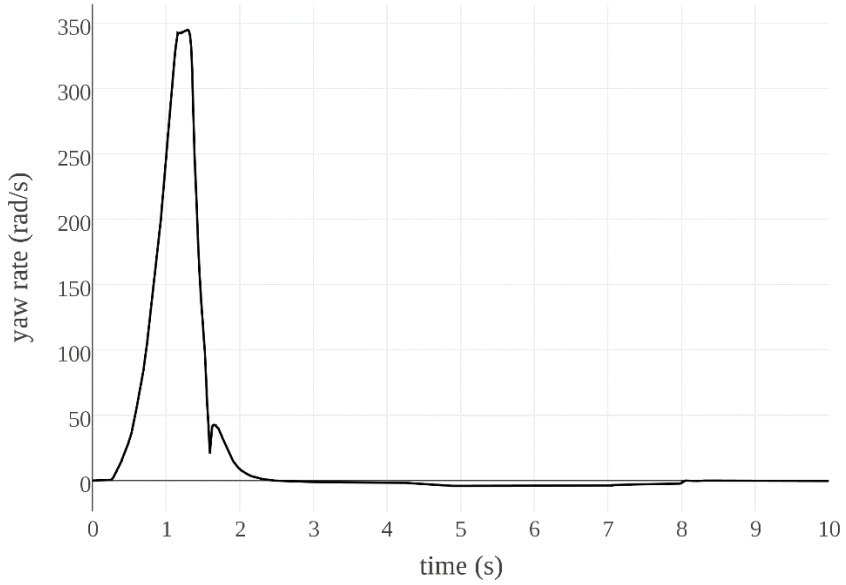

Figure 4-15 Yaw rate during NHTSA maneuver with controller on a low friction road

4.6 Conclusions

A steering based rollover mitigation controller was presented using sliding mode control design method. The controller was able to limit lateral load transfer at a predetermined value even in the presence of large vehicle parameter uncertainty. The performance degraded slightly when higher than actual values for inertial parameters were used for controller. It is suggested that vehicle parameters corresponding to an un-laden state be used for conservative limit on lateral load transfer, effectively mitigating rollover.

The controller action can be interpreted as limiting the maximum steering angle for a particular speed of the vehicle with due regard to transient chassis motion. For large steering input by the driver, this may lead to an artificial under steering behavior of the vehicle.

CHAPTER 5

BRAKE AND STEERING BASED INTEGRATED CONTROL FOR ROLLOVER PREVENTION AND DIRECTIONAL STABILITY

In this chapter to augment the steering controller, two brake based control schemes are studied. The objective of these controllers is to maintain directional stability on low friction roads and ensure steer-ability when the rollover controller limits road steer angle at higher friction roads.

5.1 Brake Based Dynamic Stability Controller Design

To overcome the limitations of steering in its ability to maintain directional stability during high yaw rate state of the vehicle, a brake based, Dynamic Stability control systems (DSC) is proposed. Desired yaw rate is calculated using equation (5-1)

$$\dot{\psi}_{des} = \frac{v_x}{L + K_{us} v_x^{\,2}} \delta \tag{5-1}$$

The dynamics of the vehicle using lateral velocity v_x and yaw rate $\dot{\psi}$ as state variables is given in equation(5-2). M_t is the external yaw moment required to stabilize the vehicle. This moment would be determined using sliding mode control. The sliding surface is defined using the difference in actual and desired yaw rate as in equation(5-3).

$$\begin{bmatrix} \dot{v}_y \\ \ddot{\psi} \end{bmatrix} = \begin{bmatrix} \dfrac{-(C_f + C_r)}{m v_x^{\,2}} & \dfrac{-aC_f + bC_r}{m v_x^{\,2}} - 1 \\ \dfrac{-aC_f + bC_r}{I_z v_x} & \dfrac{-a^2 C_f - b^2 C_r}{I_z v_x} \end{bmatrix} \begin{bmatrix} v_y \\ \dot{\psi} \end{bmatrix} + \begin{bmatrix} \dfrac{C_f}{m v_x} \\ \dfrac{aC_f}{I_z} \end{bmatrix} + \begin{bmatrix} 0 \\ I_z \end{bmatrix} M_t \tag{5-2}$$

$$s = \dot{\psi} - \dot{\psi}_{des} \tag{5-3}$$

In order to keep the surface attractive and finite time convergence, the sliding condition is taken as in equation(5-4). The discontinuous control action is as defined in equation(5-5) part (a) the $sign(s)$ is replaced by $\tanh(\frac{s}{\varepsilon_{DSC}})$ as its continuous approximation in part (b) of equation (5-5)

$$\frac{1}{2}\frac{d}{dt}s^2 = s\dot{s} \le -\eta|s| \tag{5-4}$$

$$\begin{aligned} M_t &= -K_{DSC}\,sign(s) && \text{(a)} \\ M_t &= -K_{DSC}\tanh(\frac{s}{\varepsilon_{DSC}}) && \text{(b)} \end{aligned} \tag{5-5}$$

The gain K_{DSC} is calculated using equations(5-1), (5-2) and(5-4). The expression for this gain is given in equation (5-6)

$$K_{DSC} = I_z(F_{yf}\left|-\frac{av_y}{I_z v_x}-\frac{a^2\dot{\psi}}{I_z}+\frac{a\delta_f}{I_z}\right|+F_{yr}\left|-\frac{bv_y}{I_z v_x}-\frac{b^2\dot{\psi}}{I_z}\right|+|\dot{\psi}_{des}|+\eta) \tag{5-6}$$

Brake force applied on single or all of the wheels on one side of the vehicle produces a corrective yaw moment. In four wheeled vehicles, brake based Dynamic Stability control systems (DSC) apply braking effort to the outer front wheels as shown in the Figure 5-1 and discussed in [114] as the rear wheel is either saturated or close to saturation and hence less breaking potential is available. In case of a delta configuration of a TWV the front wheel mounted in the middle cannot contribute towards corrective yaw moment due to negligible moment arm.

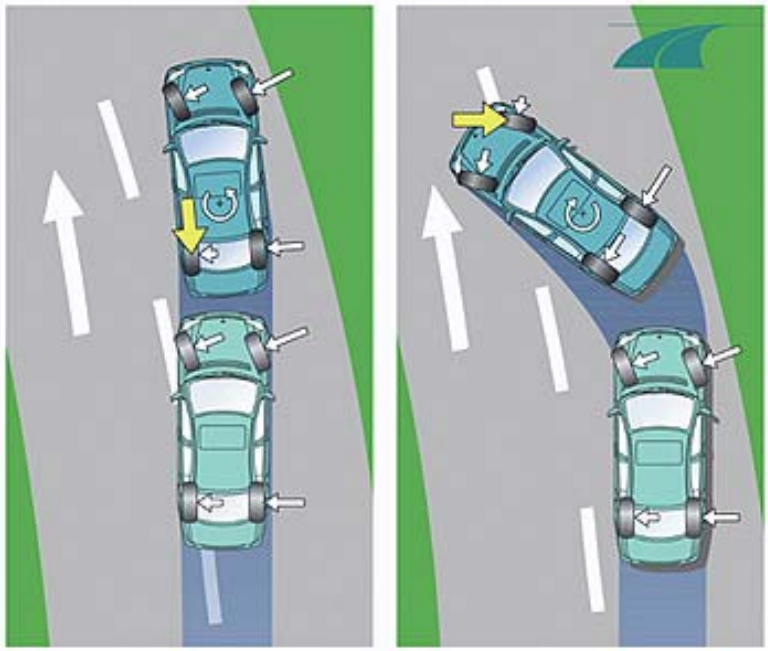

Figure 5-1 Typical DSC operation to correct under steering and over steering behaviour of vehicle

The braking force on the left and right rear wheels is calculated using the relation in equation(5-7)

$$F_{brr} = \frac{M_t}{t_w}$$
$$F_{brl} = -\frac{M}{t_w} \tag{5-7}$$

Only positive values are used as the brakes cannot generate tractive force. The rear wheels also need to be prevented from saturating from the braking and lateral forces. The requirement for DSC intervention is required on low friction surface hence a limit on the amount of brake force that can be applied without causing the wheel to skid is based on the

friction circle of the rear wheels as in equation (5-8) and the value of η is chosen as a small value.

$$\begin{aligned} F_{br} &< \rho_{b\max} \left| \sqrt{\mu F^{2}{}_{zr(\max)} - F^{2}{}_{yr}} \right| \\ F_{br} &> 0 \end{aligned} \tag{5-8}$$

The pressure supplied to the rear wheels is calculated based on the equations(5-9) where K_b is the respective factor relating brake pressure to brake torque and r_{wheel} is the wheel radius.

$$\begin{aligned} P_{brr} &= K_{br} F_{brr} r_{wheel} \\ P_{brl} &= K_{br} F_{brl} r_{wheel} \\ P_{bf} &= \rho_f K_{bf} \max(F_{brr}, F_{brl}) \mathrm{r}_{wheel} \end{aligned} \tag{5-9}$$

During a limit over steer condition the rear wheels are at or nearing saturation, hence the control effort has to be effected before a limiting situation arises. The limiting value of braking force available also slows down convergence and at time would not be as desired by equation(5-6). To compensate this, the front wheel is also braked by a fraction ρ_f of the maximum braking effort on any of the rear wheels. This would reduce the speed of the vehicle and enable the driver to take remedial control actions to recover from an impending limit over steer behavior. This additional front braking can make the tuning of the controller less intensive as the information about the friction and the lateral forces would not be required if a reasonable gain is tuned for a typical very low friction surface anticipated. This would be at the cost of speed of the vehicle which would be reduced further as compared to a situation in which only the rear wheels are used for braking.

The controller is evaluated using the same test maneuver as for rollover stability as it includes both high rate steering inputs and reversals. The limiting amount of braking

force restricts the controllability on low friction surfaces. The response of the vehicle with maneuver entry speed set at 35 km/h is shown in Figure 5-2. The controller was not able to make the vehicle track the desired yaw rate and the vehicle enters into a limit over steer and spins out. The peak yaw rate was however reduced but is insignificant as the vehicle would have already left the road or hit another vehicle. The controller was tested for lower maneuver entrance speeds and it was only at 20 km/h speed that the controller became effective in stabilizing the vehicle and avoiding the limit over steer condition.

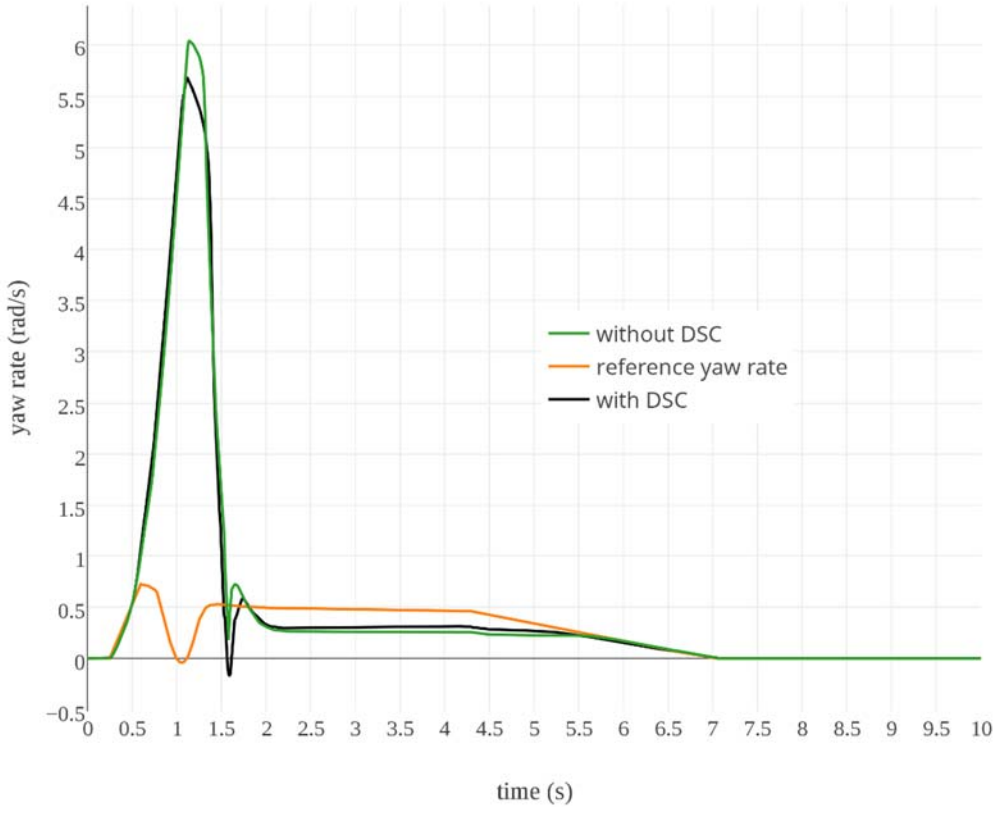

Figure 5-2 Yaw rate with and without DSC controller on a low friction road at 35 km/h speed

The response of the vehicle is as shown in Figure 5-3 for maneuver entrance speed of 20 km/h. The vehicle without DSC enters into a limit over steer and spins out of control during steering reversal. The controlled vehicle followed the desired yaw rate based upon the steering input of the driver.

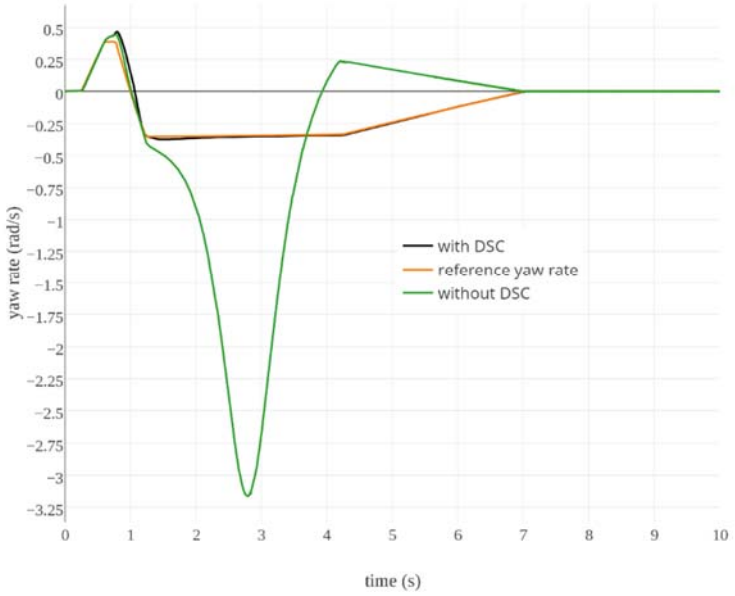

Figure 5-3 Yaw rate with and without DSC at low friction road at 20km/h speed

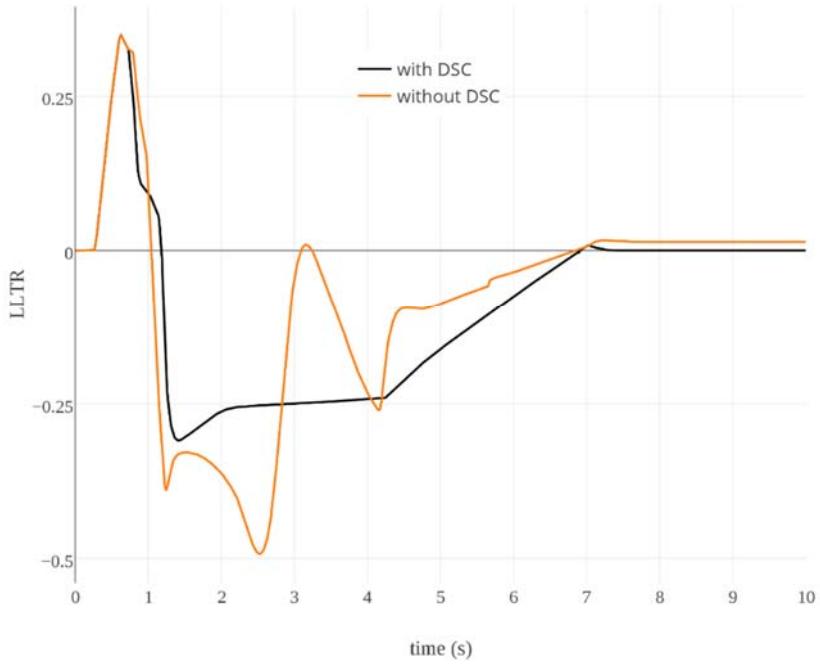

Figure 5-4 LLTR with and without DSC on a low friction road at 20km/h

The LLTR during this maneuver is shown in Figure 5-4 which shows that the spinning vehicle has more lateral load transfer during the maneuver. It is almost double at 2.6 sec for that of an uncontrolled vehicle. This increases the possibility of tripped rollover. As with any brake based control, the speed of the vehicle is reduced as shown in Figure 5-5. For this scenario, the speed during the maneuver got reduced by less than 2 km/hr which would not be that noticeable for the driver. The longitudinal speed of the vehicle without DSC decreases significantly as the energy of this motion mode is transferred to lateral and yaw motion. The brake maximum brake force is hence based on a trade-off between priorities of lateral stability and longitudinal speed.

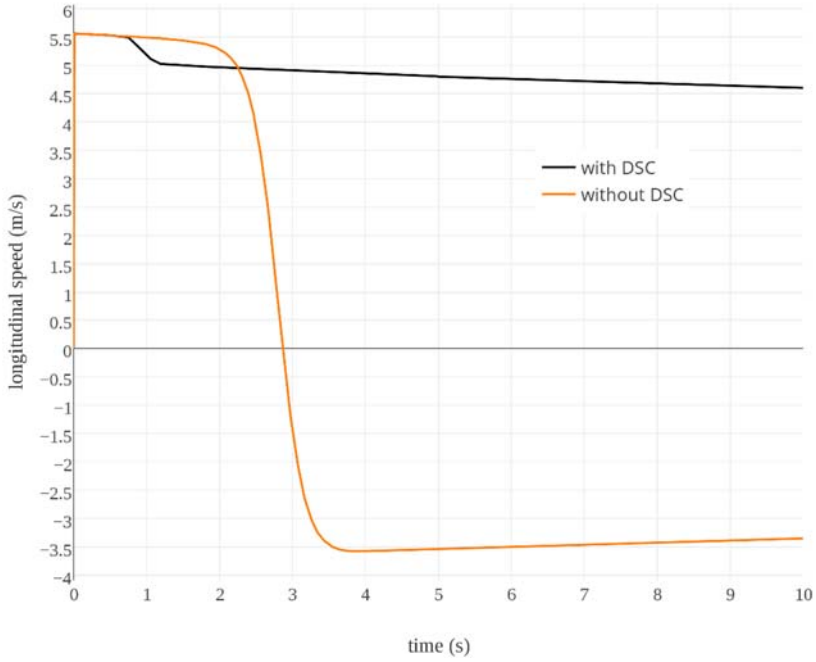

Figure 5-5 Longitudinal speed with and without DSC on low friction road at 20 km/h speed

5.2 Integration of RMC and DSC controllers

The DSC and the rollover mitigation controller (RMC) would have no interaction on the low friction road where limit over steer dominates the planner dynamics. Roll over occurs at higher speeds due to high yaw rate and even with the steer control is enabled, it is not able to mitigate rollover. On normal roads when the threshold LLTR is crossed, the RMC limits the road steer angle of the vehicle to reduce limit lateral acceleration. This when compared with the driver intent based on steering wheel angle appears as an under steer condition. This would lead to larger turn radii and at reasonably high speeds, large departures from the intended path would occur. Any increase in steer angle would enhance the LLTR and may lead to rollover. Both under steer correction and LLTR reduction require opposite yaw moment corrections. A purely brake based system for four wheeled

vehicles as reported by Yoon et al [90] would reduce speed along with corrective moments added to the vehicle. This reduces the lateral acceleration and hence reduces some strain from the roll mitigation. The reduction in LLTR is not effected by deceleration in the longitudinal direction. Where as in a three wheeled delta configuration the unloading of the rear wheels coupled with corrective yaw moment for under steer affects LLTR more adversely. When the DSC is enabled along with RMC on a normal high friction road the results obtained are shown in Figure 5-6,Figure 5-7 and Figure 5-8 . The oscillations in LLTR and yaw rate results are most significant in relating the conflicting effect of DSC and RMC. The increase in yaw rate by application of brakes leads to an increase in the LLTR which is then compensated by the steer angle correction by the RMC. The RMC was still able to mitigate rollover. The yaw rate in the initial phase (first 0.8 seconds) still remains much lower than the desired yaw rate based upon the driver intent. Reduction in speed later makes the yaw rate close to the desired value easier as the load on steering based RMC is reduced.

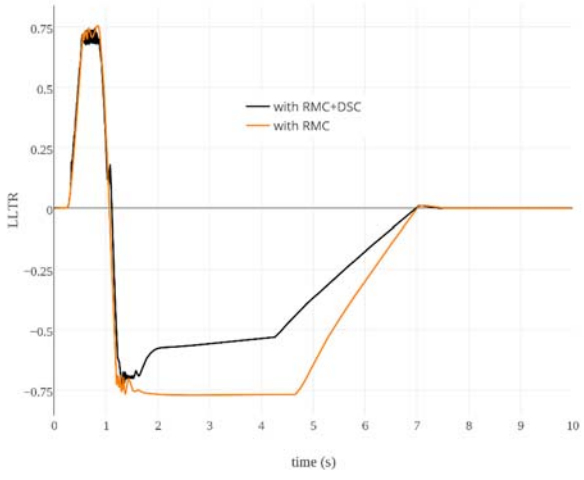

Figure 5-6 LLTR on high friction road with DSC and RMC controller at 35 km/hr speed

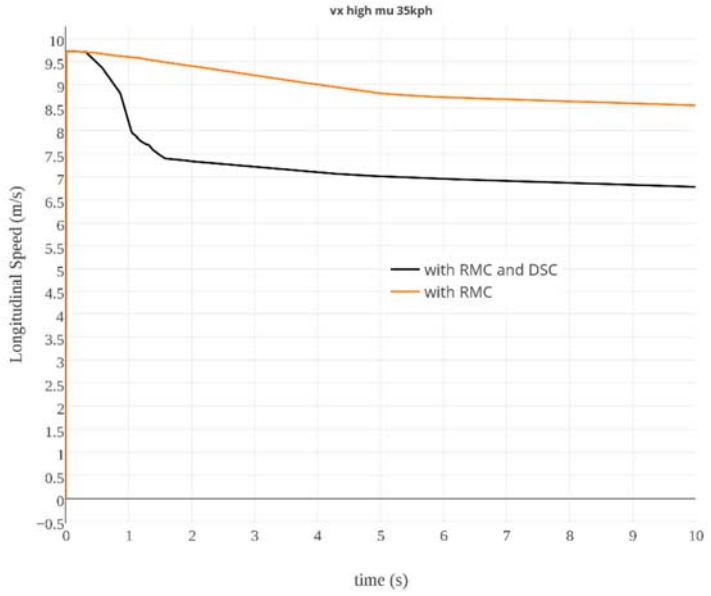

Figure 5-7 Longitudinal speed on high friction road using RMC and DSC at 35 km/hr speed

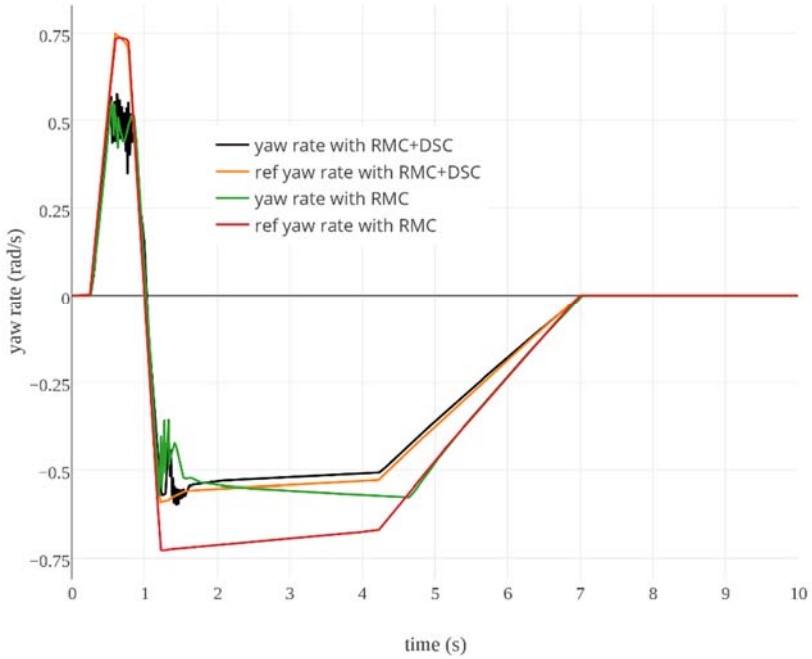

Figure 5-8 Yaw rate on high friction road using RMC and DSC at 35km/hr speed

.

5.3 Proportional Braking Controller for Augmenting RMC

With the undesired extra oscillations and a limited ability to track desired yaw rate on high friction surfaces, a simple proportional braking on all wheels is proposed which is modulated by the forward speed based on the equation(5-10)

$$F_b = v_x k_2 \{|(\dot{\psi} - \dot{\psi}_{des})| - \Delta\dot{\psi}_{threshold} \tag{5-10}$$

$$\begin{aligned} F_{brl} &= \min(F_b, F_{brl(\max)}, F_{brr(\max)}) \\ F_{brr} &= \min(F_b, F_{brl(\max)}, F_{brr(\max)}) \\ F_{bf} &= \min(F_b, F_{bf(\max)_{\text{with RMC}}}) \end{aligned} \tag{5-11}$$

The brake force is converted into brake pressure using

$$\begin{aligned} P_{brr} &= K_{br} F_{brr} r_{wheel} \\ P_{brl} &= K_{br} F_{brl} r_{wheel} \\ P_{bf} &= K_{bf} F_{bf} r_{wheel} \end{aligned} \tag{5-12}$$

Hence the braking pressure is equally distributed to the rear wheels and a fraction of it would be sent to the front wheel to keep the lateral tire force budget available to the steering based rollover mitigation controller, based on typical tire friction circle limits as in equation

$$F_{bf(\max)_{\text{with RMC}}} < 0.2\left|\sqrt{\mu F^2_{zf} - F^2_{yf}}\right| \tag{5-13}$$

The results are shown in Figure 5-9 which indicate almost the same yaw rate tracking with SMC based DSC but with far less demand on the steering based RMC.

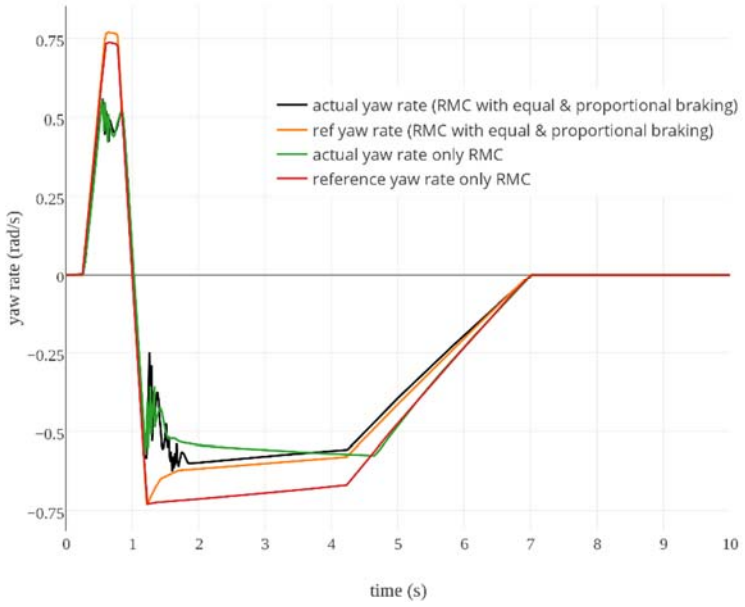

Figure 5-9 Yaw rate on high friction road using RMC and proportional braking at 35km/hr speed

The effect on LLTR is shown in Figure 5-10 . The application of brakes is significantly effecting the roll moment resistance of the rear axle and hence with the application of significant brake force, the increase in LLTR is evident. The RMC controller still manages to limit the LLTR in a safe margin. These results also indicate that the three wheeled setup with delta configuration are very sensitive to braking in near rollover conditions or when LLTR is to be regulated. In four wheeled vehicles, such proportional schemes have been able to successfully mitigate rollover and yaw rate limitations as in [141][142]. Even full braking in a four wheeled vehicle would not affect the LLTR as it is based on all axles and not as in the case of a TWV, where the rear axle unloads, increasing the LLTR.

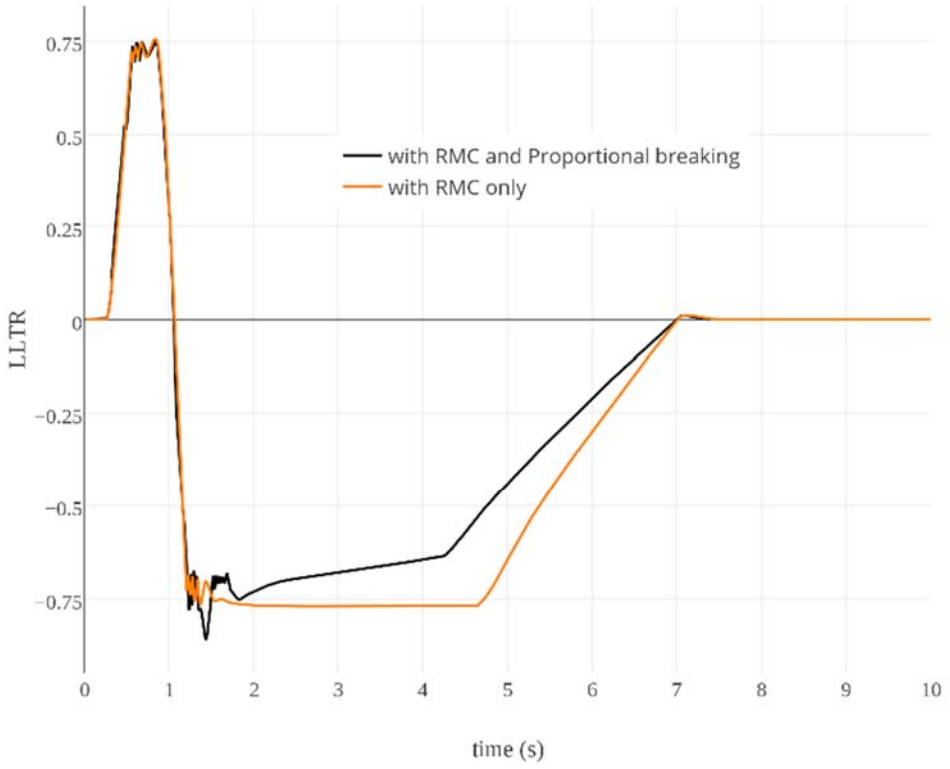

Figure 5-10 LLTR on high friction road using RMC and proportional braking at 35km/hr speed

5.4 Rule Based Integration of Steering and Brake based controllers

As the suggested controllers have a beneficial role in specific conditions, it is suggested that they should be used only when needed to conserve energy. Hence a rule based integration of RMC, DSC and proportional breaking control is suggested and shown in the Figure 5-11. To avoid conflict between DSC and RMC the two controllers are not activated together. Priority is given to rollover mitigation and a threshold LLTR is used to activate RMC. As shown in the results earlier, the vehicle would appear to under steer relative to the driver steering input. A proportional braking controller is activated when this deviation

is beyond a predetermined limit. This would ensure braking intervention does not penalize longitudinal behaviour of the vehicle. The break controller would initially increase the LLTR by unloading the rear axle and the steering based controller would respond by further increasing this error in yaw rate. The reduction in speed takes over and would result in lower values of LLTR and yaw rate. The yaw rate error would be increasing in magnitude with lower LLTR only on low friction road. This would happen when a limit over (under) steer condition is approached. This instability in case of over steer increases rapidly. A robust control action by SMC based DSC is able to handle this situation and activated when the deviation in yaw rate exceeds limiting value while the LLTR is still within safe limits.

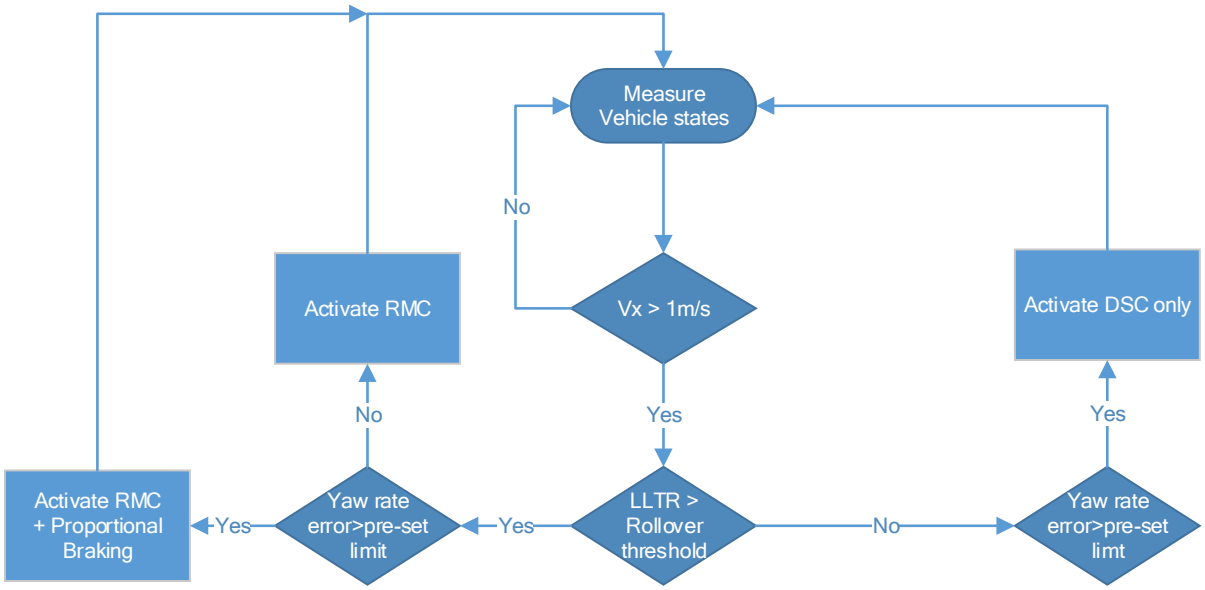

Figure 5-11 Integrated Control Flow Process using DSC, RMC and Proportional braking

The results indicate that the proposed RMC can successfully mitigate maneuver induced un-tripped rollover of a delta TWV, even under parameter uncertainty and modeling

imperfections in controller design. A brake based yaw stability system has a proven efficacy in four wheeled vehicles, performs well when rollover mitigation is not a priority. In case of impending rollover brake based system has limited efficacy which can be more effectively utilised with focusing on speed reduction to indirectly reduce desired yaw rate, corresponding to driver steering inputs.

5.5 Conclusions

Brake based controls for directional stability were integrated with steering based rollover control to prevent un-tripped rollovers and reduce the possibility of tripped rollovers. Due to the peculiar setup, differential braking at the front as preferred for an over-steering vehicle is not possible. Brake based yaw controller has a conflicting action with respect to the rollover mitigation controller. In this research, rollover avoidance was given the highest priority. This priority is based on the high rollover propensity. The relatively smaller size on road and lower average speeds allow relaxed directional behavior restrictions.

To assist saturating rear tires, front wheel brakes have been employed in both DSC and proportional braking controller design. The rules for integration in its present form are more subjective in nature and depend more on preference as heading correction and rollover reduction have contradictory yaw moment demand.

CHAPTER 6

CONCLUSIONS

In this thesis, the research focused on mitigating rollover of three wheeled vehicles particularly delta configuration. Analysis of nonlinear vehicle model and previous studies reveal that a delta configuration enters into a limit over steer state if tires of the vehicle saturate before rollover. This leads to vehicle spin out and the wheels may laterally strike road boundaries or other imperfections to generate sufficient lateral loads to tip over the vehicle. Typical aircraft ground maneuvers and commercial TWV operating on low friction surface are vulnerable to such scenarios. A phase plane analysis using yaw rate and vehicle side slip as states is used to establish vehicle behavior over a wide range of initial conditions. Increase in track width and decrease in height of center of gravity from ground, increase rollover resistance and also slightly increase the stability bounds against limit over steer behavior. Moving the center of gravity rearward however slows down yaw rate recovery when vehicle sideslip and yaw rate are in the same direction. Hence would be beneficial to rollover but would put extra burden on the driver while moving on low friction surfaces which might become challenging in the absence of any controllers for directional behavior.

The effect of adding an anti-roll bar on rollover and directional behavior is studied. The results indicate that addition auxiliary roll stiffness with the help of an anti-roll bar increases rollover resistance up to a limit, after which increase in stiffness does not have any significant effect on rollover threshold. The increase in ARB stiffness may lead to low ride quality and also a very negligible effect on directional behavior. This can be attributed

to the absence of roll stiffness based lateral load transfer between the front and rear axles. However the perceptible reduction in roll angle may encourage the driver for even tighter turns at higher speeds making the vehicle vulnerable to rollovers.

A sliding mode directional stability control, based on differential braking is proposed based upon its proven efficacy on low friction surfaces for four wheeled vehicles. Despite not being able to utilize front axle moment due to single wheel, the rear wheel braking was able to retain directional stability. The yaw rate error is based on linear vehicle behavior on normal road conditions.

Due to increased rollover vulnerability when brakes are applied during turning a steering based rollover mitigation controller is proposed. Unique modeling of roll dynamics is used which links the steering control effort to the roll dynamics directly. Roll angle corresponding to vehicle rollover limit in steady state is used with sufficient margin. Due to lag between steering input and roll motion an adaptive sliding surface is proposed based upon current roll angle and lateral load transfer ratio. The sliding mode based controller is able to limit the roll angle and lateral load transfer ratio at desired values even in the presence of vehicle parameter variations. The Robustness study results suggest that the controller should be designed using parameters for the least loaded vehicle configuration. The steering controller limits the steer angle to prevent rollover. Steering input from the driver if given priority as it is based upon visual feedback of the surrounding involving lane keeping and crash avoidance, would appear as an under steering (sluggish) response of the vehicle. To cater for this proportional braking along with the steering based rollover control is proposed. A rule based integration scheme is presented for maximum efficacy of the controllers and keeping rollover mitigation at the highest priority level. The

proposed controllers have shown significant rollover mitigation in both un-tripped and vehicle behavior leading to a possible tripped rollover.

CHAPTER 7

FUTURE WORK

The proposed controllers have been developed considering low complexity and adaptability to existing vehicles and designs. This may lead to a limited efficiency of the controllers in some scenarios. It would be appropriate to incorporate some online optimization of inputs and switching of the various controllers. An envelope control and stabilization based on the phase plane may enhance the operational bounds on vehicle states. Higher order sliding mode controllers may be considered based on high capacity electronic control units' availability. A study of vehicle near rollover is needed. This can help develop controllers with possibly relaxed limits on lateral load transfer.

The application of brake based controllers would require a similar hardware configuration as of an ABS system. In this study any existing ABS system was not accounted for in controller design. The peculiar layout of delta three wheeled vehicles require a dedicated study on efficacy of ABS, traction control systems and their possible interaction with rollover, and handling/directional stability controllers.

REFERENCES

[1] "'The Top Ten Causes of Death,'" *World Health Organisation*, 2015. [Online]. Available: http://www.who.int/mediacentre/factsheets/fs310/en/. [Accessed: 23-Jun-2015].

[2] "Global Status Report On Road Safety," *World Health Organisation*. p. 286, 2009.

[3] A. K. Jain, "Sustainable Urban Mobility in Southern Asia, A regional Report for Global Report on Human Settlements," Nairobi, 2013.

[4] The Partnership for Clean Fuels and Vehicles (PCFV) and CAI-Asia, "Managing Two and Three-wheelers in Asia," 2010.

[5] A. Mani, M. Pai, and R. Aggarwal, "Sustainable urban transport in india, Role of the Auto-rickshaw Sector," 2012.

[6] M. Breithaupt, "Two and Three Wheelers, Module 4c, Sustainable Transport: A Sourcebook for Policy-makers in Developing Cities," 2009.

[7] H. Huo, M. Wang, L. Johnson, and D. He, "Projection of Chinese Motor Vehicle Growth, Oil Demand, and CO2 Emissions Through 2050," 2008.

[8] H. Huo, M. Wang, L. Johnson, and D. He, "Projection of Chinese Motor Vehicle Growth, Oil Demand, and CO2 Emissions Through 2050," *Energy Systems Division, Argonne National Laboratory, USA*. 2006.

[9] Government of India, "Road Accidents in India 2011." New Dehli, 2011.

[10] Government of India, "Road Accidents in India 2010," New Dehli, 2010.

[11] Government of India, "Road Accidents in India 2009," New Dehli, 2009.

[12] A. Ahmed, "Road Safety In Pakistan," *National Road Safety Secretariat, Ministry of Communications, Govt. of Pakistan*. 2007.

[13] R. Jooma, A. Jehangir, J. Razzak, M. S. Ali, and S. A. Hussain, “Road Casualities Report 2011,” Karachi Pakistan, 2011.

[14] “Standards for All Terrain Vehicles and Ban of Three-Wheeled All Terrain Vehicles; Notice of Proposed Rulemaking,” *Fed. Regist. Consum. Prod. Saf. Comm. USA*, vol. 71, no. 154, pp. 45904–45962, 2006.

[15] U. Schmucker, R. Dandona, G. A. Kumar, and L. Dandona, “Crashes Involving Motorised Rickshaws in Urban India : Characteristics and Injury Patterns,” *Injury*, vol. 42, no. 1, pp. 104–11, Jan. 2011.

[16] T. Acarman and Ü. Özgüner, “Rollover prevention for heavy trucks using frequency shaped sliding mode control,” *Veh. Syst. Dyn.*, vol. 44, no. 10, pp. 737–762, Oct. 2006.

[17] C. Zong, Q. Miao, and B. Zhang, “Research on rollover warning algorithm of heavy commercial vehicle based on prediction model,” in *Internaltional Conference on Computer, Mechatronics, Control and Electronic Engineering (CMCE)*, 2010, pp. 432–435.

[18] Z. Tianjun and Z. Changfu, “A Real-Time Rollover Warning System for Heavy Duty Vehicle,” *2010 Int. Conf. Challenges Environ. Sci. Comput. Eng.*, pp. 324–327, 2010.

[19] B. Ji-hua, L. Jin-liang, and Y. Yan, “Lateral stability analysis of the tractor/full trailer combination vehicle,” *2011 Int. Conf. Electr. Inf. Control Eng.*, pp. 2294–2298, Apr. 2011.

[20] J. N. Dang, “Preliminary Results Analyzing The Effectiveness of Electronic Stability Control (ESC) Systems,” 2004.

[21] P. G. Van Valkenburgh, R. H. R. H. Klein, J. Kanianthra, P. G. Van Valkenburgh, R. H. R. H. Klein, and J. Kanianthra, “Three-Wheel Passenger Vehicle Stability and Handling,” *SAE Tech. Pap. 820140*, vol. 820140, pp. 604–627, 1982.

[22] J. C. Huston, B. J. Graves, and D. B. Johnson, “Three Wheeled Vehicle Dynamics,” in *SAE Technical Series Paper No. 820139*, 1982, vol. 820139.

[23] “Nicolas-Joseph Cugnot (French engineer),” *Britannica Online Encyclopedia*. [Online]. Available: http://www.britannica.com/EBchecked/topic/145966/Nicolas-Joseph-Cugnot.

[24] M. K. Gupta, D. Bhatt, V. K. Goel, D. V Singh, and A. Eiber, “Wind drag characteristics of two- and three-wheeled vehicles,” *J. Inst. Eng. India Mech. Eng. Div.*, vol. 76, pp. 100–104, 1995.

[25] K. L. D’Entremont and R. L. Barnett, “On the Maneuverability and Stability of Turf Work Trucks,” *SAE Tech. Pap. Ser. 961761*, pp. 1–8, 1996.

[26] “Groupe 2: Les 3-Roues à une seule roue avant.” [Online]. Available: http://cll.qc.ca/Professeurs/Mecanique/ethierp/3-roues/class2.htm. [Accessed: 30-May-2015].

[27] T. Aoki, Y. Murayama, and S. Hirose, “Mechanical design of three-wheeled lunar rover; Tri-Star IV,” in *2011 IEEE International Conference on Robotics and Automation*, 2011, pp. 2198–2203.

[28] B. Kim, D. Necsulescu, and J. Sasiadek, “Model Predictive Control of an Autonomous Vehicle,” no. July, pp. 1279–1284, 2001.

[29] “Piaggio Ape.” [Online]. Available: http://www.3wheelers.com/piaggio.html. [Accessed: 22-Aug-2012].

[30] “Carver (automobile) - Wikipedia, the free encyclopedia.” [Online]. Available: http://en.wikipedia.org/wiki/Carver_(automobile). [Accessed: 13-Nov-2011].

[31] “CLEVER - Wikipedia, the free encyclopedia.” [Online]. Available: http://en.wikipedia.org/wiki/CLEVER. [Accessed: 13-Nov-2011].

[32] “A to Z database of three Wheelers.” [Online]. Available: http://www.3wheelers.com/AZDatabase/AZ_view.php. [Accessed: 13-Nov-2011].

[33] “Tuk Tuks replace mules on Gaza streets,” 2010. [Online]. Available: http://www.maannews.net/eng/ViewDetails.aspx?ID=314523. [Accessed: 13-Nov-

2011].

[34] “Auto rickshaw crucial for sustainable transport: Study - Economic Times.” [Online]. Available: http://articles.economictimes.indiatimes.com/2012-02-25/news/31099871_1_urban-transport-auto-rickshaw-public-transport. [Accessed: 15-Aug-2012].

[35] “Three wheeled car - Wikipedia, the free encyclopedia.” [Online]. Available: http://en.wikipedia.org/wiki/Three-wheeled_car.

[36] “ALIAS Electric Car.” [Online]. Available: http://www.zapworld.com/zap-alias-electric-car. [Accessed: 14-Nov-2011].

[37] “h2 three-wheelers.” [Online]. Available: http://www.unido-ichet.org/index.php?option=com_content&view=article&id=258:h2-three-wheelers&catid=15:demonstration-projects&Itemid=42&lang=en. [Accessed: 13-Nov-2011].

[38] S. Herman, W. Lee, T. Vu, and B. Warda, “Project 10 Xebra : Hydraulic-Electric Hybrid,” 2007.

[39] “Three-wheelers on auto majors’ radar.” [Online]. Available: http://www.business-standard.com/india/news/three-wheelersauto-majors-radar/278616/. [Accessed: 13-Dec-2011].

[40] M. Kojima, C. Brandon, and J. J. Shah, “Improving urban air quality in South Asia by reducing emissions from two-stroke engine vehicles,” World Bank, Dec. 2000.

[41] A. Mani, M. Pai, and R. Aggarwal, “Sustainable Urban Transport in India,” 2012.

[42] M. Walz, “Trends in the static stability factor of passenger cars, light trucks, and vans,” 2005.

[43] A. Raman, J. S. Rao, and S. R. Kale, “Overturning Stability of Three Wheeled Motorized Vehicles,” *Veh. Syst. Dyn.*, vol. 24, no. 2, pp. 123–144, Mar. 1995.

[44] T. Gillespie, *Fundamentals of vehicle dynamics*. SAE International, 1992.

[45] J. Rao, “Overturning stability analysis of three wheeled motorized vehicles using simulink,” *Adv. Vib. Eng.*, vol. 8, no. 4, pp. 301 – 311, 2009.

[46] A. Zandieh, “Dynamics of a Three-Wheel Vehicle with Tadpole Design,” University of Waterloo, 2014.

[47] S. Saha and J. Angeles, “Kinematics and dynamics of a three-wheeled 2-DOF AGV,” in *Robotics and Automation*, 1989.

[48] O. Honorati, R. Caricchi, R. Crescimbini, L. Solero, F. Caricchi, and F. Crescimbini, “Lightweight, compact, three-wheel electric vehicle for urban mobility,” in *International Conference on Power Electronic Drives and Energy Systems for Industrial Growth*, 1998, vol. 50, no. 4, pp. 1085–1091.

[49] F. Caricchi, L. Del Ferraro, F. Giulii Capponi, O. Honorati, and E. Santini, “Three-wheeled electric maxi-scooter for improved driving performances in large urban areas,” *IEEE Int. Electr. Mach. Drives Conf. 2003. IEMDC’03.*, vol. 3, pp. 1363–1368, 2003.

[50] V. Cossalter and A. Doria, “Potentialities of a three-wheeled vehicle for zero emission mobility,” in *ecologic vehicles renewable energies*, 2009.

[51] P. Mulhall and A. Emadi, “Comprehensive simulations and comparative analysis of the electric propulsion motor for a solar/battery electric auto rickshaw three-wheeler,” in *2009 35th Annual Conference of IEEE Industrial Electronics*, 2009, pp. 3785–3790.

[52] V. Cossalter, N. Ruffo, and F. Biral, “Development of a novel three-wheeled vehicle,” *3rd IfZ Int. …*, pp. 1–19, 2000.

[53] J. Darling, A. Harrison, and B. Shalders, “Design evolution of a novel tilting three-wheeled motorcycle for city environments,” *Am. Soc. Mech. Eng. Des. Eng. Div. Publ.*, vol. 106, pp. 129–134, 2000.

[54] A. Chawla, S. Mukherjee, D. Mohan, R. Kumar, and T. Gavade, “FE Simulation Studies of a Three-Wheeled Scooter Taxi,” *Mech. Eng.*, 2001.

[55] C.-C. Yu and T. Liu, “Full control modes of three-wheeled vehicles with zero body sideslip angle and zero body motions,” *Proc. Inst. Mech. Eng. Part K J. Multi-body Dyn.*, vol. 215, no. 2, pp. 103–117, Jan. 2001.

[56] Y. Yavin, “Modelling the motion of a three-wheeled car,” *Math. Comput. Model.*, vol. 39, no. 4–5, pp. 473–478, Feb. 2004.

[57] T. Gawade, S. Mukherjee, and D. Mohan, “Wheel Lift-off and Ride Comfort of Three-wheeled Vehicle over Bump,” *J. Inst. Eng. Part MC, Mech. Eng. Div.*, vol. 85, no. I, pp. 78–87, 2004.

[58] T. R. Gawade, S. Mukherjee, D. Mohan, and T. G, “Rollover propensity of three-wheel scooter taxis,” in *SAE Technical Paper Series 2004-01-1622*, 2004, no. September, pp. 309–310.

[59] T. R. Gawade, S. Mukherjee, and D. Mohan, “Six-degree-of-freedom three-wheeled-vehicle model validation,” *Proc. Inst. Mech. Eng. Part D J. Automob. Eng.*, vol. 219, no. 4, pp. 487–498, Jan. 2005.

[60] S. Mukherjee, D. Mohan, T. Gawade, and T. G, “Rollover Stability of Three Wheeled Vehicles,” in *IRCOBI Conference*, 2004, no. September, pp. 309–310.

[61] S. Mukherjee, D. Mohan, and T. R. Gawade, “Three-wheeled Scooter Taxi: A Safety Analysis,” *Sadhana*, vol. 32, no. 4, pp. 459–478, Dec. 2007.

[62] R. J. Whitehead, W. E. Travis, D. D. M. D. M. Bevly, and G. T. Flowers, “A study of the effect of various vehicle properties on rollover propensity,” in *SAE 2004 Automotive Dynamics, Stability & Controls Conference and Exhibition*, 2004, pp. 3381–3386.

[63] B. Chen, Z. Jiao, and S. S. Ge, “Nonlinear control of aircraft on ground runway keeping,” *Proc. 2011 Int. Conf. Fluid Power Mechatronics*, pp. 576–581, Aug. 2011.

[64] A. Rankin, B. Krauskopf, M. Lowenberg, and E. Coetzee, “Bifurcation and stability analysis of aircraft turning manoeuvres,” *Am. Inst. Aeronaut. Astronaut.*, vol. 32, no. 2, pp. 1–24, 2008.

[65] S. Lei, Y. Hua, Y. Xufeng, M. Cong, and H. Jun, “A study of instability in a miniature flying-wing aircraft in high-speed taxi,” *Chinese J. Aeronaut.*, Apr. 2015.

[66] E. Coetzee, B. Krauskopf, and M. Lowenberg, “Nonlinear aircraft ground dynamics,” in *International Conference on Nonlinear Problems in Aviation and Aerospace* -, 2006, pp. 1–8.

[67] J. RANKIN, E. COETZEE, B. KRAUSKOPF, and M. LOWENBERG, “Bifurcation and Stability Analysis of Aircraft Turning on the Ground,” *J. Guid. Control. Dyn.*, vol. 32, no. 2, pp. 500–511, 2009.

[68] J. Duprez, “Control of the aircraft-on-ground lateral motion during low speed roll and manoeuvers,” in *Proceedings. 2004 IEEE Aerospace Conference*, 2004.

[69] J. Duprez, F. Mora-Camino, and F. Villaume, “Robust control of the aircraft on ground lateral motion,” *Proc. 24th ICAS Conf., Yokohama, …*, pp. 1–10, 2004.

[70] “Fedral Aviation Administration, Part 25.” pp. 252–439, 1980.

[71] D. O. Tipps, J. Rustenburg, D. Skinn, and T. Defiore, “Side Load Factor Statistics From Commercial Aircraft Ground Operations,” Washington, D.C., 2003.

[72] E. Coetzee, B. Krauskopf, and M. Lowenberg, “Application of Bifurcation Methods to the Prediction of Low-Speed Aircraft Ground Performance,” *J. Aircr.*, vol. 47, no. 4, pp. 1248–1255, Jul. 2010.

[73] E. Coetzee, “Modelling and Nonlinear Analysis of Aircraft Ground Manoeuvres,” 2011.

[74] C. Roos and J.-M. Biannic, “Aircraft-on-ground lateral control by an adaptive LFT-based anti-windup approach,” in *2006 IEEE Conference on Computer Aided Control System Design, 2006 IEEE International Conference on Control Applications, 2006 IEEE International Symposium on Intelligent Control*, 2006, pp. 2207–2212.

[75] Y. Li, Z. Jiao, and Y. Shang, “Research on aircraft taxiing lateral control based on fuzzy controller,” *Proc. 2011 Int. Conf. Fluid Power Mechatronics*, pp. 582–587, Aug. 2011.

[76] Y. Zhaohui and W. Yi, “A Design of Airplane’s Integrated Ground Directional System with Fuzzy Control,” *2009 Sixth Int. Conf. Fuzzy Syst. Knowl. Discov.*, vol. 6, pp. 13–17, 2009.

[77] C. M. . Farmer, “Effects of Electronic Stability Control on Fatal Crash Risk,” Arlington, VA 22201, 2010.

[78] B.-C. Chen and H. Peng, “Differential-Braking-Based Rollover Prevention for Sport Utility Vehicles with Human-in-the-loop Evaluations,” *Veh. Syst. Dyn.*, vol. 36, no. 4–5, pp. 359–389, Nov. 2001.

[79] S. Yim, “Design of a rollover prevention controller with differential game theory and a coevolutionary genetic algorithm,” *J. Mech. Sci. Technol.*, vol. 25, no. 6, pp. 1565–1571, Aug. 2011.

[80] V. Cherian, R. Shenoy, A. Stothert, and J. Shriver, “Model-Based Design of a SUV Anti-Rollover Control System,” *Veh. Dyn. Simul.*, vol. SP-2157, 2008.

[81] B. Hopkins, S. Taheri, and M. Ahmadian, “Yaw Stability Control and Emergency Roll Control for Vehicle Rollover Mitigation,” *SAE Tech. Pap.*, 2010.

[82] S. Solmaz, M. Corless, and R. Shorten, “A methodology for the design of robust rollover prevention controllers for automotive vehicles: Part 2-Active steering,” *2007 Am. Control Conf.*, no. 1, pp. 1606–1611, Jul. 2007.

[83] J. Ackermann, “Damping of vehicle roll dynamics by gain scheduled active steering,” in *Proceedings of European Control Conference*, 1999.

[84] X. Qiu, F. Yi, M. Yu, and L. Zhou, “Vehicle Active Anti-Roll Control Simulation,” in *2011 3rd International Workshop on Intelligent Systems and Applications*, 2011, pp. 1–4.

[85] M. Islam and C. Ha, “Road vehicle rollover avoidance using active steering controller,” in *International Conference on Computer and Information Technology (ICCIT)*, 2011, pp. 22–24.

[86] S. Solmaz, “Switched stable control design methodology applied to vehicle rollover prevention based on switched suspension settings,” *IET Control Theory Appl.*, vol. 5, no. 9, p. 1104, 2011.

[87] J. Yoon and K. Yi, “A rollover mitigation control scheme based on rollover index,” in *American Control Conference, 2006*, 2006, pp. 5372–5377.

[88] D. J. M. Sampson, D. Cebon, and T. St, “Active Roll Control of Single Unit Heavy Road Vehicles,” *Veh. Syst. Dyn.*, vol. 40, no. 4, 2003.

[89] J. Tjonnas and T. Johansen, “Stabilization of automotive vehicles using active steering and adaptive brake control allocation,” *IEEE Trans. Control Syst. Technol.*, vol. 18, no. 3, pp. 545–558, 2010.

[90] J. Yoon, W. Cho, J. Kang, B. Koo, and K. Yi, “Design and evaluation of a unified chassis control system for rollover prevention and vehicle stability improvement on a virtual test track,” *Control Eng. Pract.*, vol. 18, no. 6, pp. 585–597, Jun. 2010.

[91] B. C. B.-C. Chen and H. Peng, “Rollover prevention for sports utility vehicles with human-in-the-loop evaluations,” in *5th Int’l Symposium on Advanced Vehicle Control*, 2000.

[92] N. Amati, A. Festini, L. Pelizza, and A. Tonoli, “Dynamic modelling and experimental validation of three wheeled tilting vehicles,” *Veh. Syst. Dyn.*, vol. 49, no. 6, pp. 889–914, Jun. 2011.

[93] R. Bartolozzi, F. Frendo, M. Guiggiani, O. Di Tanna, O. Di Tanna, and C. S. A, “Comparison between experimental and numerical handling tests for a three-wheeled motorcycle,” *SAE Int. J. Engines*, vol. 1, no. 1, pp. 1389–1395, 2009.

[94] A. Sponziello, F. Frendo, and M. Guiggiani, “Stability Analysis of a Three-Wheeled Motorcycle,” *SAE Int. J. Engines*, vol. 1, no. 1, pp. 1396–1401, 2009.

[95] M. Barker, B. Drew, J. Darling, K. A. Edge, and G. W. Owen, “Steady-state steering of a tilting three-wheeled vehicle,” *Veh. Syst. Dyn.*, vol. 48, no. 7, pp. 815–830, Jul. 2010.

[96] J. J. H. Berote, “Dynamics and Control of a Tilting Three Wheeled Vehicle,”

University of Bath, 2010.

[97] J. Gohl, R. Rajamani, L. Alexander, and P. Starr, “Active Roll Mode Control Implementation on a Narrow Tilting Vehicle,” *Veh. Syst. Dyn.*, vol. 42, no. 5, pp. 347–372, Dec. 2004.

[98] S. Kidane, R. Rajamani, L. Alexander, P. J. Starr, and M. Donath, “Development and Experimental Evaluation of a Tilt Stability Control System for Narrow Commuter Vehicles,” vol. 18, no. 6, pp. 1266–1279, 2010.

[99] P. Tsai, L. Wang, and F. Chang, “Modeling and hierarchical tracking control of tri-wheeled mobile robots,” in *IEEE Transactions on Robotics*, 2006, vol. 22, no. 5, pp. 1055–1062.

[100] a Ghaffari, a Meghdari, D. Naderi, and S. Eslami, “Enhancement of the tipover stability of mobile manipulators with non-holonomic constraints using an adaptive neuro-fuzzy-based controller,” *Proc. Inst. Mech. Eng. Part I J. Syst. Control Eng.*, vol. 223, no. 2, pp. 201–213, Mar. 2009.

[101] A. Elahidoost and C. Cao, “Control and navigation of a three wheeled unmanned ground vehicle by L1 adaptive control architecture,” *2012 IEEE Int. Conf. Technol. Pract. Robot Appl.*, pp. 13–18, Apr. 2012.

[102] N. Roqueiro, E. F. Colet, and M. G. de Faria, “A Sliding Mode Controlled Tilting Three Wheeled Narrow Vehicle,” in *XVIII Congresso Brasileiro de Automatica*, 2010, no. x, pp. 1596–1602.

[103] T. Gawade, S. Mukherjee, and D. Mohan, “Rollover Propensity of Three-Wheel Scooter Taxis,” Mar. 2004.

[104] T. Shim and C. Ghike, “Understanding the limitations of different vehicle models for roll dynamics studies,” *Veh. Syst. Dyn.*, vol. 45, no. 3, pp. 191–216, Mar. 2007.

[105] J. Y. Wong, *Theory of Ground Vehicles*, 3rd ed. Wiley-Interscience, 2001.

[106] R. M. Brach and R. M. Brach, “Tire Models for Vehicle Dynamic Simulation and Accident Reconstruction,” *SAE Tech. Pap. 2009-01-0102*, vol. 7323, 2009.

[107] Hans B. Pacejka, *Tire and Vehicle dynamics*, 2nd Editio. SAE International, Warrendale, Pennsylvania, USA, 2006.

[108] H. Slimi, H. Arioui, L. Nouveliere, and S. Mammar, "Motorcycle Lateral Dynamic Estimation and Lateral Tire-Road Forces Reconstruction Using Sliding Mode Observer."

[109] E. Coetzee, "Nonlinear Aircraft Ground Dynamics," pp. 1–8, 2006.

[110] H. B. Pacejka and R. S. Sharp, "Shear Force Development by Pneumatic Tyres in Steady State Conditions: A Review of Modelling Aspects," *Veh. Syst. Dyn.*, vol. 20, no. 3–4, pp. 121–175, Jan. 1991.

[111] "Tire Modelling Reference: CarSim Software." Carsim.

[112] G. J. Forkenbrock, W. R. Garrott, M. Heitz, and B. C. O'Harra, "A Comprehensive Experimental Evaluation of Test Maneuvers That May Induce On-Road , Untripped , Light Vehicle Rollover Phase IV of NHTSA ' s Light Vehicle Rollover Research Program," no. October. NHTSA, US Dept of Transport, 2002.

[113] V. Nguyen, "Vehicle Handling, Stability, and Bifurcation Analysis for Nonlinear Vehicles Models," University of Maryland, College Park, 2005.

[114] B.-C. Chen, C.-C. Yu, W.-F. Hsu, and M.-F. Lo, "Design of electronic stability control for rollover prevention using sliding mode control," *Int. J. Veh. Des.*, vol. 56, no. 1/2/3/4, pp. 224 – 245, 2011.

[115] H. Imine, L. M. Fridman, and T. Madani, "Steering Control for Rollover Avoidance of Heavy Vehicles," *IEEE Trans. Veh. Technol.*, vol. 61, no. 8, pp. 3499–3509, Oct. 2012.

[116] L. D. Metz, "What Constitutes Good Handling," in *SAE Technical Paper 2004-01-3532*, 2004.

[117] "Types of Rollover," *National Highway Traffic Safety Admnistration (NHTSA)*. [Online]. Available: http://www.safercar.gov/Vehicle+Shoppers/Rollover/Types+of+Rollovers. [Accessed: 22-Jun-2015].

[118] M. Nuessle, R. Rutz, M. Leucht, M. Nonnenmacher, and H. Volk, "Objective test methods to assess active safety benefits of ESP," in *International Technical Conference on the Enhanced Safety of Vehicles (ESV)*, 2007.

[119] G. Mavros, "On the objective assessment and quantification of the transient-handling response of a vehicle," *Veh. Syst. Dyn.*, vol. 45, no. 2, pp. 93–112, Feb. 2007.

[120] D. A. Crolla, R. P. King, and H. a S. Ash, "Subjective and Objective Assessment Of Vehicle Handling Performance," pp. 1–7, 2000.

[121] R. GSG, G. R. D, T. R. Gawade, K. V. Santosh, and M. N. Reddy, "Parametric Study of Three - Wheeler Directional Stability using MBD Simulations," *SAE Tech. Pap. 2010-32-0102*, Sep. 2010.

[122] Saeedi and Kazemi, "Stability of Three-Wheeled Vehicles with and without Control System," *Int. J. Automot. Eng.*, vol. 3, no. 1, pp. 343–355, Mar. 2013.

[123] A. Soltani, A. Goodarzi, and A. Khajepour, "An Investigation on Dynamic Behavior of Different Three-Wheeled Vehicle Configurations," in *AVEC'14*, 2014.

[124] E. Ono, "Bifurcation in Vehicle Dynamics and Robust Front Wheel Steering Control," *IEEE Trans. Control Syst. Technol.*, vol. 6, no. 3, p. 412420, Oct. 1998.

[125] F. Farroni, M. Russo, R. Russo, M. Terzo, and F. Timpone, "A combined use of phase plane and handling diagram method to study the influence of tyre and vehicle characteristics on stability," *Veh. Syst. Dyn.*, vol. 51, no. 8, pp. 1265–1285, Aug. 2013.

[126] C. G. Bobier, "A Phase Portrait Approach To Vehicle Stabilization And Envelope Control," STANFORD UNIVERSITY, 2012.

[127] T. Chung and K. Yi, "Design and evaluation of side slip angle-based vehicle stability control scheme on a virtual test track," *IEEE Trans. Control Syst. Technol.*, vol. 14, no. 2, pp. 224–234, Mar. 2006.

[128] C. J. Wenzinger and A. R. Kantrowitz, “Notes of Factors Affecting Geometrical Arrangement of Tricycle-Type landing Gears,” 1937.

[129] S. Shen, J. Wang, P. Shi, and G. Premier, “Nonlinear dynamics and stability analysis of vehicle plane motions,” *Veh. Syst. Dyn.*, vol. 45, no. 1, pp. 15–35, Jan. 2007.

[130] S. Chen and N. Moshchuk, “Vehicle Rollover Avoidance,” *IEEE Control Systems Magazine*, no. August, 2010.

[131] J. P. Perruquetti, Wilfrid/Barbot, *Sliding Mode Control in Engineering*. Marcel Dekker, Inc., 2002.

[132] R. W. Ogden, R. Andrzejewski, and Ja. Awrejcewicz, *Nonlinear dynamics of a wheeled vehicle*, vol. 10. Springer Verlag, 2005.

[133] C. Vecchio, “Sliding Mode Control: Theoretical Developments and Applications to Uncertain Mechanical Systems,” 2008.

[134] H. K. Khalil, *Nonlinear Systems*, 3rd ed. New Jersey: Prentice Hall Inc, 2002.

[135] Y. Shtessel, C. Edwards, L. Fridman, and A. Levant, *Sliding Mode Control and Observation*. New York, NY: Springer New York, 2014.

[136] A. Hac, “Rollover Stability Index Including Effects of Suspension Design,” in *SAE World Congress*, 2002, no. 724.

[137] J. Gertsch, J. Jung, and T. Shim, “A Vehicle Roll-Stability Indicator Incorporating Roll-Center Movements,” *IEEE Trans. Veh. Technol.*, vol. 58, no. 8, pp. 4078–4087, Oct. 2009.

[138] J. Yoon, W. Cho, B. Koo, and K. Yi, “Unified Chassis Control for Rollover Prevention and Lateral Stability,” *IEEE Trans. Veh. Technol.*, vol. 58, no. 2, pp. 596–609, Feb. 2009.

[139] F. Joachim and J. Boerner, “Superposition-Drive for Steering System,” US Patent No. 20100331133A12010.

[140] G. Tarchala, “Influence of the sign function approximation form on performance of the sliding-mode speed observer for induction motor drive,” in *2011 IEEE International Symposium on Industrial Electronics*, 2011, pp. 1397–1402.

[141] S. Yim, “Design of a Preview Controller for Vehicle Rollover Prevention,” *IEEE Trans. Veh. Technol.*, vol. 60, no. 9, pp. 4217–4226, Nov. 2011.

[142] Ch. R. Carlson and J. C. Gerdes, “Optimal rollover prevention with steer by wire and differential braking,” in *Proceedings of IMECE 03*, 2003.